



2007-07-18

# Soft Surface Roll Mechanics Parameters for Light Vehicle Rollover Accident Reconstruction

Kevin Claude Henry

*Brigham Young University - Provo*

Follow this and additional works at: <https://scholarsarchive.byu.edu/etd>

 Part of the [Civil and Environmental Engineering Commons](#)

---

## BYU ScholarsArchive Citation

Henry, Kevin Claude, "Soft Surface Roll Mechanics Parameters for Light Vehicle Rollover Accident Reconstruction" (2007). *All Theses and Dissertations*. 1436.

<https://scholarsarchive.byu.edu/etd/1436>

This Thesis is brought to you for free and open access by BYU ScholarsArchive. It has been accepted for inclusion in All Theses and Dissertations by an authorized administrator of BYU ScholarsArchive. For more information, please contact [scholarsarchive@byu.edu](mailto:scholarsarchive@byu.edu), [ellen\\_amatangelo@byu.edu](mailto:ellen_amatangelo@byu.edu).

SOFT SURFACE ROLL MECHANICS PARAMETERS FOR LIGHT  
VEHICLE ROLLOVER ACCIDENT RECONSTRUCTION

by

Kevin C. Henry

A thesis submitted to the faculty of

Brigham Young University

in partial fulfillment of the requirements for the degree of

Master of Science

Department of Civil and Environmental Engineering

Brigham Young University

August 2007



Copyright © 2007 Kevin C. Henry

All Rights Reserved



BRIGHAM YOUNG UNIVERSITY

GRADUATE COMMITTEE APPROVAL

of a thesis submitted by

Kevin C. Henry

This thesis has been read by each member of the following graduate committee and by majority vote has been found to be satisfactory.

---

Date

---

David W. Jensen, Chair

---

Date

---

Steven E. Benzley

---

Date

---

Kenneth W. Chase



## BRIGHAM YOUNG UNIVERSITY

As chair of the candidate's graduate committee, I have read the thesis of Kevin C. Henry in its final form and have found that (1) its format, citations, and bibliographical style are consistent and acceptable and fulfill university and department style requirements; (2) its illustrative materials including figures, tables, and charts are in place; and (3) the final manuscript is satisfactory to the graduate committee and is ready for submission to the university library.

---

Date

---

David W. Jensen  
Chair, Graduate Committee

Accepted for the Department

---

E. James Nelson  
Graduate Coordinator

Accepted for the College

---

Alan R. Parkinson  
Dean, Ira A. Fulton College of Engineering  
and Technology





## ABSTRACT

### SOFT SURFACE ROLL MECHANICS PARAMETERS FOR LIGHT VEHICLE ROLLOVER ACCIDENT RECONSTRUCTION

Kevin C. Henry

Department of Civil and Environmental Engineering

Master of Science

Light vehicle rollover accidents on soft surfaces can be modeled assuming constant drag with linear motion equations and other engineering principles. The concept of using segment average results to evaluate roll mechanics parameters throughout a roll sequence, and specifically, segment duration to evaluate vehicle trajectory between ground impacts is developed. The trajectory model is presented, explained and compared to values obtained by analyzing digital video of rollover crash tests.

Detailed film analysis procedures are developed to obtain data from rollover crash tests that are not otherwise documented. Elevation of the center of gravity of vehicles is obtained where instrumentation does not explicitly yield this data.



Instantaneous center of gravity elevation data throughout a roll sequence provides the opportunity to calculate descent distances as a vehicle travels from one ground contact to another. This data is used to quantify severity of ground impacts as a vehicle interact with the ground throughout a roll sequence.

Segment average analysis is a reasonable method for determining general roll mechanics parameters. Because of the chaotic nature of rollover accidents, the range of effective drag factors for a given roll surface may be quite large. Choosing an average of typical drag factors is a reasonable approach for a first-order approximation although certain parameters may be predicted less accurately than if actual values were known.

The trajectory results demonstrate the influence of drag factor descent height calculations. Typical constant drag factors tend to overestimate descent height early in a roll sequence and underestimate descent height later in the sequence.

The trajectory model is a useful tool to aid in understanding rollover mechanics although a rolling vehicle may be in contact with the ground for a significant fraction of a roll segment. The model should not be used at locations in roll sequences where there are extremes in translational center of gravity decelerations. These extremes include the segments immediately following overturn where there are large angular accelerations and large differences between the tangential velocity of the vehicle perimeter and the translational velocity of the center of gravity, as well as segments that include vehicle impacts with irregular topography.



## ACKNOWLEDGMENTS

The research included in this thesis was made possible by General Motors® and Ford Motor Company®. I thank the gracious individuals at these corporations for allowing me access to proprietary crash test data for analysis in this work. I also thank Geoff Germane and the entire Germane Engineering staff for their input and assistance. I thank Dr. Jarrod Carter of Origin Engineering and Pete Luepke of Exponent®. I thank Dr. David W. Jensen as my thesis advisor, and Dr. Steven E. Benzley and Dr. Kenneth W. Chase as committee members for their input on this project. I also thank my family for their support.



## TABLE OF CONTENTS

<b>LIST OF TABLES.....</b>	<b>xvii</b>
<b>LIST OF FIGURES.....</b>	<b>xix</b>
<b>1 Introduction .....</b>	<b>1</b>
1.1 Motivation .....	1
1.2 Collision Type Overview .....	4
1.3 Prior Work .....	6
1.4 Contribution.....	12
1.5 Approach .....	12
<b>2 Current Industry Standard Analysis Procedures .....</b>	<b>15</b>
2.1 Segment Average Analysis.....	15
2.2 Trajectory Analysis Based on Segment Average Results .....	20
<b>3 Equations Governing Analysis of a “Rolling” Body .....</b>	<b>29</b>
3.1 Kinetic Energy .....	29
3.2 Moments of Inertia .....	30
3.3 Tangential Velocity .....	34
3.4 Instantaneous Center of Rotation .....	37
3.5 Euler Equations of Motion .....	39
<b>4 Rollover Testing.....</b>	<b>41</b>
4.1 Description of FMVSS 208 Dolly Rollover Testing.....	41
4.2 Description of Analyzed Rollover Tests .....	43



4.3	Data Reduction for Test 1 (1989 Chevrolet Blazer).....	44
4.4	Data Reduction for Test 2 (1998 Ford Expedition).....	48
4.5	Data Reduction for Test 3 (2004 Volvo XC90) .....	48
4.6	Data Reduction for Test 4 (1985 Toyota Pickup) .....	51
<b>5</b>	<b>Roll Mechanics Parameters and Results .....</b>	<b>53</b>
5.1	Ground Contact Ratio .....	57
5.2	Drag Factors .....	59
5.3	Roll Angle .....	60
5.4	Translational Velocity .....	62
5.5	Roll Rate .....	65
5.6	Energy.....	69
<b>6</b>	<b>Trajectory Analysis and Results .....</b>	<b>75</b>
6.1	Test 1 (1989 Chevrolet Blazer) .....	76
6.2	Test 2 (1998 Ford Expedition) .....	82
6.3	Trajectory Summary .....	88
<b>7</b>	<b>Discussion of Results .....</b>	<b>91</b>
<b>8</b>	<b>Conclusions, Contributions and Recommendations .....</b>	<b>95</b>
	<b>References .....</b>	<b>99</b>
	<b>Appendix A – Nomenclature .....</b>	<b>101</b>
	<b>Appendix B – Detailed Crash Test documentation .....</b>	<b>103</b>
	<b>Appendix C – Energy Correlations.....</b>	<b>109</b>
	<b>Appendix D – Filmstrip for Test 1 .....</b>	<b>113</b>
	<b>Appendix E – Impact Effects on Roll Rate .....</b>	<b>115</b>
	<b>Appendix F – Tabular Data for Test 1 .....</b>	<b>117</b>
	<b>Appendix G – Tabular Data for Test 2.....</b>	<b>155</b>

## LIST OF TABLES

Table 1-1. Published Drag Factors Based on Combined Trip and Roll [4] .....	11
Table 1-2: Published Drag Factors Based on Roll Only [4].....	11
Table 2-1. Example Roll Sequence Spreadsheet.....	19
Table 2-2: Reconstructed Roll Position Data .....	22
Table 3-1: Example Tangential Velocity Calculations .....	37
Table 4-1—General Vehicle and Test Information Pertaining to Three Dolly Rollover Tests.....	44
Table 4-2 – Placement and Type of ATDs in Dolly Rollover Tests .....	44
Table 4-3: Frame Rate Summary for Test 1 .....	45
Table 5-1: Initial Conditions of the Rollover Tests.....	53
Table 5-2: Summary of Selected Results for the Rollover Tests .....	57
Table 6-1: Roll Mechanics Based on Reconstructed Roll Positions for Test 1.....	76
Table 6-2: Trajectory Parameters and Results Using Drag Factor of 0.425- 0.475g .....	80
Table 6-3: Trajectory Parameters and Results Using Drag of 0.38-0.64g .....	82
Table 6-4: Test 2 — Roll Mechanics Based on Reconstructed Roll Positions .....	85
Table 6-5: Test 2 — Trajectory Parameters and Results Using Drag of 0.425- 0.475 .....	85
Table 6-6: Test 2 — Trajectory Parameters and Results Using Drag of 0.38- 0.64 .....	87



## LIST OF FIGURES

Figure 1-1: Phases of a Rollover Accident.....	5
Figure 1-2: Principal Axes.....	6
Figure 1-3: Comparison of Roll Distance and Number of Rolls.....	7
Figure 1-4: Example of Material Flow .....	9
Figure 1-5: Example of Material Flow and Vegetation Accumulation.....	10
Figure 2-1: Trajectory Nomenclature .....	21
Figure 2-2: Theoretical Trajectory Diagram: a) Plan View; and, b) Elevation View.....	22
Figure 2-3: Theoretical Velocity-Time Diagram .....	26
Figure 3-1: Angles from Arbitrary Axis to Inertial Frame of Reference .....	32
Figure 3-2: Ejected Occupant in a Dolly Rollover Test.....	34
Figure 3-3: Tangential Velocity Diagram .....	35
Figure 3-4: Significant Vehicle Perimeter Points.....	36
Figure 3-5: Vector Diagram for Tangential Velocity Computations .....	36
Figure 3-6: Instant Center — Pure Rolling Motion.....	38
Figure 3-7: Instant Center — Tangential Velocity > Translational Velocity.....	38
Figure 3-8: Instant Center—Tangential Velocity < Translational Velocity.....	39
Figure 4-1: Typical Device for Rollover Tests [Adapted From Reference 22] .....	42
Figure 4-2: a) Raw Video Frame, b) Video Frame with Digital Model Overlaid .....	47

Figure 4-3: Test 2 – Documented Roll Path for Test 2 .....	49
Figure 4-4: Test 3 – Documented Roll Path.....	50
Figure 5-1: Test 1 – Dolly Rollover Sequence.....	54
Figure 5-2: Test 2 – Dolly Rollover Sequence.....	55
Figure 5-3: Test 3 – Dolly Rollover Sequence.....	56
Figure 5-4: Test 1 – Combined Roll Angle vs. Distance for Tests 1, 2, & 3 .....	61
Figure 5-5: Test 1—Translational Speed vs. Distance Compared With Computed Translational Speed.....	63
Figure 5-6: Test 2—Translational Speed vs. Distance Compared With Computed Translational Speed.....	64
Figure 5-7: Test 3—Translational Speed vs. Distance Compared With Computed Translational Speed.....	64
Figure 5-8: Test 1 — Roll Rate vs. Distance.....	66
Figure 5-9: Test 1 — Roll Rate vs. Time Compared With Computed Roll Rate.....	66
Figure 5-10: Test 2 — Roll Rate vs. Time Compared With Computed Roll Rates .....	67
Figure 5-11: Test 3 — Roll Rate vs. Time Compared With Computed Roll Rates .....	67
Figure 5-12: Roll Rate Comparison of Remote-Steered Rollover Test and Tests 1, 2 & 3.....	68
Figure 5-13: Test 1 — Translational, Rotational and Potential Energy vs. Distance .....	70
Figure 5-14: Test 1 — Translational, Rotational and Potential Energy vs. Time .....	70
Figure 5-15: Test 2 — Translational, Energy Rotational and Total vs. Distance .....	71
Figure 5-16: Test 2 — Translational, Rotational and Total Energy vs. Time.....	71
Figure 5-17: Test 3 — Translational, Rotational and Total Energy vs. Distance .....	72
Figure 5-18: Test 3 — Translational, Rotational and Total Energy vs. Time.....	72

Figure 5-19: Non-Dimensional Correlation of Combined Rollover Energy for Tests 1, 2, and 3 .....	73
Figure 6-1: Reconstructed Roll Sequence for Test 1.....	77
Figure 6-2: Test 1 — Center of Gravity Elevation vs. Distance For Three Successive Trajectories.....	78
Figure 6-3: Test 1 — Center of Gravity Elevation vs. Distance for Three Successive Airborne Segments Showing Multiple Parabolic Fit .....	79
Figure 6-4: Predicted and Measured Trajectories with $\mu_{low}=0.425$ and $\mu_{high}=0.475$ .....	81
Figure 6-5: Predicted and Measured Trajectories with $\mu_{low}=0.38$ and $\mu_{high}=0.64$ .....	82
Figure 6-6: Test 2—Reconstruction Diagram with Three Trajectory Templates .....	83
Figure 6-7: Beginning of First Trajectory .....	84
Figure 6-8: Maximum Elevation of First Trajectory .....	84
Figure 6-9: End of First Trajectory and Beginning of Second Trajectory .....	84
Figure 6-10: Maximum Elevation of Second Trajectory .....	84
Figure 6-11: End of Second Trajectory .....	84
Figure 6-12: Predicted and Measured Trajectories with $\mu_{low}=0.425$ and $\mu_{high}=0.475$ .....	86
Figure 6-13: Magnified View of Predicted and Measured Trajectories with $\mu_{low}=0.425$ and $\mu_{high}=0.475$ .....	86
Figure 6-14: Predicted and Measured Trajectories with $\mu_{low}=0.38$ and $\mu_{high}=0.64$ .....	87
Figure 6-15: Magnified View of Predicted and Measured Trajectories with $\mu_{low}=0.38$ and $\mu_{high}=0.64$ .....	88



# **1 Introduction**

Traffic accident reconstruction is the effort to determine from all available information and evidence how an accident happened [1]. This thesis addresses parameters and the methods used in rollover accident reconstruction. Four rollover crash tests are extensively documented and analyzed to determine parameters useful in accident reconstruction, and to demonstrate the use of certain accident reconstruction techniques. Segment average analysis, trajectory mechanics and general roll mechanics are the topics addressed.

## **1.1 Motivation**

With the increased popularity of SUVs in recent years the number of vehicle rollover accidents has increased due to the nature and use of the vehicles. Approximately 19.5% of all fatal crashes involve a rollover in the crash sequence (and 20-25% of all vehicle fatalities occur in rollovers), although rollover accidents account for less than 5% of all tow-away vehicle crashes [2]. Rollover accidents are generally more violent and more severe than planar collisions [3]. “The comprehensive cost of the injuries and fatalities in rollovers is about \$40 billion per year. As a class, rollover crashes constitute about 2.2% of the crashes, but 33% of the injury costs.” [2]



Quite often as a result of a fatality or injury that occurs during a rollover accident, a lawsuit ensues and allegations about the subject vehicle's integrity are made. Injured people often seek compensation for the adverse actions of others and file a lawsuit against all other parties involved, including the manufacturer of the vehicle and/or the manufacturer of the safety equipment installed in the vehicle. In the process of the suit attorneys hire reconstruction experts to determine the underlying causes of the accident and the injuries. There are numerous factors that cause or affect the results of an automobile accident. Often, accident reconstruction experts are employed to determine who may be at fault and/or what the causes and effects of the accident. These determinations are based on physical evidence documented by investigating police officers, evidence at the accident site, and/or evidence on the subject vehicle. The responsibility of the reconstructionist is to determine what data are useful and to use those data to form accident reconstruction opinions.

Aside from litigation, there are other reasons to perform accident reconstructions. One reason is to improve product designs based on long term experience from real world situations. If history and research shows that a vehicle can be designed in such a way that the vehicle will be safer, then research is continued to implement better safety features.

One objective during the reconstruction process is to determine how much energy the vehicle absorbed during a specific impact. Typical energy dissipation trends throughout an entire roll sequence are instructive for analysis of energy absorption by the vehicle for a single impact. Energy is dissipated in the deformation of the vehicle structure and in the disruption of the roll surface. Energy is also

converted from kinetic to potential energy and vice-versa. Kinetic energy is converted from translational to rotational energy and rotational back to translational energy. The desired result is to document what percentage of total energy is typically dissipated in a vehicle-to-ground impact and to understand typical values of energy conversion during a rollover accident.

Another question that is commonly asked is: “What is the magnitude of the forces on the vehicle during ground contact at various locations along the roll path?” One influential parameter needed to quantify ground contact forces is vertical velocity of the center of gravity toward the ground as a result of the conversion from potential energy to kinetic energy.

The purpose of this research is to quantify the exchange in velocity components and the exchange of energy in three dolly rollover crash tests. This research demonstrates a new method for accounting for exchanges in velocity and energy in a systematic manner. Spreadsheets are created that make this accounting easier. These spreadsheets are created in such a way that the reconstructionist is able to test a reconstruction for physical errors (i.e., “Are the laws of physics violated?”) quickly and easily. The accounting of these variables can only be performed on accidents where there is very little ambiguity about the vehicle motion. The accounting of velocity and energy gives the accident reconstructionist a standard or sample to measure other rollover accident reconstructions against.

## **1.2 Collision Type Overview**

The most common type of vehicle accident is a planar collision. There are many types of planar collisions. The simplest type of planar collision is a collision where one vehicle strikes a fixed rigid object like a tree, power pole, bridge abutment or any type of rigid guard rail structure. Single vehicle accidents can be classified as frontal, side, or rear end collisions and can have numerous variables defining the outcome of such a collision.

Another very common type of planar collision involves two or more vehicles that may impact one another at any orientation. For example, two cars may strike each other head-on. There are also offset frontal collisions, angled collisions, side impact collisions, and rear impact collisions. Any of these types of accidents may include two or more vehicles in any series of events.

Another type of vehicle accident involves rollovers. Most often, these accidents are caused by a single vehicle losing control and ultimately traveling a significantly different direction than the vehicle heading. In this circumstance a large torque is applied to the vehicle about its wheels or tires. If this torque is caused by striking an object like a curb or a similar fixed object or if the leading tires and wheels furrow into a soft surface, the impulse can become quite large and often leads to a rollover accident. If the vehicle torque is applied solely as a result of tire friction this may also lead to a rollover accident, although this is much less common.

On occasion a vehicle may roll as a result of a planar collision with another vehicle. This sometimes happens when there is a height difference between the centers of gravity of the vehicles involved. One vehicle overrides the other and in the

process receives a vertical force that causes a vehicle to overturn. A rollover may also result from a planar collision if a high yaw rate is imparted.

A vault is another type of rollover. A vault occurs if a vehicle rotates about its pitch axis far enough to overturn. This can occur only if a vehicle contacts an object that imparts a reaction force that acts below the center of gravity. The reaction must cause a moment that is greater than the moment acting in the opposite direction caused by the inertial force acting through the center of gravity of the vehicle. This type of rollover is a result of very unusual circumstances and is therefore, very uncommon.

As shown in Figure 1-1, rollover accidents consist of three phases [4]: 1) pre-trip (yaw phase); 2) trip; and, 3) roll. The pre-trip and trip phases are not directly approached in this work. This thesis focuses on the analysis of the roll phase of rollover accidents.

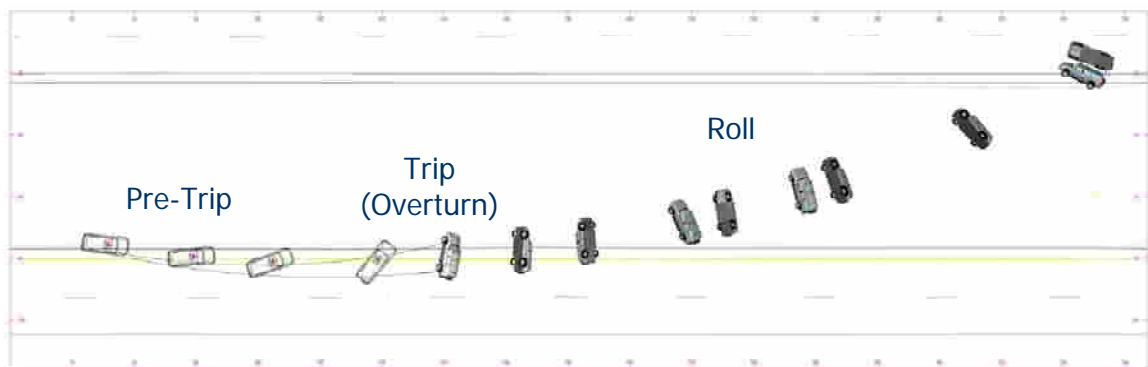


**Figure 1-1: Phases of a Rollover Accident**

Generally, once a vehicle enters the roll phase, the roll axis becomes the principal axis of rotation. The definitions of the principal axes of rotation are defined in Figure 1-1 where X is the roll axis, Y is the pitch axis and Z is the yaw axis.

Oscillation about the pitch and yaw axes generally involve small rotations compared to the roll angles produced.

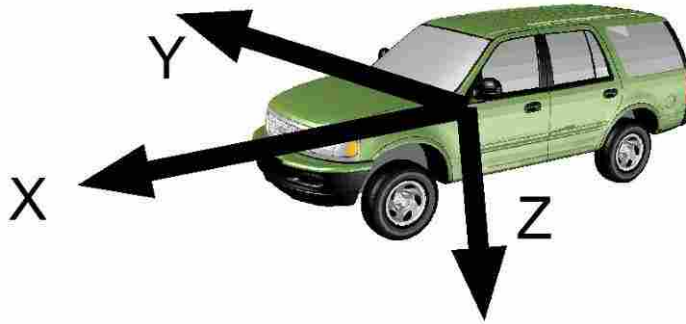


**Figure 1-2: Principal Axes**

### **1.3 Prior Work**

Rollover research and testing has been conducted on different levels since the early days of the automobile until the present day. Many of these tests were performed to determine the general crashworthiness of production vehicles. Rollover accident reconstruction, simulation and research has rapidly increased and improved in recent years in response to the increased number of vehicle rollover accidents. The National Highway Traffic Safety Administration (NHTSA) has standards for occupant crash protection (FMVSS 208) and roof crush resistance (FMVSS 216) but does not have a standard requirement for rollover propensity or any standard defining how a vehicle moves after entering the rollover phase of an accident. A rating system to statically quantify rollover propensity of light vehicles has been developed, but a dynamic rating system is still in the development stages [5,6].

Many works have been published regarding different aspects of rollover accidents. The Society of Automotive Engineers (SAE) publishes a majority of the scholarly work in the fields of accident reconstruction and occupant protection. The published research is generally provided by automotive experts and industry consultants. The Northwestern University Center for Public Safety is also a major contributor to the accident reconstruction sciences.

The following sections describe previous published research conducted relating to light vehicle roll mechanics that apply to this thesis.

### 1.3.1 Roll Distance vs. Number of Rolls

There are limited data available from crash tests and real world rollover accidents where roll distance and number of rolls are known. Several publications compile these data [7,8,13,16]. Figure 1-2 and shows the relation between roll distance and number of rolls.

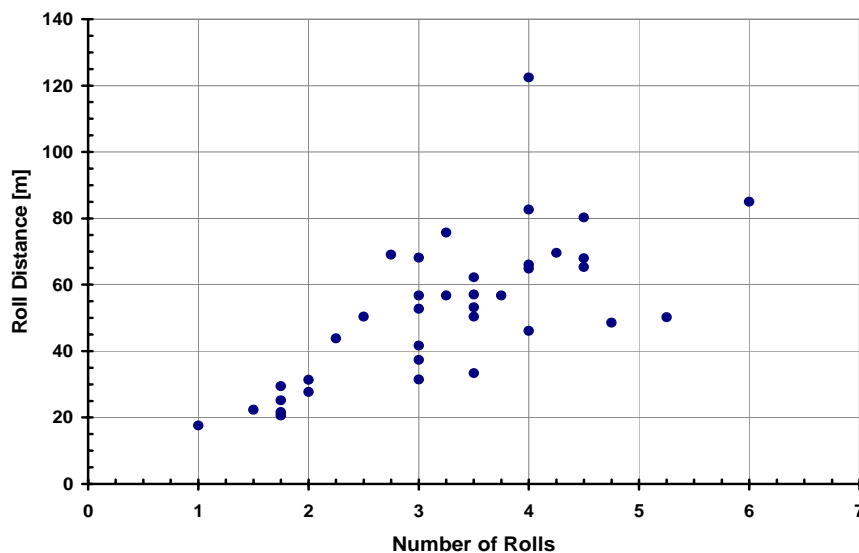


Figure 1-3: Comparison of Roll Distance and Number of Rolls

### **1.3.2 Vehicle Abrasions as a Tool to Understand Vehicle Dynamics**

Several writers have discussed vehicle abrasions as forensic evidence on rollover vehicles [7,8]. Each vehicle revolution in a roll sequence typically produces an independent set of abrasions on the body panels. Therefore, if a vehicle has  $n$  independent abrasion directions then the vehicle went through at least  $n$  roll revolutions [8].

The direction of an abrasion is a function of translational velocity along the roll path, rotational velocity, and vertical velocity. The vehicle orientation along the roll path can be calculated directly if the velocity variables are known [8]. The vehicle yaw angle at certain positions is useful when trying to determine the trajectory of unbelted occupants.

Abrasion sense is also useful. When a vehicle rolls and the roll direction (passenger-side leading or driver-side leading) is not immediately obvious from either tire marks leading up to overturn, or rest position, an understanding of abrasion direction and also the sense of the abrasions is critical. Typically, tangential velocity relative to the center of gravity does not exceed the translational velocity of the center of gravity of a vehicle. If this is assumed to be true, knowing the abrasion sense can readily indicate the roll direction. The perimeter of the vehicle typically has a relative velocity with the ground in the direction of travel. This velocity difference causes abrasions to be made on the body panels opposite the direction of travel.

By examining material flow, abrasion sense can be determined. For example, if a vehicle overturns passenger-side leading, plastic on a body panel, mirror housing, or bumper cover tends to show a flow of material downward on the passenger side,

upward on the driver-side and toward the passenger side on the roof and hood panels. In some situations, careful examination of abraded rubber weather stripping, pinstripes, paint or bare metal also indicates direction and sense as shown in Figure 1-4 and Figure 1-5. Note the shadows of the plastic tailings on the upper side of the bumper cover ridge in Figure 1-4. Vegetation or accumulation of other debris may also aid in this analysis as shown in Figure 1-5 under the plastic antennae mount trim piece.

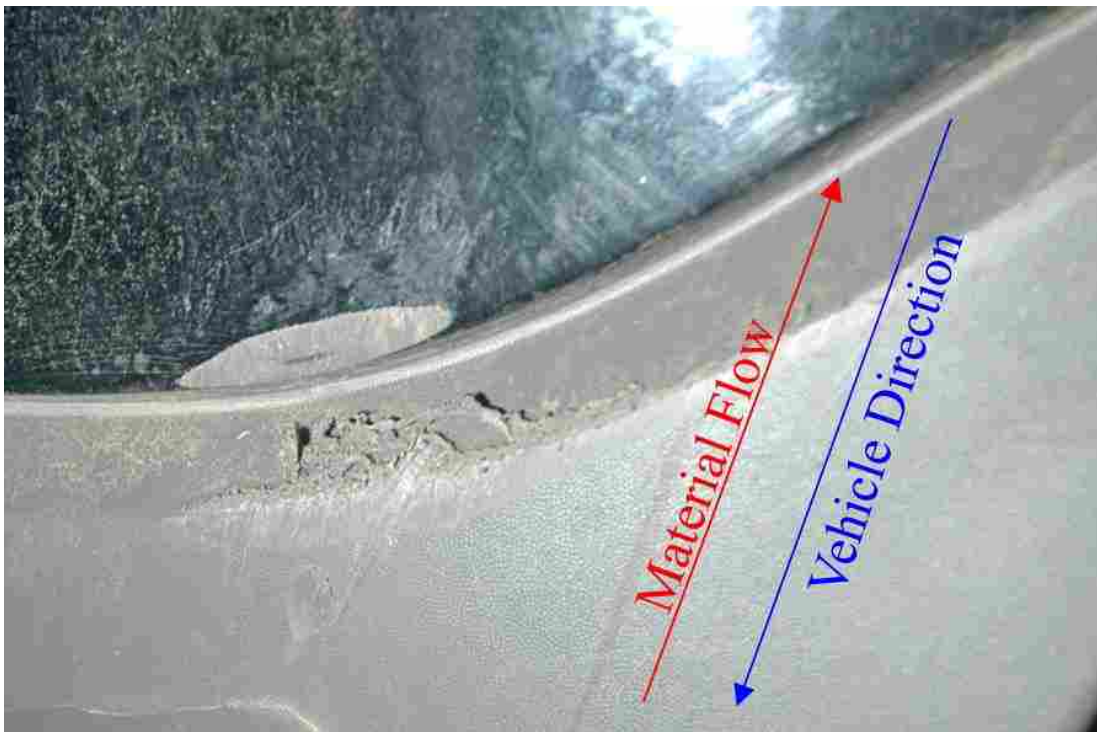


**Figure 1-4: Example of Material Flow**



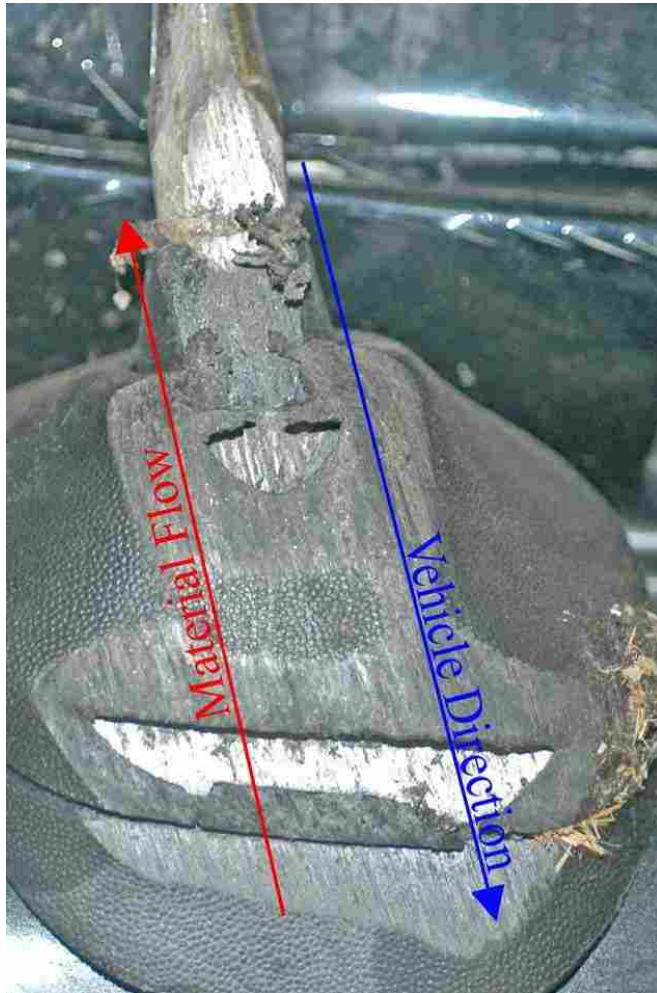


**Figure 1-5: Example of Material Flow and Vegetation Accumulation**

### **1.3.3 Rollover Drag Factors**

Roll sequence deceleration rates have been documented and discussed by numerous researchers as summarized in Table 1-1 [4,9,14,15,17,18]. Documented deceleration rates for the rollover phase range from 0.36 to 0.61 g. This range includes rollovers tests on a variety of roll surfaces including pavement and soft soil. Care should be taken to note whether these decelerations include the deceleration

resulting from the impulse that causes the vehicle to overturn [4]. This impulse should be accounted for in the trip phase and not the rollover phase.

**Table 1-1. Published Drag Factors Based on Combined Trip and Roll [4]**

Paper, Author Roll Surface	Effective Drag Factor	Speed at Start of Trip [kph]	Vehicle
SAE 98022, Cooperrider et al.			
Soil	0.8	37.0	1984 Oldsmobile Cutlass Ciera
Soil	0.8	69.0	1984 Oldsmobile Cutlass Ciera
Soil	0.9	54.2	1981 Dodge Challenger
Soil	0.9	43.5	1979 Datsun B210
SAE 2000-01-1641, Larson et al.			
Soil	0.8	65.5	1991 Jeep Wrangler
Soil	0.8	66.1	1986 Chevrolet S10 Blazer
Pavement	0.7	112.7	1979 Datsun B210

**Table 1-2: Published Drag Factors Based on Roll Only [4]**

Paper, Author Roll Surface	Effective Drag Factor	Speed at Start of Roll (kph)	Vehicle
SAE 2002-01-0694, Carter et al.			
Asphalt	0.44	82.1	1999 Ford E-350
Asphalt	0.46	89.0	1999 Ford E-350
SAE 980022, Cooperider et al.			
Soil	0.48/0.30*	69.0	1984 Oldsmobile cutlass Ciera
SAE 900366, Cooperrider et al.			
Soil	0.48	~48.3	1981 Dodge Challenger
Soil	0.47	~48.3	1979 Datsun B210
SAE 851734, Orlowski et al.			
Pavement	0.43	51.5	1983 Chevrolet Malibu
SAE 890857, Orlowski et al.			
Unknown	Min: 0.36 Avg: 0.42 Max: 0.61	Unknown	41 separate tests based on various sources
*The first number corresponds with the end of trip at $\omega=100$ deg/sec and the second number corresponds with the end of trip for the center of mass positioned over the leading tires.			

## **1.4 Contribution**

The work in this thesis contributes to the areas of rollover mechanics and trajectory mechanics for rollover accident reconstruction. The included work helps to improve the accuracy and substantiates the scientific basis used to determine the dynamics of a rolling vehicle.

This thesis demonstrates that by applying linear motion equations and other engineering principles that rollover accidents on soft surfaces can be accurately reconstructed; and therefore, many questions regarding forces and accelerations experienced by a vehicle and its occupants can be estimated with reasonable accuracy.

Film analysis procedures are developed to obtain data from rollover crash tests that are not otherwise documented. Specifically, elevation of the center of gravity of vehicles is obtained from the video where instrumentation does not explicitly yield this data.

Instantaneous center of gravity elevation data throughout a roll sequence provides the opportunity to calculate descend distances as a vehicle travels from one ground contact to another. This data is used to quantify severity of ground impacts as vehicles interact with the ground throughout a roll sequence.

## **1.5 Approach**

The approach of this research was to apply several years of experience relating to rollover accident reconstruction, old and new reconstruction practices, engineering dynamics equations and crash test data to explain and validate some specific reconstruction theories. Certain practices have become the industry standards for

analysis and some new ideas have not been presented or validated. Given access to data from several off-road rollover crash tests, an explanation of current unpublished practices and a validation of new ideas are made possible.

First, the explanation of the current practice of segment average rollover reconstruction analysis is given, and the theory behind the new ideas of refined roll mechanics analysis is presented. Relevant mathematical theory is discussed. Four staged rollover tests are analyzed to reduce data to critical reconstruction parameters. These parameters are compared to parameters available in published literature. Conclusions are drawn about the relevance and accuracy of the roll mechanics parameters and theory.



## **2 Current Industry Standard Analysis Procedures**

Several undocumented practices have been developed by industry leaders that are very useful in the reconstruction of rollover accidents. Detailed segment average analysis and trajectory analysis are two previously undocumented procedures outlined here.

### **2.1 Segment Average Analysis**

A rolling vehicle is airborne for a certain percentage of the roll sequence and is in contact with the ground for the remaining time. The aerodynamic drag on the vehicle is assumed to be negligible. Using this assumption along with Newton's first law ("a particle will remain in a state of rest or will continue to move with a constant velocity unless an unbalanced external force acts on it" [12]), the motion can be simplified into translational motion along the roll path, translational motion in the direction of gravity, and rotational motion. This simplification implies that the only forces that alter the vehicle motion are those that result from the vehicle-ground impacts.

It is often difficult, in the reconstruction process to accurately determine when the vehicle is in contact with the ground and for how much time. In these cases an overall average deceleration is a good simplification for entire sequence analysis,

yielding a reasonably accurate overturn speed range, and therefore a reasonably accurate range of time for the entire sequence.

### **2.1.1 Segment Length and Angle**

Segment length is defined as the translation distance along the roll path between the location of the center of gravity at the midpoint of one ground impact and the location of the center of gravity at the midpoint of the next ground impact. If the available evidence documents some portion of two sequential ground contacts of the vehicle, estimation of segment length between those two contacts can be reasonably accurate. Since the segment lengths are measured from the center of gravity location at one impact to the center of gravity location of the next impact, the location of the center of gravity relative to the contacting portion of the vehicle is important to know. The roll angle of the vehicle yields this relationship. Determining which part of the vehicle contacted the ground at each location is often necessary and possible using accident site and subject vehicle evidence. This information gives the roll angle.

One method of determining vehicle location and orientation is by using glass fragments from the subject vehicle. Design tolerances and manufacturing processes are such that glass panels in a vehicle often differ by at least 0.025-0.050 mm in thickness. Glass panels often have different shades of tint also. Glass fragments discovered at the accident site at the time of inspection are documented. The measurements and shades of tint of the glass fragments found at the site are compared to the measurements and shades of tint of glass fragments remaining on the vehicle after the accident. This comparison is used to determine the source of the glass

deposits found at the site. For example, if a large deposit of light-tint tempered glass is found at the accident site with a thickness of 3.84 mm and the right front passenger window glass is the only panel on the subject vehicle that fits the same description, then the right front window and/or surrounding structure contacted the ground at that location. On occasion, two or more window panels fit the same description. In these situations, evidence immediately prior to and following the glass deposit is used to determine which window was the source of the deposit.

Other vehicle components often become imbedded in the soil as a result of impacting the ground, especially in off-road rollovers. Entire outside rearview mirror assemblies, headlight or taillight assemblies, or other trim pieces of a vehicle are commonly found driven into the ground as a result of direct impact under the load of a rolling vehicle. Shallow digging is often required to uncover such evidence.

Irregularities in the roll path like sign posts, roadway edges, or dirt berms may cause unique damage patterns on vehicle body panels. Roadway lane lines may also leave paint transfer on a vehicle that may accurately describe the vehicle orientation at a certain position.

When a vehicle rolls on or across an asphalt surface gouges are usually created, that remain until the roadway is either repaved or resurfaced. During the trip phase of the rollover the leading wheel rim flanges often make contact with the road surface and create gouges in the roadway. During the roll phase the lower edge of the outboard rim flanges often leave semi-circular imprints or gouges. These features are often the most definitive evidence in rollovers that occur at least partially on-road.



With the use of this type of data, vehicle impact locations and orientations can often be definitively determined. With distance measurements and estimation of vehicle roll angle, segment average analysis can be performed.

### 2.1.2 Segment Average Velocity and Duration

Knowing the segment length, and having an estimation of the average drag acting through that length, lends to a simple calculation to estimate a change in speed. Working backwards from the end of segment, the translational velocity at the beginning of a segment,  $V$ , is defined as:

$$V = \sqrt{V_0^2 + 2\mu g \Delta x} \quad (2.1)$$

where  $V_0$  is the translational velocity at the end of the segment,  $\mu$  is the average effective drag factor in g's,  $g$  is the acceleration of gravity, and  $\Delta x$  is the segment length (A consolidated list of nomenclature is found in Appendix A). To calculate the speed for the final segment, or to calculate the speed at trip only,  $V_0$  is zero, therefore Equation 2.1 becomes:

$$V = \sqrt{2\mu g \Delta x} \quad (2.2)$$

If the change in roll angle for a segment is known, the segment time can be used to determine the average roll rate for the segment. Using the same variable definitions as in Equation 2.1, the segment time,  $t$ , is defined as:

$$t = \frac{V - V_0}{\mu g} \quad (2.3)$$

Using a range of effective drag factors,  $\mu_{low}$  to  $\mu_{high}$ , rollover sequence calculations are often performed in a spreadsheet, as shown in Table 2-1, with the first velocity calculation performed being the beginning of the last segment, which ends at rest. The spreadsheet is populated using Equations 2.1 and 2.3, reconstructed segment lengths, and other basic equations of linear motion.  $\varpi$  is the overall average roll rate for the entire roll sequence.

**Table 2-1. Example Roll Sequence Spreadsheet**

Roll Position	Dist. [m]	Speed [kph]		Time [sec]		Roll Angle [deg]		Change in Roll Angle [deg]	Roll Rate [deg/sec]	
		Low	High	Low	High	Initial	Final		Low	High
1		80.7	85.4							
	13.31			0.596	0.630	45	425	380	637	603
2		71.3	75.4							
	15.11			0.791	0.837	425	1,305	880	1,112	1052
3		58.7	62.1							
	13.25			0.871	0.920	1,305	2,083	778	894	845
4		44.9	47.5							
	18.68			2.832	2.994	2,083	2,880	797	281	266
5		0.0	0.0							
$\Sigma$	60.35			5.090	5.381			$\varpi$ :	557	527
$\mu_{low}=0.425g, \mu_{high}=0.475g$										

Knowing the magnitude of acceleration at specific points relative to the center of gravity can be instructive in understanding the tendency of occupants to move in certain directions in the vehicle. Average centripetal accelerations,  $a_n$ , for any point on a vehicle can be calculated using:

$$a_n = \frac{V_t^2}{r} \quad (2.4)$$

where  $r$  is the radial distance from the center of rotation to the point where the acceleration value is desired, and  $V_t$  is the tangential velocity at that point.

## 2.2 Trajectory Analysis Based on Segment Average Results

Another unpublished practice, that has not been validated, is to use the segment average results to calculate vehicle trajectories between ground contacts. The practice assumes a ballistic trajectory in which the vehicle is acted upon by acceleration of gravity alone. Once the segment time is estimated the vehicle can be analyzed as a projectile to obtain the vertical velocity of the center of gravity at the end of the segment. Nomenclature for the trajectory Model is shown in Figure 2-1.

The trajectory model predicts the descent height,  $h_d$ , as the vehicle center of gravity follows a parabolic trajectory from the minimum elevation,  $z_i$ , at one ground impact to the minimum elevation,  $z_f$ , at the next ground impact. The descent height is simply the vertical distance between the maximum center of gravity elevation,  $h_{cg,max}$ , and the minimum elevation at the second impact.

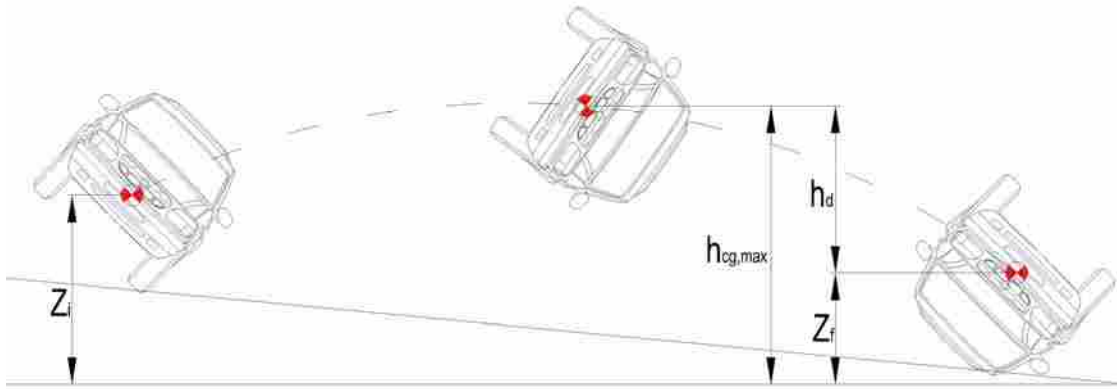


**Figure 2-1: Trajectory Nomenclature**

An example partial reconstruction diagram is shown in Figure 2-2. Each vehicle template is placed using reconstruction evidence. Figure 2-2a is a plan view showing distances between ground contacts. Figure 2-2b is a plan view of the same vehicle positions. Exaggerated lines are drawn in the diagram to show the theoretical trajectory of the center of gravity of the vehicle. Arrows at each plan view template show approximate translational and rotational rotation directions. Table 2-2 summarizes the position, orientation and time related data included in Figure 2-2.

Given the data in Table 2-2, a reconstructionist might accurately determine the height of the center of gravity of the vehicle at the maximum elevation between each ground contact. Knowing the maximum center of gravity height and the minimum height at the subsequent ground contact, a maximum vertical velocity can be calculated for the vehicle center of gravity using Equation 2.1, where  $V_0$  is zero,  $\mu$  is 1, and  $\Delta x$  is the descent height from maximum elevation to minimum elevation at the following ground impact. A trajectory model using initial and final center of gravity elevations and total segment time to calculate descent height is described.

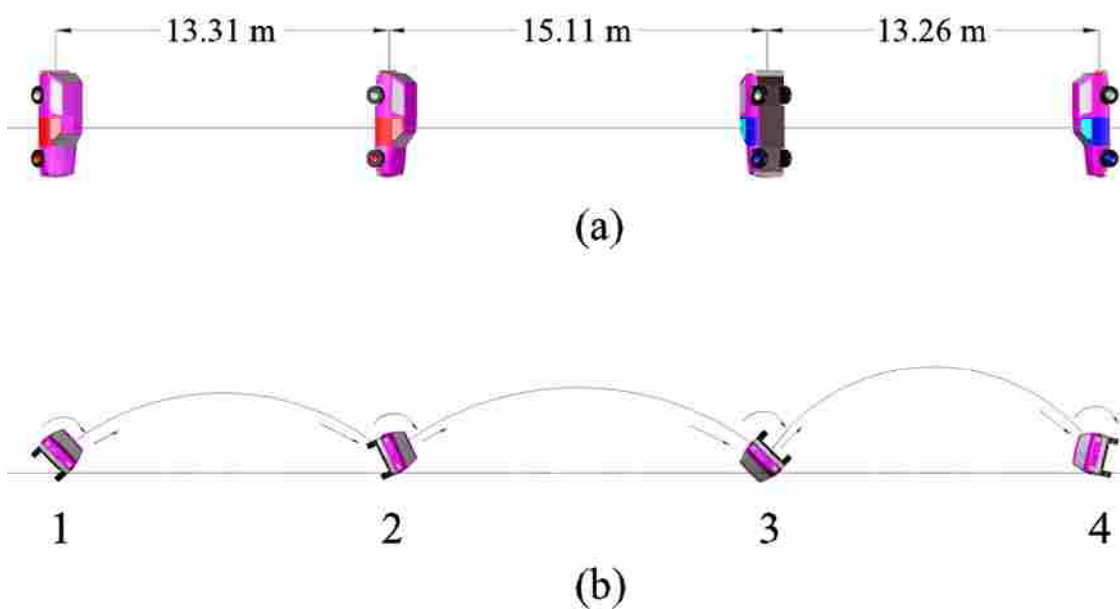


Figure 2-2: Theoretical Trajectory Diagram: a) Plan View; and, b) Elevation View

Table 2-2: Reconstructed Roll Position Data

Vehicle Position	Time $t$ [s]	Coordinate		Roll Angle $\theta$ [deg]
		Horizontal $x$ [m]	Vertical $z$ [m]	
1	0.235	1.83	0.652	45
2	0.890	15.14	0.710	425
3	1.998	30.25	0.707	1305
4	3.374	43.50	0.765	2083

This analysis is useful only when applied to a segment where there are no intermediate ground contacts of sufficient magnitude or duration to significantly alter the trajectory of the center of gravity. A liberal estimate for segment time yields an overestimate form descent distance.

Given that the model assumes parabolic motion between ground impacts, the total segment time,  $t_s$ , is assumed to be comprised of ascend time,  $t_a$ , and descent time,  $t_d$ , only; i.e.,

$$t_s = t_a + t_d \quad (2.5)$$

The travel time measured from the location where the vehicle center of gravity begins an upward motion to the location where the center of gravity reaches maximum elevation is defined as  $t_a$ . The time measured from the location where the center of gravity reaches maximum elevation where vertical velocity equals zero to the point of full engagement with the ground is defined as  $t_d$ . From Newton's equations descent distance,  $h_d$ , for an object with no initial vertical velocity is defined as:

$$h_d = \frac{gt_d^2}{2} \quad (2.6)$$

where  $g$  is the acceleration of gravity. Solving for descent time,  $t_d$ :

$$t_d = \sqrt{\frac{2h_d}{g}} \quad (2.7)$$

Substituting in the total ascent height,  $h_d + (z_f - z_i)$ , for the descent height,  $h_d$ , where

$(z_f - z_i)$  is center of gravity elevation difference between ground impacts, ascent time,  $t_a$ , is defined as:

$$t_a = \sqrt{\frac{2[h_d + (z_f - z_i)]}{g}} \quad (2.8)$$

where  $z_i$  and  $z_f$  are the initial and final cg elevations, respectively, which are a function of roll surface terrain, vehicle geometry and the orientation of the vehicle at each impact. Solving this equation for  $h_d$ , yields:

$$h_d = \frac{t_a^2 g}{2} - (z_f - z_i) \quad (2.9)$$

Substituting this result into Equation 2.7,  $t_d$  becomes:

$$t_d = \sqrt{t_a^2 - \frac{2(z_f - z_i)}{g}} \quad (2.10)$$

which by substituting in Equation 2.5 becomes:

$$t_d = \sqrt{(t_s - t_d)^2 - \frac{2(z_f - z_i)}{g}} \quad (2.11)$$

and by expanding the first term on the right yields:

$$t_d = \sqrt{t_s^2 - 2t_d t_s + t_d^2 - \frac{2(z_f - z_i)}{g}} \quad (2.12)$$

Squaring both sides of the equation, and simplifying, yields:

$$t_d = \frac{t_s}{2} - \frac{z_f - z_i}{gt_s} \quad (2.13)$$

Since descent height, where initial velocity equals zero, can be defined as a function of descent distance, as described in Equation 2.7, descent height is defined as:

$$h_d = \frac{1}{2} g \left( \frac{t_s}{2} - \frac{z_f - z_i}{gt_s} \right)^2 \quad (2.14)$$

Once  $h_d$  is known, vertical ground impact velocity,  $V$ , can be solved:

$$V = \sqrt{2gh_d} \quad (2.15)$$

This analysis simplifies the segment trajectory of a rolling vehicle as free flight motion of a projectile between vehicle positions. During large percentages of each segment the vehicle is in contact with the ground. During the initial portion of the ground contact the vehicle is moving toward the ground as the vehicle structure and



the roll surface are deformed. During the latter portion of each ground contact the vehicle and roll surface restore to a plastically deformed state. The trajectory model neglects these transitions from airborne to full engagement and from full engagement back to airborne by simplifying the impulses as instantaneous.

Figure 2-3 is a generic diagram showing ground contacts labeled with the integers 1, 2, 3, and 4. The sloped lines represent periods of time when the vehicle is in contact with the ground and decelerating. The horizontal lines represent airborne segments when deceleration is essentially zero.

Reconstructed roll positions are chosen based on physical evidence. Generally, evidence is deposited at locations where the subject vehicle is fully engaged with the ground and there are large forces at the contact surfaces of the vehicle. Forces need to be large enough to break vehicle components. These forces occur in the middle portion of each contact, not while the vehicle and ground are only lightly engaged at the transitions from airborne to full contact and full contact back to airborne.

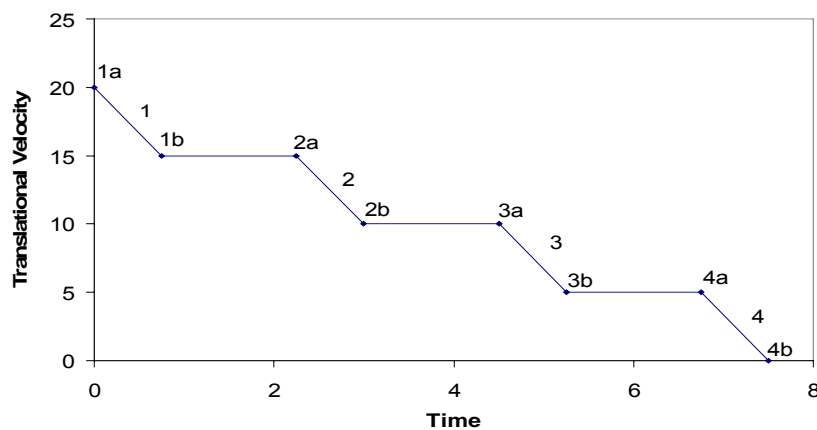


**Figure 2-3: Theoretical Velocity-Time Diagram**

Based on vehicle geometry and the original location of the vehicle components, an experienced reconstructionist can estimate the location and orientation of the vehicle at the point where the center of gravity is at the lowest elevation during the impact.

The analysis comparing the trajectory model with measured data from two extensively documented dolly rollover crash tests is presented later, along with an assessment of the validity of this analysis as a method for estimating vertical ground impact velocity.



### 3 Equations Governing Analysis of a “Rolling” Body

Accurate documentation of vehicle motion throughout a roll sequence requires definition of selected parameters. Kinetic energy is dissipated with every ground contact along the roll sequence. Accounting for losses in energy assists in ground impact severity analysis. Moment of inertia calculations are necessary to complete energy calculations. Calculation of vehicle roll moment of inertia in different rollover situations is addressed. Angular accelerations affect any free mass in a rotating body. Tangential velocity at the perimeter of a vehicle partially defines occupant ejection mechanics. Euler’s equations of motion aid in ground impact torque analysis. These parameters are specifically addressed.

#### 3.1 Kinetic Energy

The kinetic energy,  $T$ , for a rotating and translating body is defined by:

$$T = \frac{1}{2}I_x\omega_x^2 + \frac{1}{2}I_y\omega_y^2 + \frac{1}{2}I_z\omega_z^2 + \frac{1}{2}mV^2 \quad (3.1)$$

where  $I_x$  is the rotational moment of inertia about the roll axis;  $\omega_x$  is the roll rate about the roll axis;  $m$  is the vehicle mass; and,  $V$  is the velocity at the center of gravity.

For a vehicle with only two degrees of freedom, the equation becomes:

$$T = \frac{1}{2} I_x \omega_x^2 + \frac{1}{2} m V^2 \quad (3.2)$$

where  $x$ ,  $y$ , and  $z$ , reference the roll, pitch and yaw axes, respectively. For vehicle motion which has relatively large roll angles and small pitch and yaw angles, Equation 3.2 is sufficient.

### **3.2 Moments of Inertia**

In order to calculate the rotational kinetic energy of a body, the moment of inertia about the axis of rotation must be known. If a vehicle rotates about a principle axis, published data can be used directly. However, a vehicle may rotate about an arbitrary axis which may or may not be parallel to a principal axis of the vehicle. This is an important correction to make especially if the vehicle is in contact with the ground and therefore is not rolling about its center of gravity.

#### **3.2.1 Moment of Inertia about a Parallel Axis**

If the axis of rotation is assumed to be parallel with the roll surface, the parallel axis theorem can be used. The moment of inertia,  $I$ , of a rotating body about an axis parallel to its roll axis but not coaxial is:

$$I = I_x + m d^2 \quad (3.3)$$

where  $m$  is the mass of the vehicle and  $d$  is the distance from the roll axis to the center of rotation. Equation 3.2 is used for ground impacts where there is not sufficient evidence to estimate a pitch angle and when a vehicle is rolling essentially perpendicular to its longitudinal axis.

### 3.2.2 Moment of Inertia about an Arbitrary Axis

For an arbitrary axis  $x'x'$  which passes through the origin of the vehicle coordinate system, the moment of inertia  $I_{x'x'}$  is [10]:

$$I_{x'} = I_x u_x^2 + I_y u_y^2 + I_z u_z^2 - 2I_{xy} u_x u_y - 2I_{yz} u_y u_z - 2I_{zx} u_z u_x \quad (3.4)$$

where  $I_x$ ,  $I_y$ , and  $I_z$ , are moments of inertia about the principal axes,  $I_{xy}$ ,  $I_{xz}$ ,  $I_{yz}$  are products of inertia, and  $u_x$ ,  $u_y$ , and  $u_z$  are the direction cosines of the axis of the rotating body relative to the inertial frame of reference. Equation 3.4 can also be written as [11]:

$$I_{x'} = I_x \cos^2 A + I_y \cos^2 B + I_z \cos^2 C - 2I_{xy} \cos A \cos B - 2I_{yz} \cos B \cos C - 2I_{zx} \cos C \cos A \quad (3.5)$$

where  $A$ ,  $B$ , and  $C$  are the angles of the longitudinal axis,  $x'$ , of the vehicle from the global reference frame axes as shown in Figure 3-1.

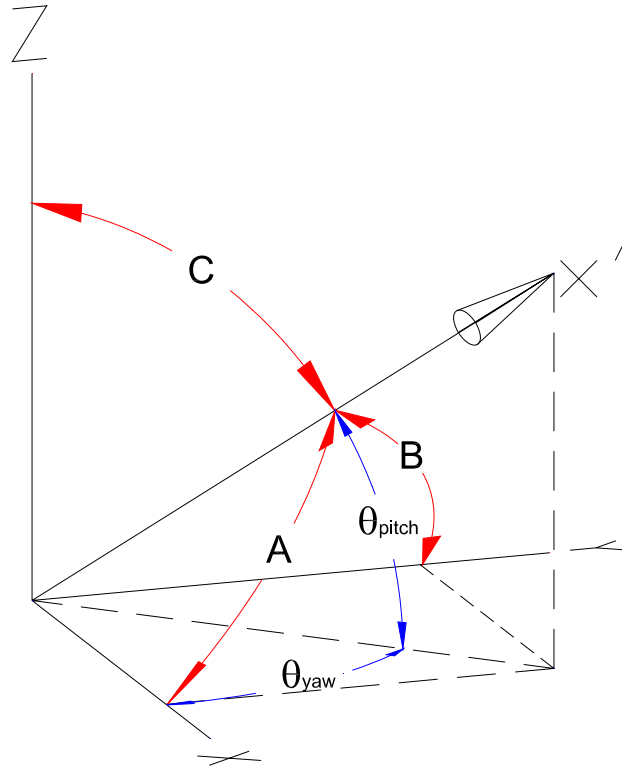


**Figure 3-1: Angles from Arbitrary Axis to Inertial Frame of Reference**

If a vehicle oriented with  $\theta_{pitch}$  degrees of pitch and  $\theta_{yaw}$  degrees of yaw measured from a heading perpendicular to the direction of travel, and  $\theta_{roll}$  degrees of roll, then:

$$A = a \cos(\cos \theta_{pitch} \cos \theta_{yaw}) \quad (3.6)$$

$$B = a \cos(\cos \theta_{pitch} \cos(90 - \theta_{yaw})) \quad (3.7)$$

$$C = 90 - \theta_{pitch} \quad (3.8)$$

Equation 3.5 is used for ground contacts where there is sufficient evidence to estimate the pitch angle and/or yaw angle.

“If either one or both of the orthogonal planes are planes of symmetry for the mass, the product of inertia with respect to these planes will be zero [10].” Since the object is symmetric about the  $xz$  plane, the products of inertia  $I_{xy}$  and  $I_{yz}$  become zero, therefore Equation 3.5 becomes:

$$I_{x'} = I_x \cos^2 A + I_y \cos^2 B + I_z \cos^2 C - 2I_{zx} \cos C \cos A \quad (3.9)$$

Rolling vehicles often tend to have a “football” type bouncing motion where one end may hit hard and then on the subsequent ground impact the other end of the vehicle receives a large impact. In cases such as this, Equation 3.5 is also employed in conjunction with Equation 3.1 to estimate the rotational energy of the vehicle while airborne.

This “football” type motion is also seen when a vehicle repeatedly strikes the same parts of the vehicle over and over again. For instance, a vehicle may strike the left side tires and suspension area and then on the next ground contact strike the right side roof rail, and repeat this cycle until the vehicle comes to rest with the left side roof rail and the right side tires and suspension essentially undamaged while the left suspension and right roof structure are compromised significantly.



### 3.3 Tangential Velocity

As shown in Figure 3-2, unbelted occupants in severe rollover accidents often get ejected from the vehicle and as a result strike the ground and receive serious injuries. Performing trajectory analysis for ejected occupants, requires an understanding of the tangential velocity at certain points around the perimeter of the subject vehicle.



**Figure 3-2: Ejected Occupant in a Dolly Rollover Test**

Tangential velocity of a rotating object is defined by:

$$V_{\text{tan}} = r\omega \quad (3.10)$$

where  $r$  is the distance from the center of rotation to the point of interest on the periphery of the vehicle and  $\omega$  is the roll rate of the vehicle, as shown in Figure 3-3.

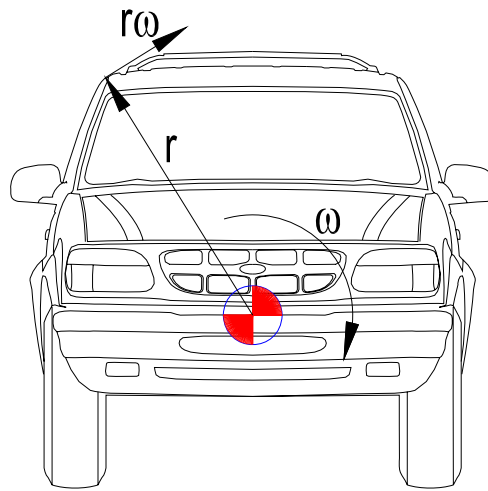


**Figure 3-3: Tangential Velocity Diagram**

Given coordinates for certain periphery locations that define the general shape of a vehicle as shown in Figure 3-4, and given orientation and velocity information, a vector diagram can be constructed that shows the absolute velocities of the periphery (see Figure 3-5).

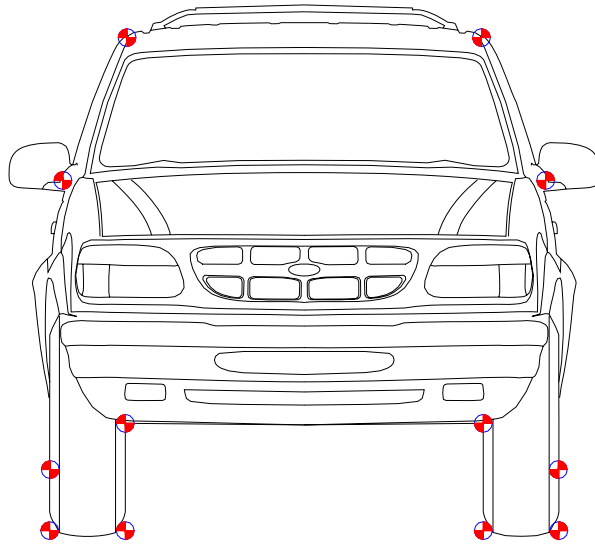


**Figure 3-4: Significant Vehicle Perimeter Points**

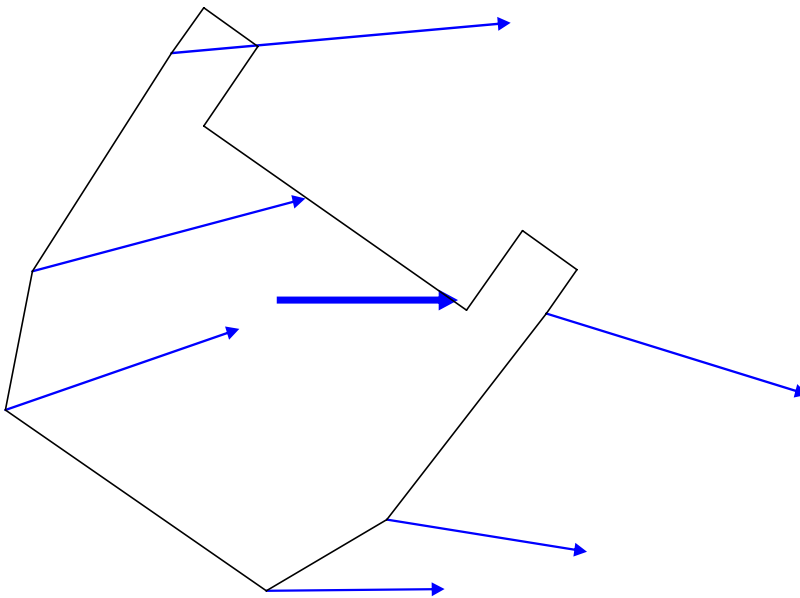


**Figure 3-5: Vector Diagram for Tangential Velocity Computations**

**Table 3-1: Example Tangential Velocity Calculations**

Veh. Periph. (+x →, +y↑)		r (ft.)	$\theta$ (rad)	$\theta$ (deg)		Velocity (ft/sec., +x →, +y↓)			
x (ft.)	y (ft.)					x	y	Mag.	$\theta$ (deg)
2.032	-1.285	2.40	-0.564	-32.3					
2.032	-2.503	3.22	-0.889	-50.9					
2.890	-2.502	3.82	-0.714	-40.9					
2.883	-1.809	3.40	-0.560	-32.1	Leading Rims	75.1	-6.9	75.4	-5.3
2.739	1.472	3.11	0.493	28.2	Leading Belt Line	60.6	-16.2	62.7	-14.9
2.011	3.092	3.69	0.994	57.0	Leading Roof Rail	51.4	-17.9	54.5	-19.2
-2.011	3.092	3.69	2.147	123.0	Trailing Roof Rail	39.4	-0.7	39.4	-1.0
-2.740	1.472	3.11	2.649	151.8	Trailing Belt Line	44.1	7.3	44.7	9.4
-2.883	-1.810	3.40	-2.581	-147.9	Trailing Rims	57.8	17.8	60.4	17.1
-2.890	-2.503	3.82	-2.428	-139.1					
-2.032	-2.503	3.22	-2.253	-129.1					
-2.032	-1.285	2.40	-2.578	-147.7					

Vehicle Coordinates and Velocity Values for Figure 3-5.

### 3.4 Instantaneous Center of Rotation

A vehicle rotates about its center of gravity while airborne, but does not necessarily rotate about a principal axis. However, when there is a torque or other forces applied, while in contact with the ground, rotation is neither about the center of gravity nor about a principal axis.

If an object is rolling on a surface with no slip, the center of rotation is the instantaneous point of contact with the ground as shown in Figure 3-6. This point of impact is defined as the “instant center [10].” If an object rotates and slides along the ground, with a tangential velocity,  $r\omega$ , greater than the translational velocity of the center of gravity,  $V_{cg}$ , then the center of rotation is in between the center of gravity and roll surface as shown in Figure 3-7. If in the same scenario the tangential velocity is less than the translational velocity of the center of gravity, the center of rotation is below the roll surface and outside the perimeter of the vehicle as shown in Figure 3-8. The latter situation is generally true for rollover accidents.

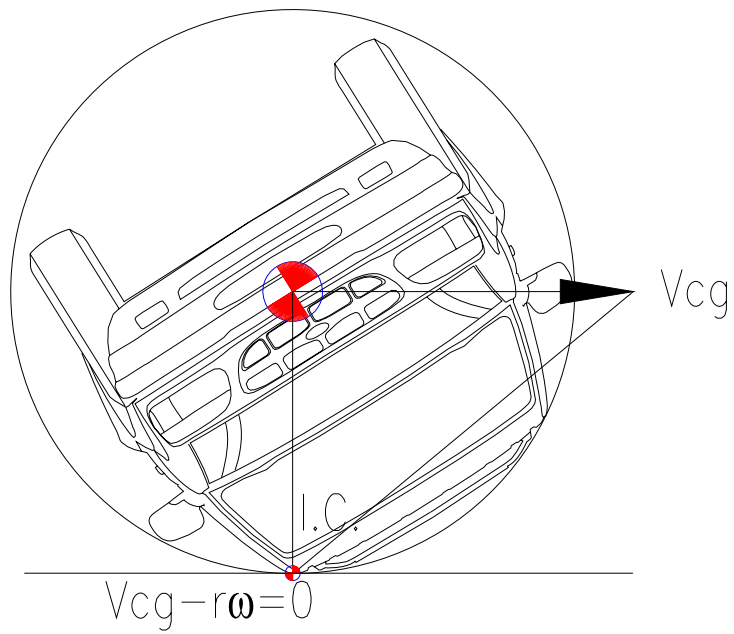


**Figure 3-6: Instant Center — Pure Rolling Motion**

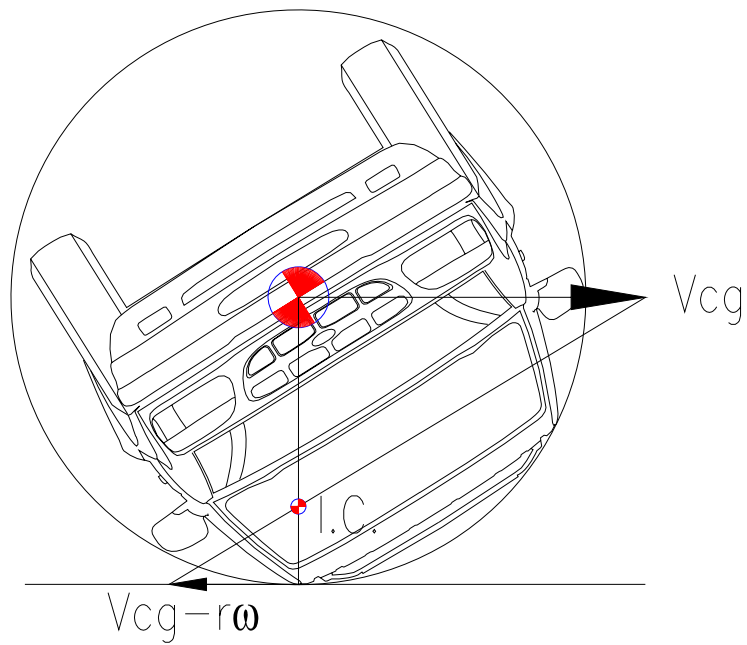


**Figure 3-7: Instant Center — Tangential Velocity > Translational Velocity**

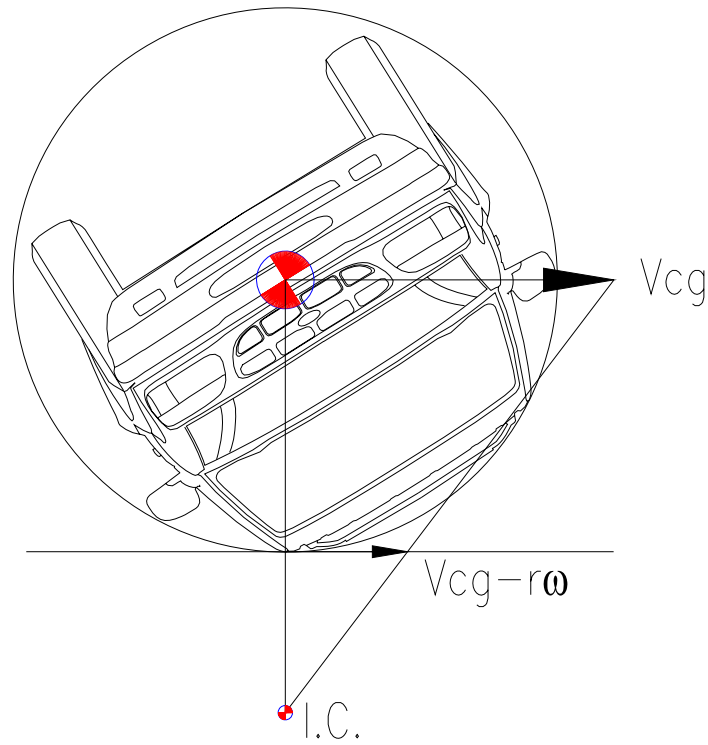


**Figure 3-8: Instant Center—Tangential Velocity < Translational Velocity**

### 3.5 Euler Equations of Motion

If detailed and specific information is known about the vehicle motion, individual ground contacts can be extensively analyzed. If, for instance, a vehicle was in contact with the ground for a known distance and the angle the vehicle traverses can be reasonably estimated, angular and linear decelerations can be calculated using the segment average pre- and post-impact velocities. By applying Euler's equations of motion [10], the moments applied to the vehicle can be calculated:

$$\begin{aligned}
\Sigma M_x &= I_x \dot{\omega}_x - (I_y - I_z) \omega_y \omega_z \\
\Sigma M_y &= I_y \dot{\omega}_y - (I_z - I_x) \omega_z \omega_x \\
\Sigma M_z &= I_z \dot{\omega}_z - (I_x - I_y) \omega_x \omega_y
\end{aligned} \tag{3.11}$$

Torque analysis aids in understanding the forces and directions of those forces that act on the vehicle structure. During vehicle-ground impact, the moment arm where the forces are acting varies drastically. Detailed torque analysis will not be demonstrated.

## **4 Rollover Testing**

There are not many well documented, real world rollover accidents available for study. For this reason staged rollover testing has been standardized for use of scientists to determine the characteristics of rolling vehicles

Four staged rollover tests are analyzed here to show the correlation of certain critical parameters relating to this work. The first three are FMVSS 208 dolly rollover tests. Test four is a steer-induced rollover test.

### **4.1 Description of FMVSS 208 Dolly Rollover Testing**

NHTSA has a standard procedure for dolly rollover tests.

“The vehicle is placed on a device, similar to that illustrated in Figure 4-1, having a platform in the form of a flat, rigid plane at an angle of 23 deg. from the horizontal. At the lower edge of the platform is an unyielding flange, perpendicular to the platform with a height of 4 inches and a length sufficient to hold in place the tires that rest against it. The intersection of the inner face of the flange with the upper face of the platform is 9 inches [22.9 cm] above the rollover surface. No other restraints are used to



hold the vehicle in position during the deceleration of the platform and the departure of the vehicle. With the vehicle on the test platform, the test devices remain as nearly as possible in the posture specified in. Before the deceleration pulse, the platform is moving horizontally and perpendicularly to the longitudinal axis of the vehicle, at a constant speed of 30 mph [48.3 kph] for a sufficient period of time for the vehicle to become motionless relative to the platform. The platform is decelerated from 30 to 0 mph [48.3 to 0 kph] in a distance of not more than 3 feet [0.91 m], without change of direction and without transverse or rotational movement during the deceleration of the platform and the departure of the vehicle. The deceleration rate is at least 20g for a minimum of 0.04 seconds.” [22]

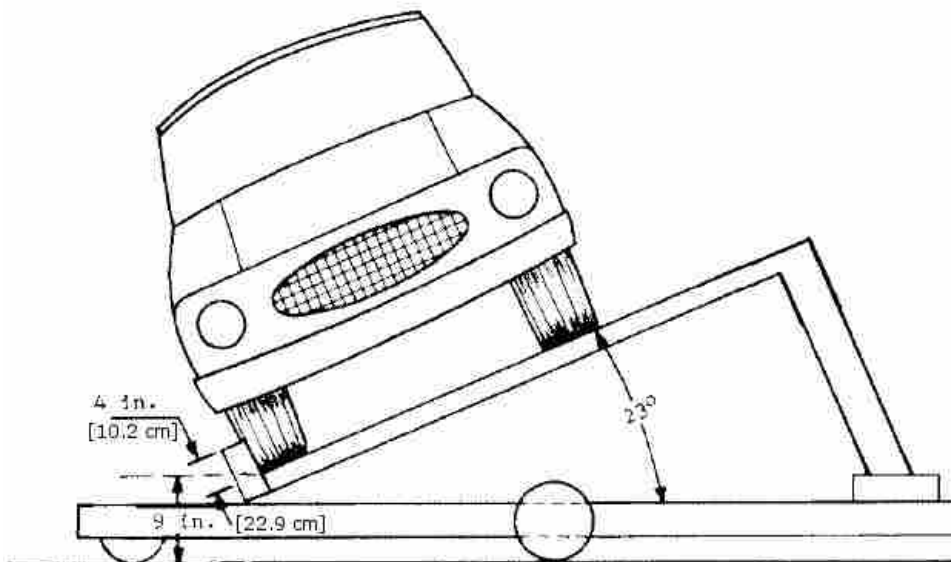


**Figure 4-1: Typical Device for Rollover Tests [Adapted From Reference 22]**

After the vehicle is released from the dolly, all control over vehicle motion ceases and the vehicle travels to rest.

#### **4.2 Description of Analyzed Rollover Tests**

Three dolly rollover tests were analyzed in great detail to determine the validity of mathematical models. All three dolly rollover tests were performed using the standard FMVSS 208 dolly; however the speeds were increased significantly above that of standard FMVSS 208 tests to model real world rollover accidents at higher speeds. Test 4 was a steering-induced rollover test.

Test 1 was a 1989 Chevrolet Blazer with a dolly speed of 89.0 kph [55.3 mph] at release and rolled 62.2 m [204 ft.] in 5.2 seconds; Test 2 was a 1998 Ford Expedition with a dolly speed of 69.5 kph [43.2 mph] at release and rolled 34.4 m [112.9 ft.] in 4.3 seconds; Test 3 was a 2004 Volvo XC90 with a dolly speed of 69.0 kph [42.9 mph] at release and rolled 34 m [111.5 ft.] in 4.3 seconds; and, Test 4 was a 1985 Toyota Pickup with an initial speed of 87 kph [54.1 mph] and roll distance of 79 m [259 ft.] in 6.5 seconds. The available documentation for Test 4 is relatively limited.

The vehicle parameters for the three dolly rollover tests are detailed in Table 4-1 with more detailed descriptions given in Appendix B. The placement and description of Anthropomorphic Test Devices (ATDs) is located in Table 4-2.

**Table 4-1—General Vehicle and Test Information Pertaining to Three Dolly Rollover Tests**

	TEST NUMBER		
	1	2	3
Test Date	1/10/1995	10/19/2005	7/17/2006
Exponent Test No.	PH04668	PH09825	PH10303
Vehicle Year	1989	1998	2004
Vehicle Make	Chevrolet	Ford	Volvo
Vehicle Model	S-10 Blazer	Expedition	XC 90
Packaging	2-dr 4X4	4-dr 4X4	4-dr 4X4
Drive train	4.3L V-6 Auto	5.4L V-8 Auto	2.5L I-5 Auto
Test Weight [N]	18073 (4063 lbf)	29510 (6634 lbf)	22300 (5013 lbf)
Distribution [F/R] %	52/ 48	45/ 55	52/ 48
CG Height [m] †	0.649 (25.56 in)	0.77 (30.32 in)	0.709 (27.93 in)

† CG Height data was obtained from inertial parameters measured by the NHTSA [19]

**Table 4-2 – Placement and Type of ATDs in Dolly Rollover Tests**

	TEST NUMBER		
	1	2	3
Driver	None	H-II 50 M	H-II 50 M
Right Front	None	H-II 50 M	H-II 50 M
2 <sup>nd</sup> Row Left	None	H-II 50 M	H-II 50 M
2 <sup>nd</sup> Row Right	H-III 5 F	H-II 50 M	H-II 50 M
3 <sup>rd</sup> Row Left	N/A	H-II 50 M	N/A
3 <sup>rd</sup> Row Right	N/A	H-II 50 M	N/A

*Only the right rear ATD in Test 1 was restrained*

*H-III 5 F – Hybrid III 5<sup>th</sup> percentile Female ATD*

*H-II 50 M – Hybrid II 50<sup>th</sup> percentile Male ATD*

### 4.3 Data Reduction for Test 1 (1989 Chevrolet Blazer)

The first test was not instrumented and the roll surface, including depressions and debris, was not documented. VHS film was the only available data source. Test 1 was video taped by 10 different cameras from outside the vehicle; 2 real-time, and 8

high-speed. Four of the high-speed cameras were panning and 4 were fixed. The 4 fixed high-speed cameras were used to analyze a majority of the rollover. Because of technology limitations at the time this test was run, exact frame rate of high speed cameras was difficult to specify with certainty. The high speed cameras used to document this test were set to a desired frame rate using an analog dial and the frame rate was approximate. Because of this problem with accuracy, a practice to use a more precise method of determining frame rate was developed. The method resulted in small red flashes appearing at the right side of the camera frame every hundredth of a second. These flashes were then used to assure accurate film analysis. The nominal frame rate was 500 frames per second. Table 4-3 shows actual frame rates for each of the high speed cameras used in the analysis of Test 1.

**Table 4-3: Frame Rate Summary for Test 1**

Camera	Frame Rate [fps]
3	468.14
4	507.92
5	493.96
6	497.67
7	471.90

Once the frame rates were determined a spreadsheet was set up having the first column as time, the next column as frame number for the respective camera view. All four camera views were synchronized to get one continuous record of the roll sequence from the time the vehicle left the dolly until the vehicle left coverage of the four lateral high speed cameras.

The tabular data was produced to a professional animator along with a digital vehicle model and the relevant segments of video. Based on crash test camera documentation, including camera position and focal length, virtual cameras were matched to the real world cameras (see Appendix B). The animator overlaid the digital model of the test vehicle on each video frame. The vehicle was placed at a position and orientation that accurately matched the vehicle in the video as shown in Figure 4-2.

This process allowed the animator to digitally measure the position and orientation of the vehicle in frames selected. Global position and rotation of the vehicle along the roll path at approximately every 0.002 sec. was acquired. The outputs received from the animation process were pitch, roll, and yaw angles, and location along roll path and elevation of the center of gravity, relative to time. The final spreadsheet is included in Appendix F.

The process used by the animator to gather quantitative data in an accurate manner is new to the crash test documentation community. This process allows information to be gathered from video that has previously been strictly qualitative.



(a)



(b)

**Figure 4-2: a) Raw Video Frame, b) Video Frame with Digital Model Overlaid**

#### **4.4 Data Reduction for Test 2 (1998 Ford Expedition)**

Test 2 was extensively documented with video coverage. For Test 2 the roll surface was documented immediately after the crash test, as shown in Figure 4-3. The documentation process included an electronic survey and extensive photographic documentation of all portions of the roll path. The vehicle position and orientation at various contact points along the roll path were unambiguous. These positions were verified by film analysis. Time and position data is presented in Appendix G.

Center of gravity elevation was not explicitly documented. Electronic instrumentation did not capture elevation data. To acquire the center of gravity elevation that would be used in trajectory analysis, five discrete positions were analyzed using the same procedures used to analyze every frame in Test 1.

#### **4.5 Data Reduction for Test 3 (2004 Volvo XC90)**

Test 3 was analyzed in the same manner as Test 2 with the exception that CG elevation data was not obtained by any means. The roll surface was documented immediately after the crash test as shown in Figure 4-4. Video documentation that would yield trusted elevations values was not readily available. Trajectory analysis was not performed for Test 3. The vehicle position and orientation at various contact points along the roll path were unambiguous. These positions were verified by film analysis.

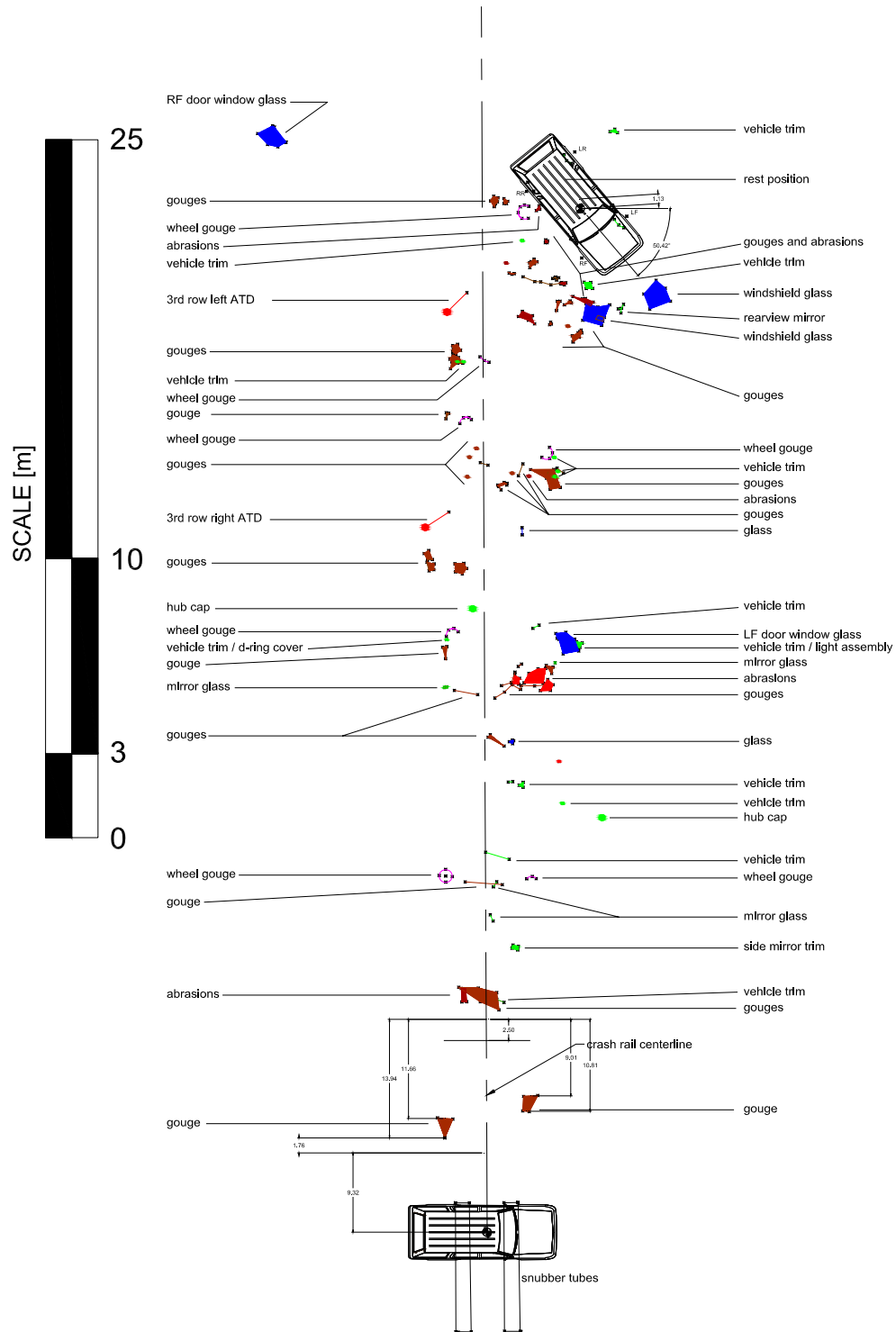


Figure 4-3: Test 2 – Documented Roll Path for Test 2



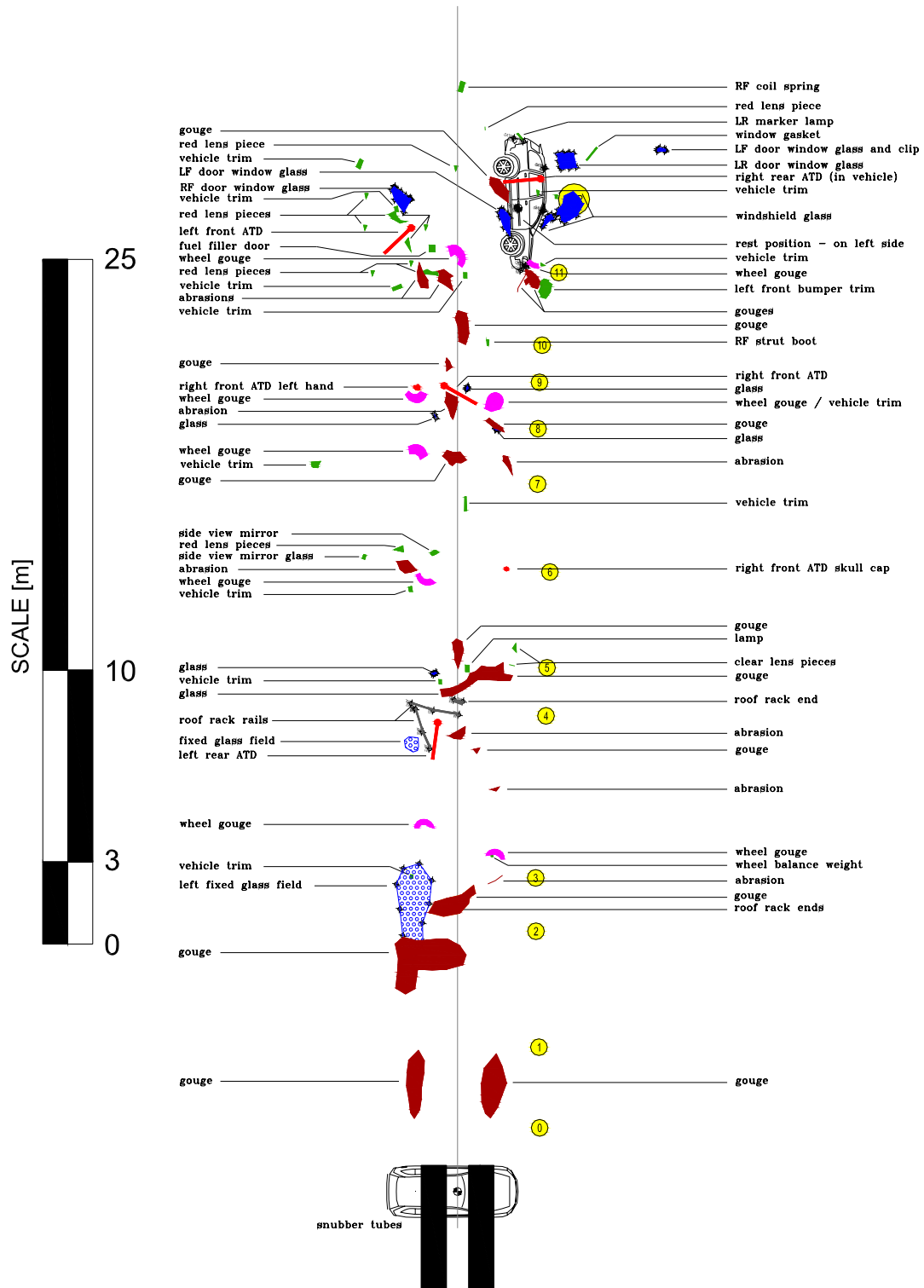


Figure 4-4: Test 3 – Documented Roll Path

#### **4.6 Data Reduction for Test 4 (1985 Toyota Pickup)**

Test 4 is a staged steer-induced rollover of a 1985 four-wheel-drive Toyota Pickup. Only limited access was granted to the data from Test 4, but certain parameters were accessible. Portions of this test were previously published [20]. Steering was input via an automated steering controller. Roll surface documentation, as provided for Tests 2 and 3, were not available. Video was also not available and therefore was not analyzed as with Test 1.



## 5 Roll Mechanics Parameters and Results

This chapter discusses the intricacies involved in getting the test vehicles from the initial conditions to the rest position where all motion ceases. Ground contact ratio, drag factors, roll angle, translational velocity, roll rate and energy are all addressed in detail. Initial conditions for the four rollover tests are summarized in Table 5-1.

**Table 5-1: Initial Conditions of the Rollover Tests**

	TEST NUMBER			
	1	2	3	4
Velocity [kph]	89.0	69.5	69.0	87.0
Kinetic Energy [N-m]	562,997	560,576	417,541	514,165

Table 5-2 summarizes the overall results of the three dolly rollover tests. Test 1 of the Chevrolet Blazer comprised 8 net roll revolutions over approximately 62 m. Figure 5-1 shows a plan view of the roll sequence for Test 1 using selected locations along the vehicle travel path.

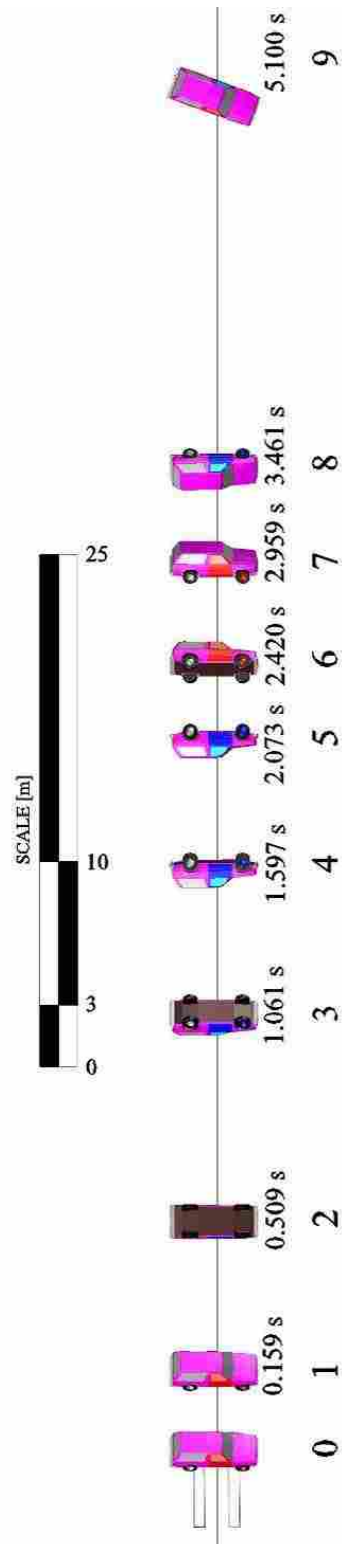
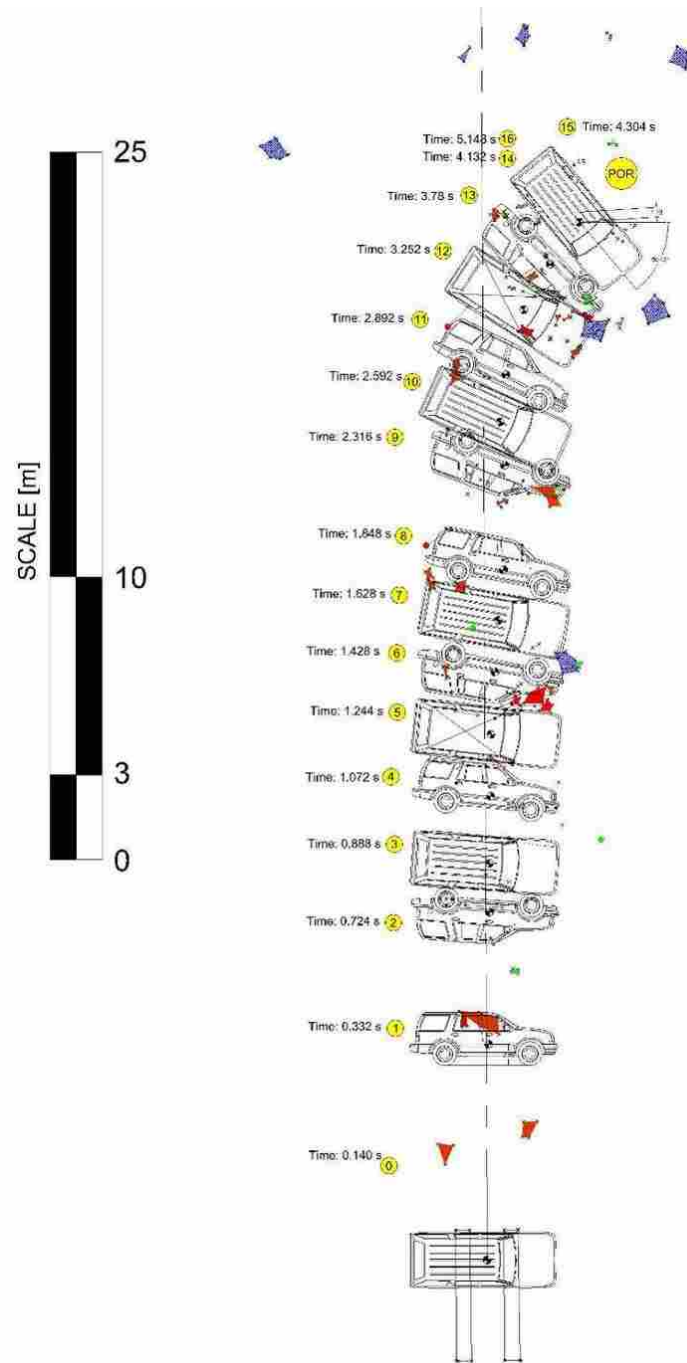


Figure 5-1: Test 1 – Dolly Rollover Sequence

In Test 2, the Expedition rolled four revolutions and came to rest on its wheels after traveling approximately 34.4 m. Figure 5-2 shows the Expedition rollover sequence.



**Figure 5-2: Test 2 – Dolly Rollover Sequence**

The XC90 in Test 3 rolled 4-1/4 revolutions and came to rest on its driver side after traveling approximately 34 m. Figure 5-3 shows the XC90 rollover sequence.

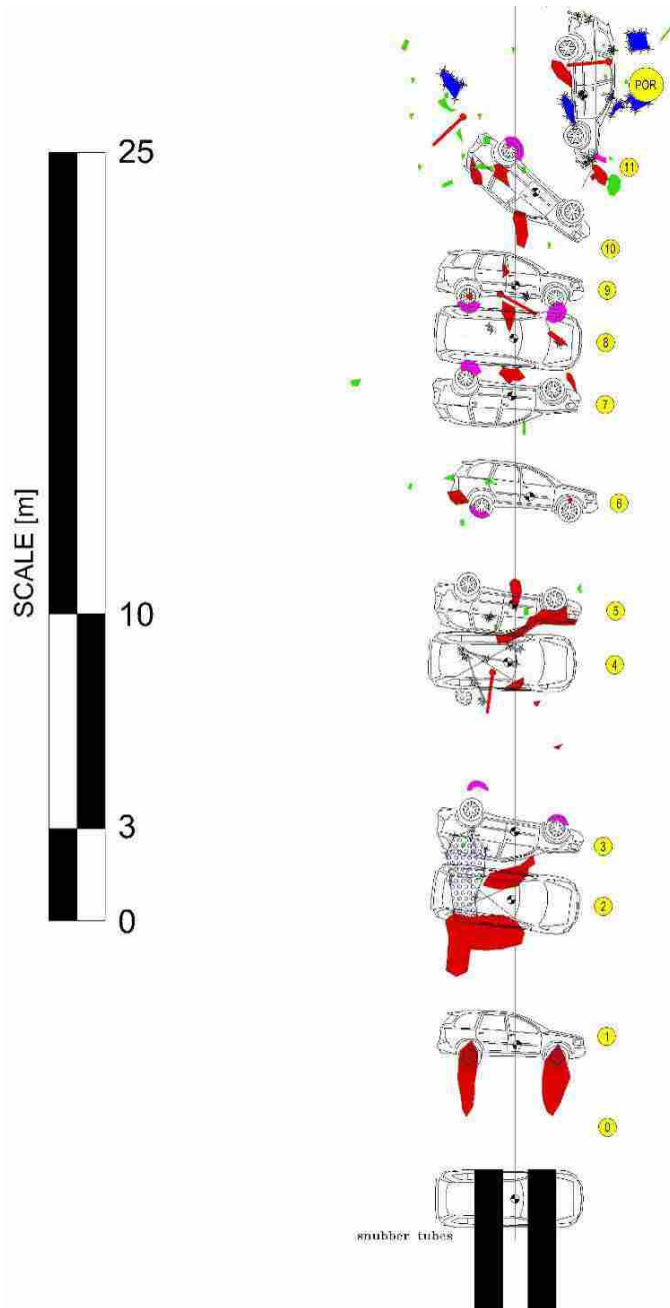


**Figure 5-3: Test 3 – Dolly Rollover Sequence**

**Table 5-2: Summary of Selected Results for the Rollover Tests**

	TEST NUMBER			
	1	2	3	4
Test Date	1/10/1995	10/19/2005	7/17/2006	1/19/2000
Test Weight [N]	18073	29510	22300	17273
Dolly Speed [kph]	89	69.5	69	87
Roll Distance [m]	62.3 †	34.4 †	34 †	79§
Drag Factor [G]	0.50 (0.64‡‡)	0.55	0.55	0.38
$\Delta$ Yaw [deg] ††	~20	50.4	88.3	--
Event Time [sec]	5.04 ‡	4.312 ‡	4.312 ‡	6.51 §§
Ground Contact [sec]	2.90	3.536	2.848	--
Airborne Travel [sec]	2.14	0.596	1.464	--
Number of Rolls	8	4	4.25	7
Peak Roll Rate [deg/s]	918	636	631	636
Mean Roll Rate [deg/s]	549	339	317	378 ¥

† - Roll distance is defined as the distance traveled by the CG along the CG path from the initial touchdown to point-of-rest.

†† - The change in yaw angle is the difference between the yaw angle at launch and the at rest yaw angle. In Test 1 the yaw angle at rest was not documented, so the yaw angle was approximated based on available camera coverage.

‡ - Event time is the total length of time from the initial ground contact following launch to the point where the CG has reached its final at rest position neglecting any additional time for the vehicle to settle.

‡‡ - This is the deceleration over the first approximately 80% of the event where photogrammetry was used to provide precise position and orientation data.

§ - Roll distance is defined as the distance traveled by the CG along the CG path from four wheel lift to point-of-rest.

§§ - Event time is the time duration from four-wheel lift to the point where the CG has reached its final at rest position neglecting any additional time for the vehicle to settle.

¥ - Mean roll rate is based on total roll angle from four-wheel lift to final rest. The roll angle at four-wheel lift was approximately 60 deg.

## 5.1 Ground Contact Ratio

The ground contact ratio is the ratio of ground contact time to airborne time.

This parameter is useful in understanding decelerations throughout a roll sequence. If the overall average drag factor for a specific roll sequence is 0.5g, for example, the actual drag factor while the vehicle is in contact with the ground is much greater. If a



reconstructionist gets specific about a single well-documented ground contact and would like to perform an energy exchange analysis, using an overall average drag factor to compute energy loss would be a mistake.

The test results show that the rolling vehicles are in contact with the ground for far more than half of the total event time. The event time was determined from the center of gravity movement at initial ground contact to the rest location. The event time therefore was generally lower than the time until cessation of vehicle motion at its rest location. The ground contact ratio for Test 1 was approximately 0.58. The ground contact ratio for Test 2 was 0.82, and that for Test 3 was 0.66.

Ground contact durations involving vehicle side body panels and pillars and the roof outer panels and rails, were as short as 0.108 sec. and as long as 0.628 sec. Most of the ground contacts ranged from 0.250 sec. to 0.400 sec. and involved extended contact from one upper side structure to the other upper side structure. The upper body structure contact of longest duration was 0.628 seconds, which occurred during the final rollover revolution.

Durations of tire and wheel contacts ranged from 0.064 sec. to 0.396 sec., with the majority between 0.100 and 0.200 seconds. These contacts varied from light ground abrasions of the tire tread to heavy contacts of the entire tire sidewall and wheel face. The approximate time duration of airborne events ranged from 0.012 sec. to 0.496 sec. These values are specific to these tests. More data may change these ranges appreciably.

## **5.2 Drag Factors**

Effective drag factor for a rolling vehicle is one of the most debated subjects in the field of accident reconstruction. There is a very broad range of effective drag factors that have been documented by different researchers under a myriad of different test conditions. Often the test documentation is sparse enough or inconsistent enough that the actual values for a specific test are even somewhat vague. The drag factors in these tests are more consistently documented, not to mention the fact that the tests were all performed using the same apparatus and had essentially the same roll surfaces. There is good reason for drag factors being one of the most debated topics in rollover accident reconstruction: As the most fundamental parameter, all other calculations are functions of the effective drag factor. Trip speed calculations are highly dependent on the value chosen for drag. Event time is also directly affected. Average roll rates along the roll path are a function of time, and therefore, affected by the drag factor.

The translational drag factors for the test vehicles are calculated over the total roll distances. The drag factors were not constant along the roll path, and tended to decrease with total roll angle. Vehicle decelerations are caused by rolling friction of the vehicle perimeter with the ground, and by mechanical interference of the vehicle with the ground. Early in a roll sequence the tangential velocity of the vehicle perimeter is significantly less than the translational velocity of the center of gravity. This contributes to higher drag factors early in a roll sequence. Near the end of a roll sequence the tangential velocity of the perimeter of the vehicle is nearly equal to that

of the center of gravity, which helps explain lower effective drag factors near the end of roll sequences.

The effective drag factor of a rolling vehicle is a function of the relative velocity of the periphery of the vehicle and the ground during each impact. If the relative velocity is large, more work is performed on the body of the vehicle and the ground than if the relative velocity is small. A torque is applied to the vehicle at every impact where there is a velocity difference as described. Each time a torque is applied there is an exchange of energy and an exchange from translational to rotational velocity or vice-versa. Other factors that influence drag factor are the distance from the center of gravity to the contact portion of the vehicle and the roll moment of inertia.

The drag factor for the detailed study portion of Test 1, determined using Equation 2.1, was approximately 0.64. The detailed study portion comprised approximately 80% of Test 1 based on number of roll revolutions captured on film by fixed lateral high speed cameras. The drag factor for the entire rollover event in Test 1 was 0.50g. The drag factor for the entire events in Tests 2 and 3 was 0.55g.

### **5.3 Roll Angle**

Often one of the first questions asked of a reconstructionist is: “How many roll revolutions did the subject vehicle experience as a result of the rollover?” Occupants in a rolling vehicle have a certain number of occasions to get injured or to get ejected while the vehicle is tumbling to rest. This number of occasions is usually directly proportional to the number of revolutions the vehicle goes through. For instance,

knowing that an occupant exited the vehicle through an adjacent window and came to rest beyond the rest position of the vehicle, indicates that the occupant exited on the high side of the vehicle at some time when the window was not against the ground. If the vehicle rolled a total of 1080 deg. (3 revolutions) then the occupant had a maximum of three opportunities to exit the vehicle, assuming the window was rolled down to start with and didn't have to be fractured by a ground impact first.

Roll angle vs. distance for Tests 1, 2, and 3 is graphed in Figure 5-4. After the first 10-15 meters in all three dolly rollover tests, the relationship between roll angle and distance is essentially linear. For Test 1 the vehicle travels approximately 6.25 meters for every roll revolution and for Tests 2 and 3 the vehicles travel approximately 8 meters for every roll revolution.

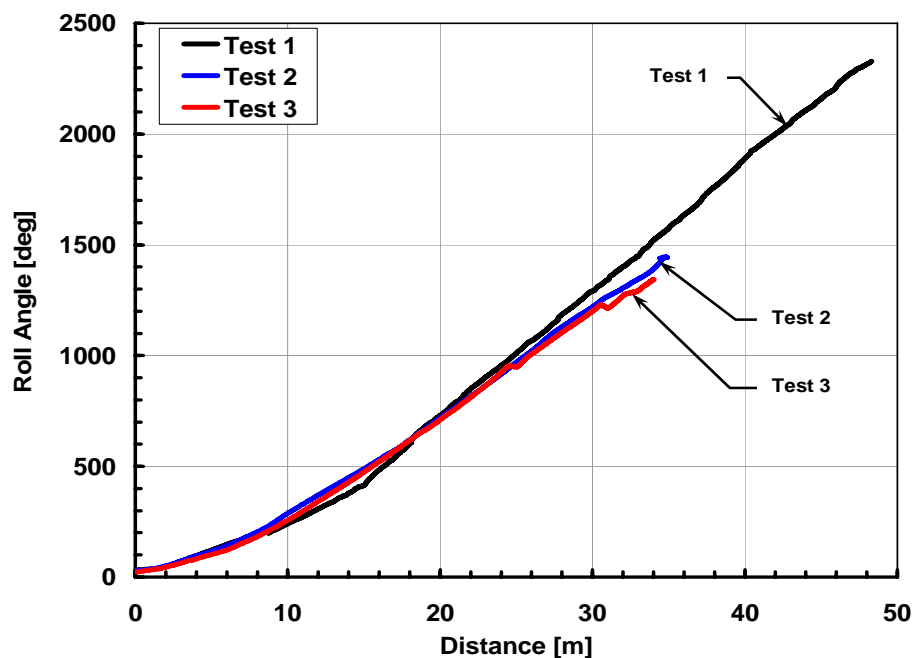


Figure 5-4: Test 1 – Combined Roll Angle vs. Distance for Tests 1, 2, & 3

Another reason to quantify the number of roll revolutions is to classify the accident by severity. Rollover accidents that involve more revolutions are rarer than those that barely tip over and are, therefore not as easily anticipated by vehicle manufacturers in the design process.

#### **5.4 Translational Velocity**

Since a large percentage of vehicle accidents have excessive speed as a contributing factor, another common goal of accident reconstruction is to determine vehicle speeds throughout the accident sequence. Since the timing and location of events throughout the analyzed rollover tests were accurately known, average velocities could be calculated for segments between discrete positions. The translational velocity of each vehicle while airborne did not change appreciably from beginning to end. Once the airborne segments were identified, velocities along the roll path could be determined from previously calculated average segment velocities. Such analysis is highly dependent upon careful examination of the high-speed camera coverage, and the times chosen for each vehicle position.

Figures 5-5 through 5-7, which contain the translational velocity histories for the three tests, show that vehicle deceleration is non-linear with distance along the rollover path. The deceleration appears to be considerably more complex than the widely utilized constant deceleration model given in Equation 2.1. The figures show that constant deceleration predictions can reasonably be made, but suggest that rolling vehicle speed may be more accurately estimated with a non-linear model.

Figure 5-5 demonstrates that if 0.64g is used for the entire sequence beginning at trip, the vehicle doesn't get to rest. If the previously published average of 0.43 g is used, calculating backwards from rest, the trip speed is grossly underestimated.

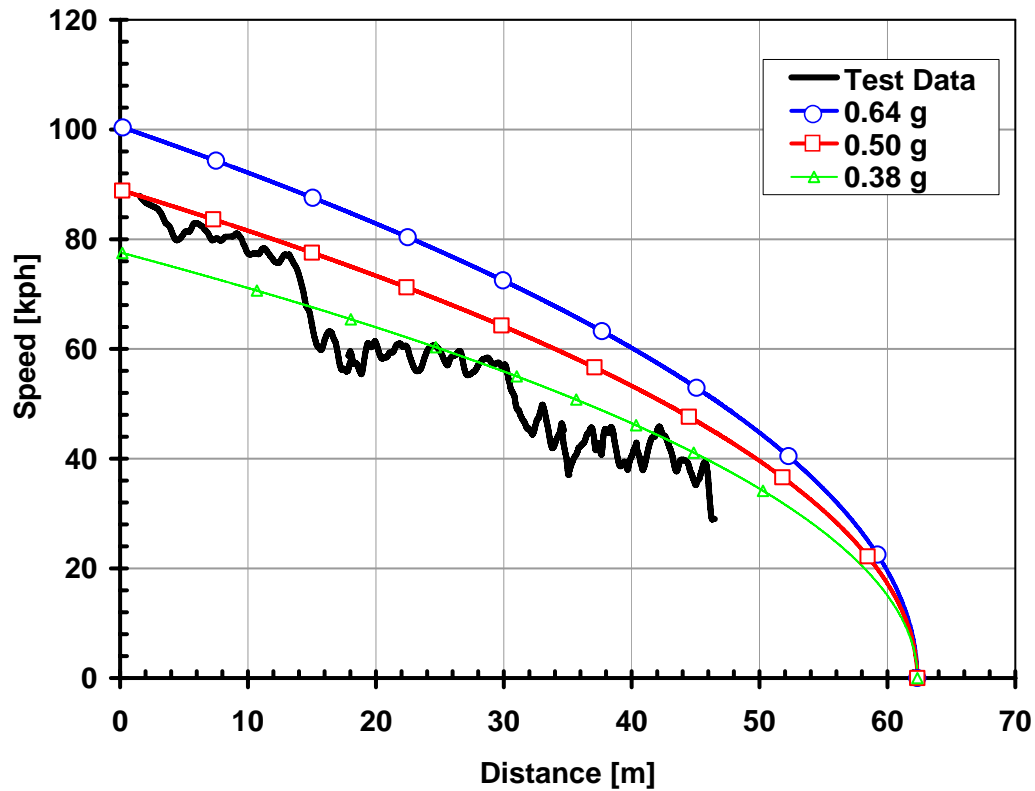


**Figure 5-5: Test 1—Translational Speed vs. Distance Compared With Computed Translational Speed**

Figure 5-6 and Figure 5-7 show similar results. Using any value less than the actual drag factor underestimates trip speed. The shape differences of the test data graphs between Test 1, and Tests 2 and 3 is a result of the differing data reduction methods. Similar general trends are, however, apparent in the graphs of all three dolly rollover tests.

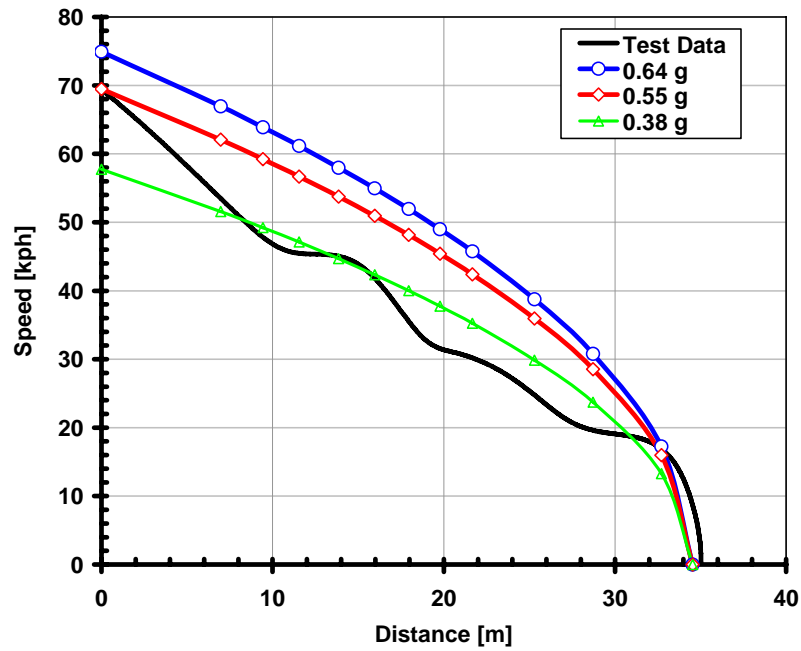


Figure 5-6: Test 2—Translational Speed vs. Distance Compared With Computed Translational Speed

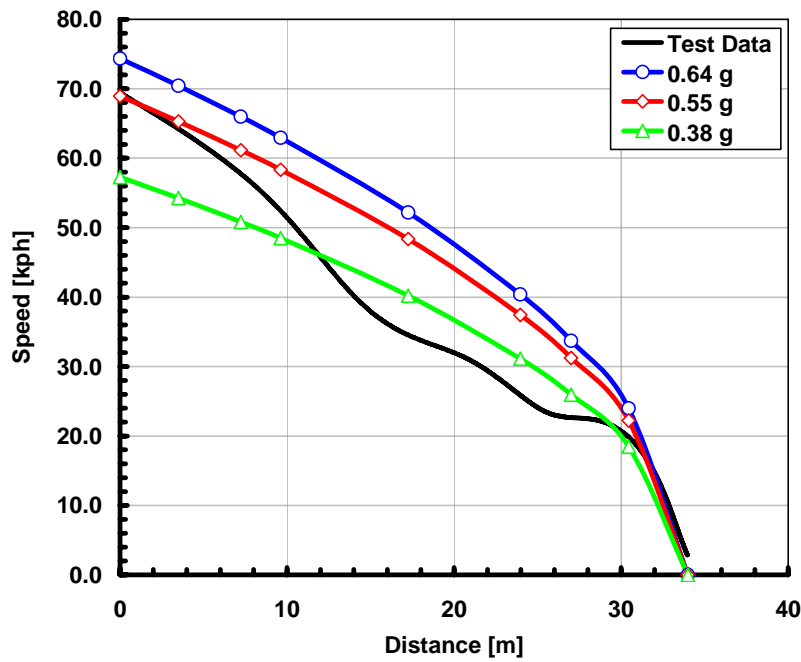


Figure 5-7: Test 3—Translational Speed vs. Distance Compared With Computed Translational Speed

## **5.5 Roll Rate**

Just as children are accelerated to the periphery of a spinning merry-go-round by centrifugal accelerations, occupants are accelerated toward the roof rails of a rolling vehicle during a violent rollover. Objects near the center of rotation are less affected by this phenomenon. Vehicle occupants commonly experience forces toward the periphery of the vehicle equivalent to several times their weight. These forces are the cause of many unbelted occupants becoming fully or partially ejected from their vehicles. Because of this, vehicle roll rate is a topic of interest for accident reconstructionists.

Test vehicle roll rate histories are depicted in Figure 5-8. Tests 2 and 3 exhibited peak roll rates approaching twice their respective averages; the peak roll rate for Test 1 was approximately 67% higher than the average of 549 deg/sec.

The angular velocity trends in the dolly tests show significant roll accelerations early in the sequences followed by decelerations throughout the remaining portion of the sequence.

Figures 5-11 through 5-13 show the same roll rate vs. time graphs overlaid with computed roll rates. In every case the computed roll rates based on the actual drag factors overestimate roll rates early in the roll sequence and underestimated the instantaneous roll rates in the latter part of the sequence. Test 1 overestimated roll rate by approximately 27%; Tests 2 and 3 by approximately 15%.



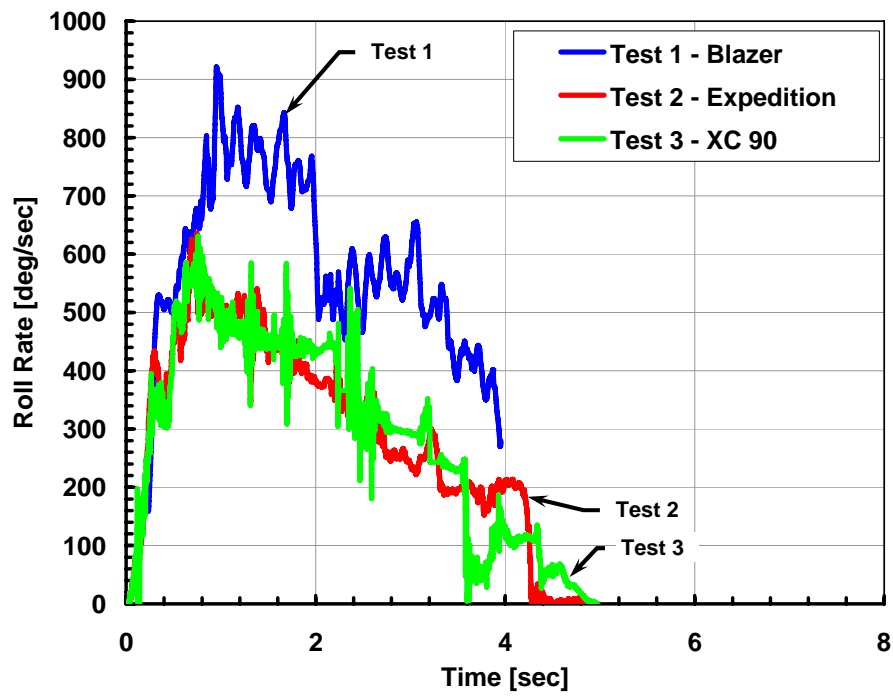


Figure 5-8: Test 1 — Roll Rate vs. Distance

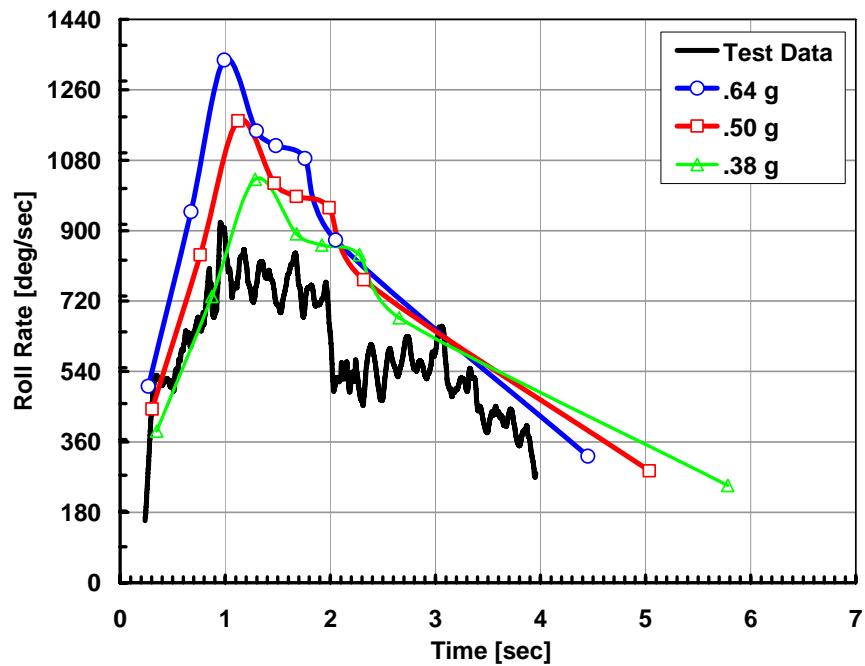


Figure 5-9: Test 1 — Roll Rate vs. Time Compared With Computed Roll Rate.

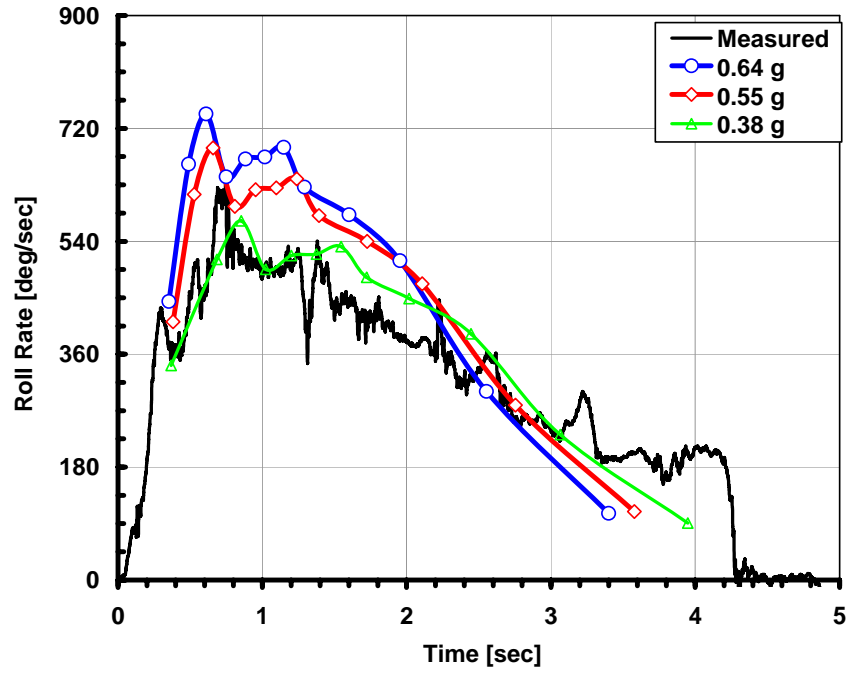


Figure 5-10: Test 2 — Roll Rate vs. Time Compared With Computed Roll Rates

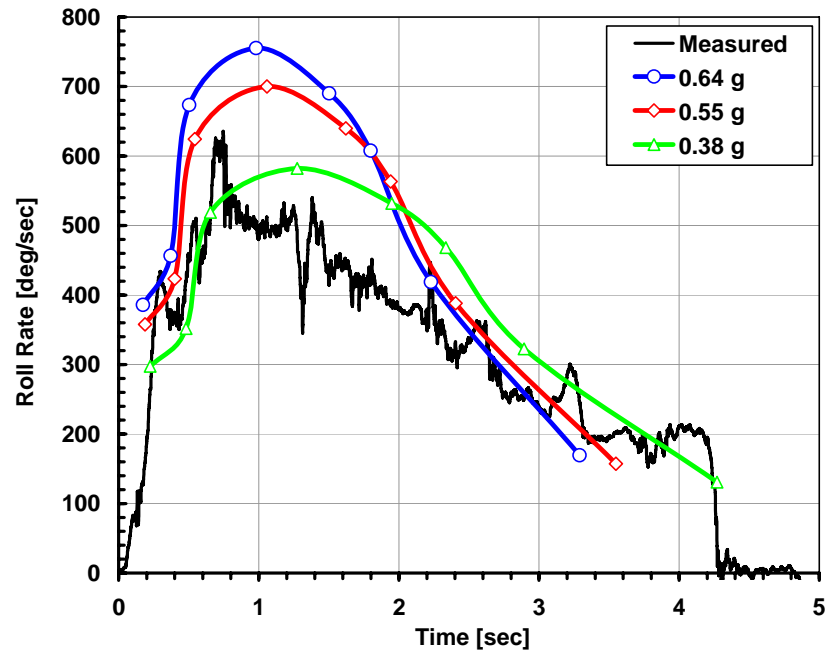


Figure 5-11: Test 3 — Roll Rate vs. Time Compared With Computed Roll Rates

Figure 5-12 compares the results of Tests 1, 2 and 3 with a rollover test in which the vehicle was tripped by remote steering. The similarity of the magnitude and general trend of the roll angular velocity suggests that the initiation mechanism of a vehicle rollover on relatively flat ground is not strongly coupled to certain aspects of rollover mechanics, such as roll accelerations and roll rates. The trend of steep angular acceleration early in a roll sequence is apparent for all four tests. The steepest portion for the steer-induced test appears to be slightly less steep than the steepest portions of the three dolly rollover tests.

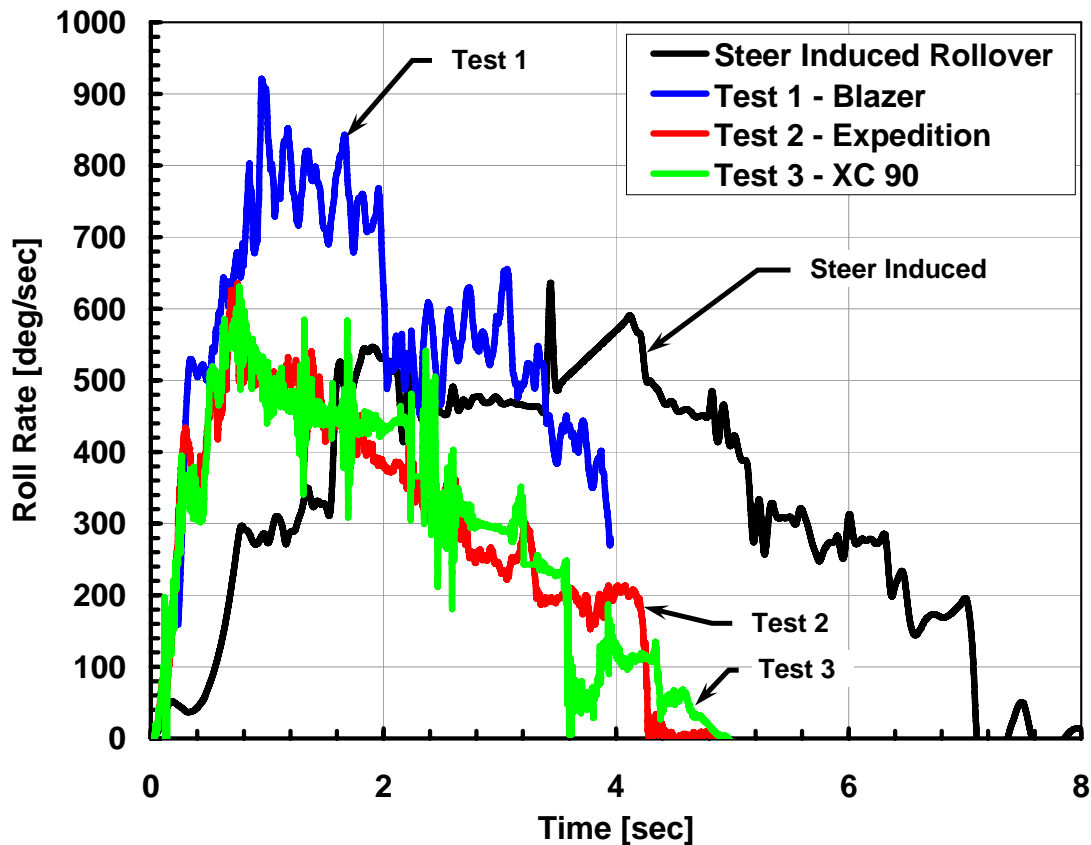


Figure 5-12: Roll Rate Comparison of Remote-Steered Rollover Test and Tests 1, 2 & 3

## 5.6 Energy

The description of energy conversion along a roll path is a useful reality check. If, in an analysis, at any instant in time the vehicle energy has increased from any previous instant in time we know that the analysis is flawed. After a vehicle leaves the rollover dolly, no energy is input into system. Energy is converted from one form to another but neither created nor destroyed. Since dolly rollover accidents constitute closed systems there is no increase in energy. A majority of the energy of the vehicle as it leaves the dolly is converted into plastic deformation of the vehicle structure and components, and disturbance of the roll surface.

Energy computations according to Equation 3.1 were performed and their temporal and spatial histories are shown in Figures 5-13—5-18. Translational and rotational kinetic energy, and potential energy are included for Test 1; only kinetic energy terms are included for Tests 2 and 3. Test 1 indicates that accounting for potential energy is superfluous. The potential energy is a negligible percentage of the total energy. The maximum rotational kinetic energy is a relatively small fraction of initial kinetic energy (~10%) but can be a much larger fraction of total energy later in the sequence, and the potential energy is generally much less than rotational kinetic energy.

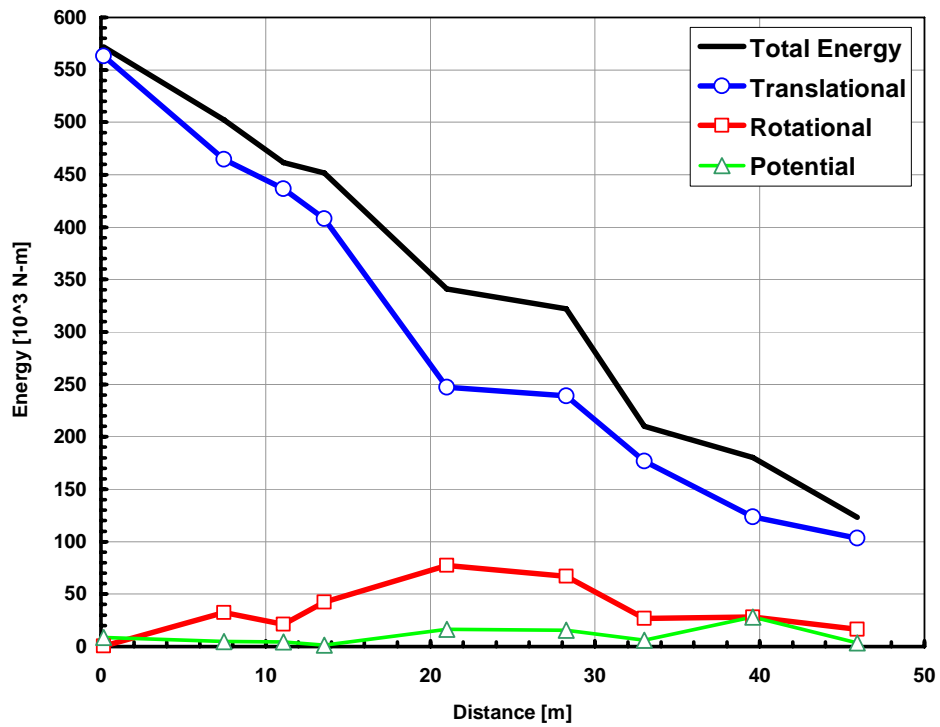


Figure 5-13: Test 1 — Translational, Rotational and Potential Energy vs. Distance

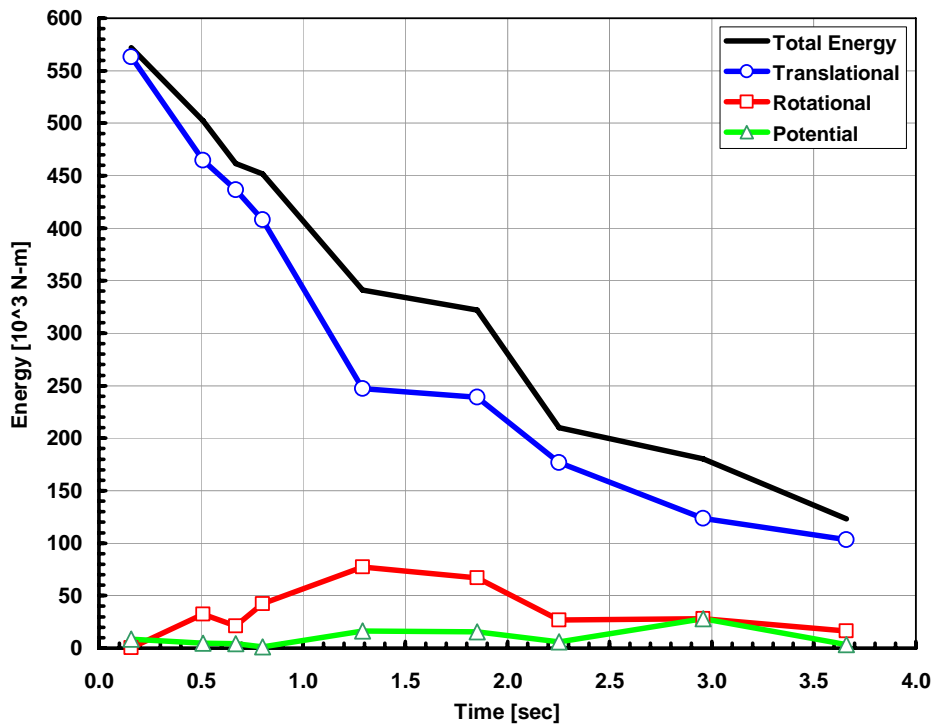


Figure 5-14: Test 1 — Translational, Rotational and Potential Energy vs. Time

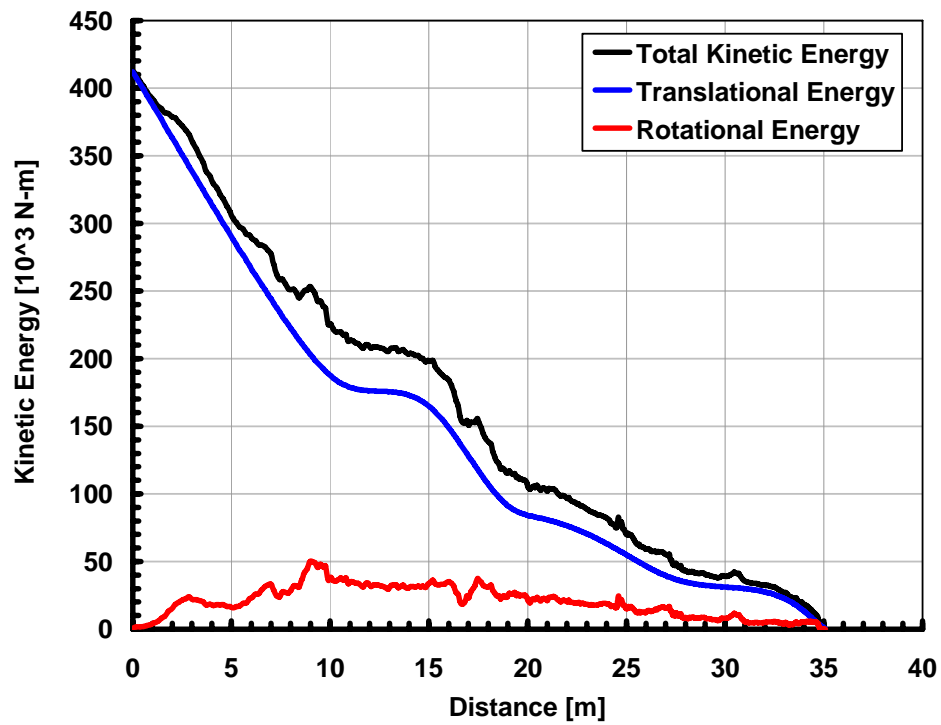


Figure 5-15: Test 2 — Translational, Energy Rotational and Total vs. Distance

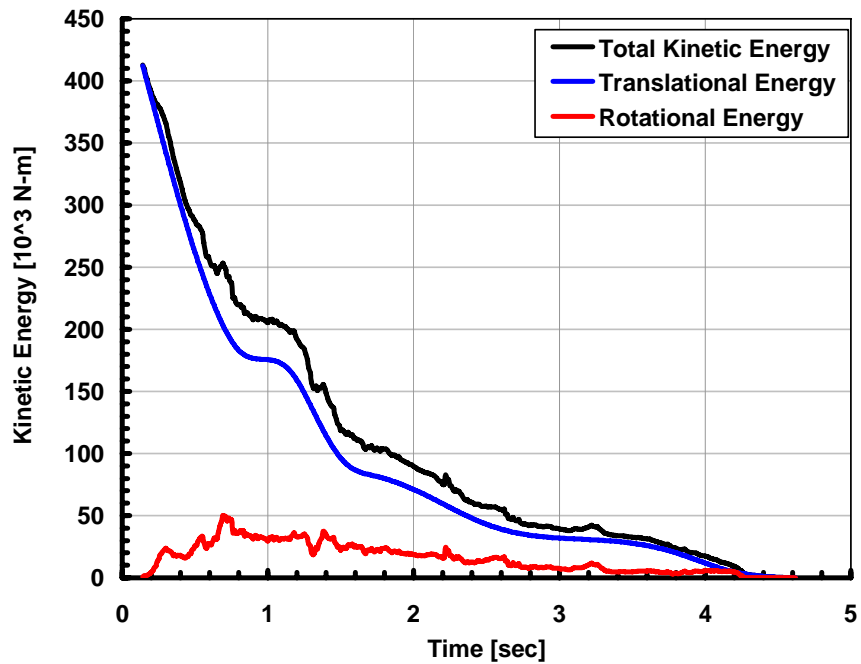


Figure 5-16: Test 2 — Translational, Rotational and Total Energy vs. Time

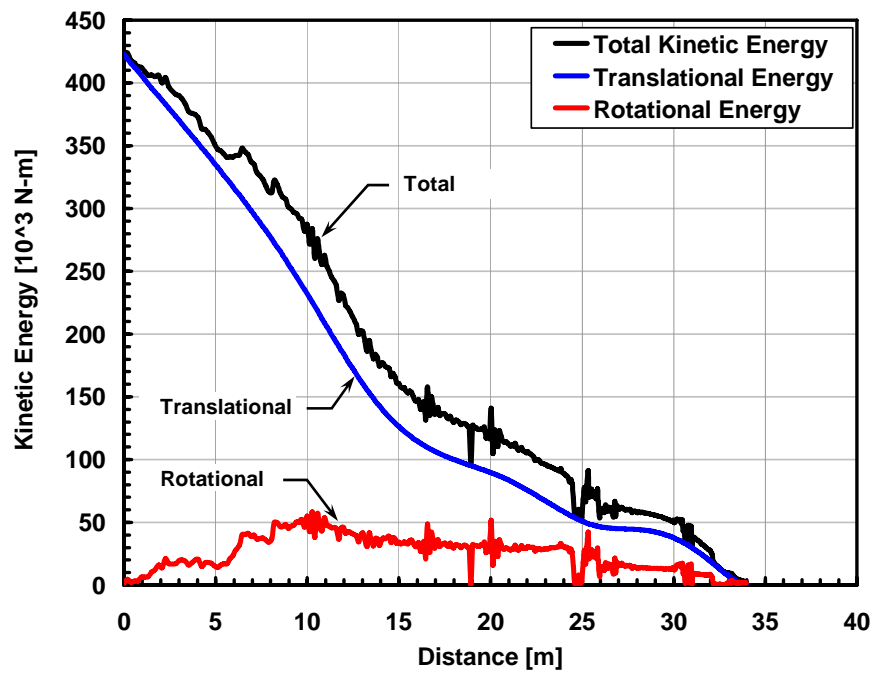


Figure 5-17: Test 3 — Translational, Rotational and Total Energy vs. Distance

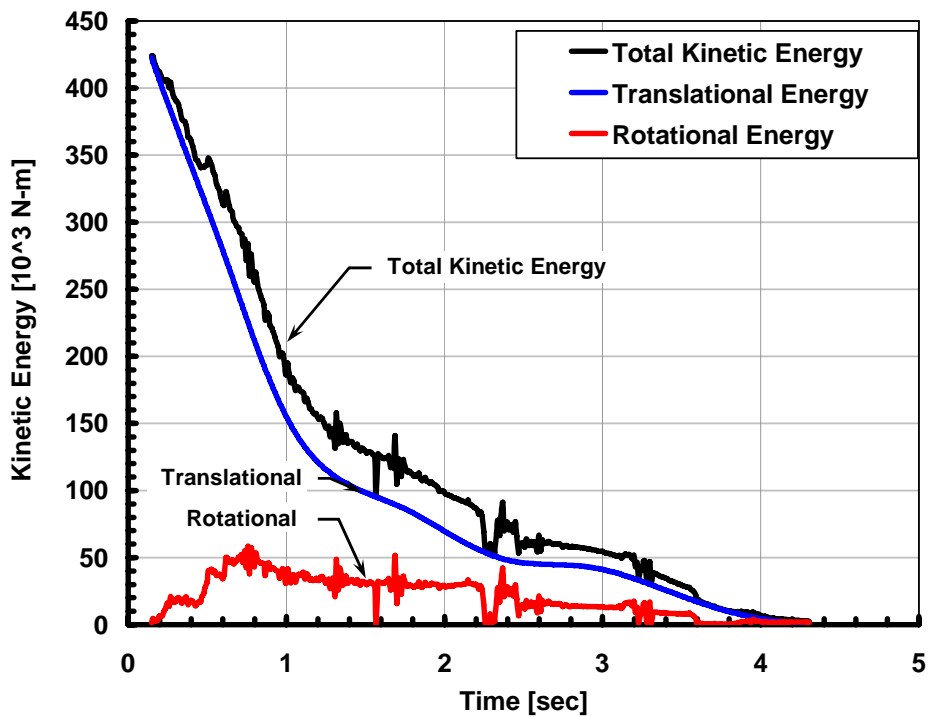
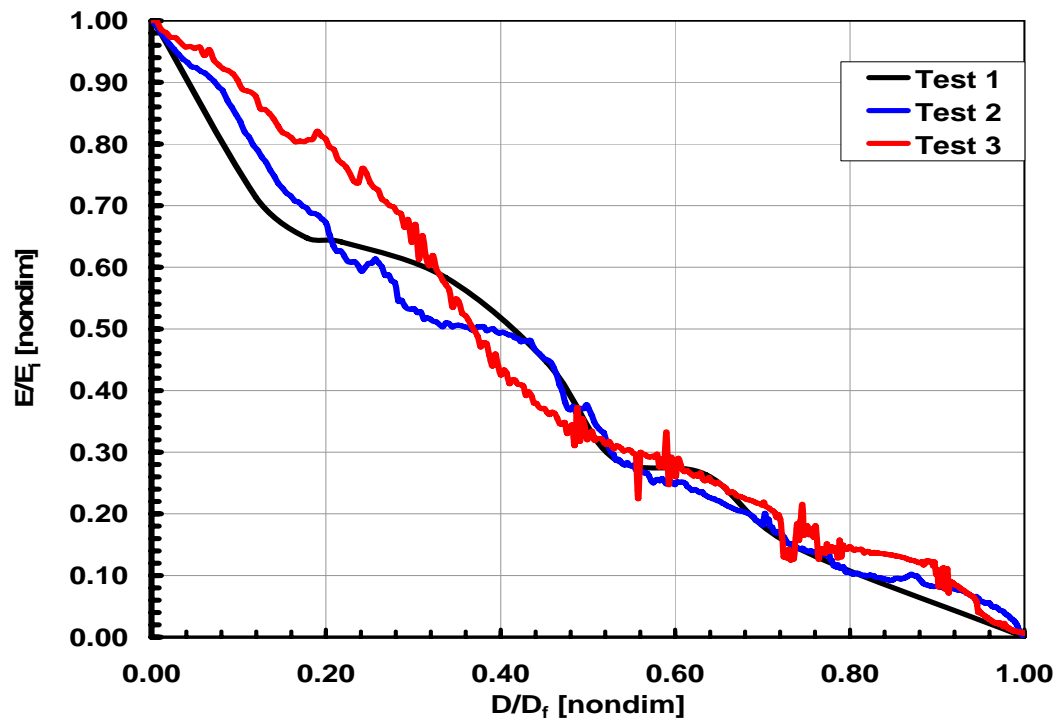


Figure 5-18: Test 3 — Translational, Rotational and Total Energy vs. Time

Combined plots of roll angle and rollover energy correlated with rollover distance are shown in Appendix C and Figure 5-19. The similarity and characteristics of the trend in roll angle for all three tests is indicative of the non-linear behavior of a rolling vehicle and an underlying fundamental relationship that may be generally applicable. The non-dimensional presentation of the energy in Figure 5-19 also reveals a similarity in dissipation mechanisms for rollovers with significantly different initial conditions and total energy. Additional combined correlations of roll angle, speed and energy with time and distance are shown in Appendix C.



**Figure 5-19: Non-Dimensional Correlation of Combined Rollover Energy for Tests 1, 2, and 3**





## **6 Trajectory Analysis and Results**

In rollover accidents where extensive roof pillar or panel deformation occurs, there is often a desire to know the magnitude of the impact forces that acted on the roof structure. The elevation of the center of gravity of a vehicle changes as it travels from one ground impact to the next significant ground contact. The simplified assumption employed in this research in the trajectory model is that the vehicle CG follows a parabolic trajectory between vehicle-ground impacts. The ground contact forces during the roll sequence are a function of the descent distance, terrain irregularities, ground frictional forces, translational velocity, and tangential velocity at the periphery of the vehicle. Often the descent distance is the most influential parameter in characterizing ground contact severity. If descent distance can be determined, then the vertical ground contact velocity can be estimated. In this study, the trajectory model is evaluated using five trajectories from two rollover crash tests to determine its validity.

A useful approach to rollover reconstruction involves a scale diagram with scale vehicle models along the roll path at positions where physical evidence suggests that the vehicle was in contact with the ground. For example, if the right front window of the vehicle is deposited at a location on the ground and that location is documented, both the roll angle and location of the vehicle can be represented by a

scale model placed on the diagram. A reconstruction diagram comprises segments defined by all such reconstructed roll positions, including the vehicle rest position.

Once a diagram is constructed, distances and roll angles are utilized to determine speeds, roll rates, and time durations for each segment based on a single drag factor. The calculated segment times are used in the trajectory model for intervals during which the vehicle is airborne or ground contacts do not significantly alter the parabolic path of the center of gravity

### 6.1 Test 1 (1989 Chevrolet Blazer)

The reconstruction diagram for Test 1 is shown in Figure 6-1. This diagram is constructed as if the roll surface and vehicle were documented and the roll positions on the diagram were a result of reconstruction evidence alone.

Table 6-1 is a summary of the reconstructed roll parameters and calculated roll mechanics. This table is populated with translational and rotational positional data from Figure 6-1, and elevation data from video tape output.

**Table 6-1: Roll Mechanics Based on Reconstructed Roll Positions for Test 1**

Roll Position	Dist. [m]	Speed [kph]		Time [sec]		Roll Angle [deg]		Change in Roll Angle [deg]	Roll Rate [deg/sec]	
		Low	High	Low	High	Initial	Final		Low	High
1		80.7	85.4							
	13.04			0.583	0.617	45	425	380	651	616
2		71.5	75.6							
	15.51			0.812	0.858	425	1305	880	1084	1025
3		58.6	62.0							
	13.12			0.863	0.913	1305	2083	778	901	852
4		44.9	47.5							
	18.68			2.832	2.994	2083	2880	797	281	266
5		0.0	0.0							
Σ	60.35			5.090	5.382				557	527
μ <sub>low</sub> =0.425g, μ <sub>high</sub> =0.475g										

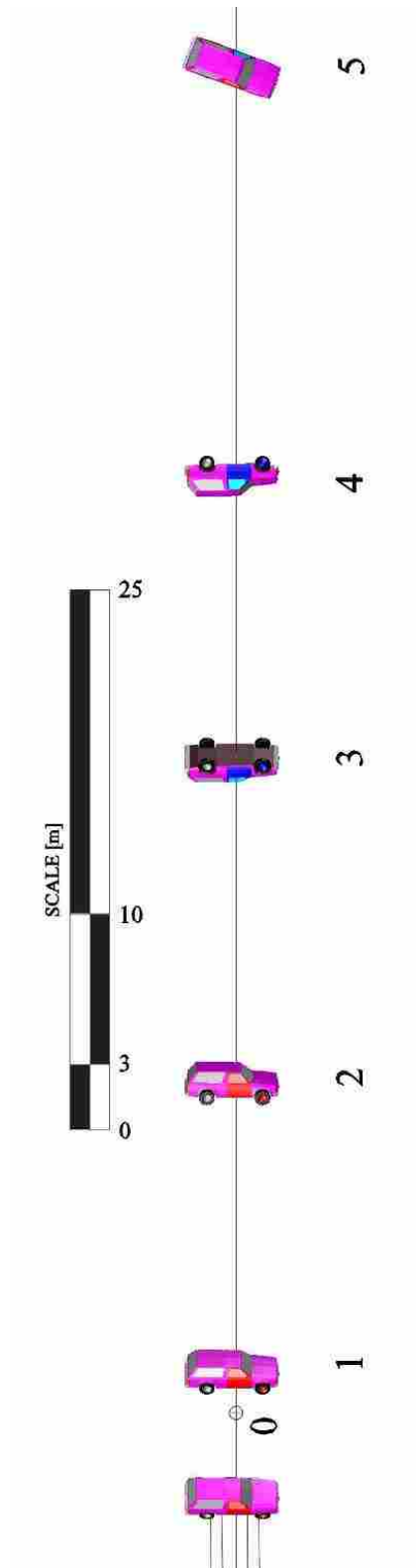


Figure 6-1: Reconstructed Roll Sequence for Test 1

The elevation of the cg relative to distance for Test 1 is shown in Figure 6-2. There are three distinct trajectories of the vehicle in the available film. Also, shown along the x-axis of Figure 6-2 are markers showing the beginning and ending points for the airborne phases along the roll path. Many of the ground contacts have very little effect on the trajectory of the vehicle as shown in Figure 6-2. These are generally contacts at the corners or wheels of the vehicle. Figure 6-3 shows that the three documented trajectories are nearly parabolic as assumed.

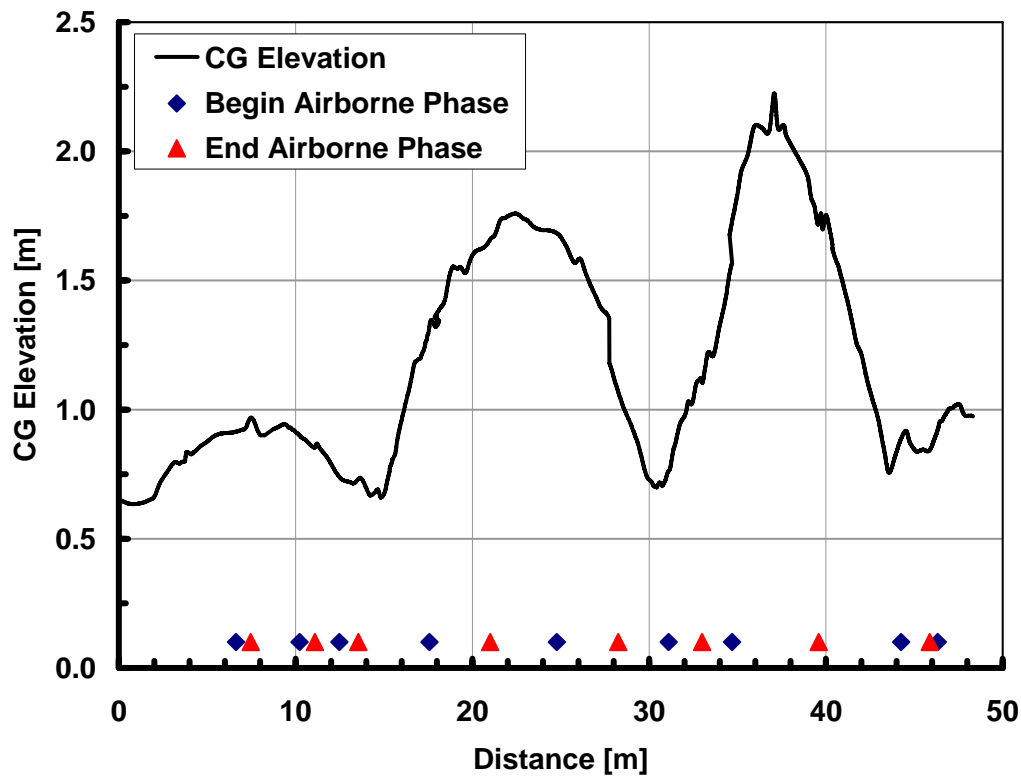
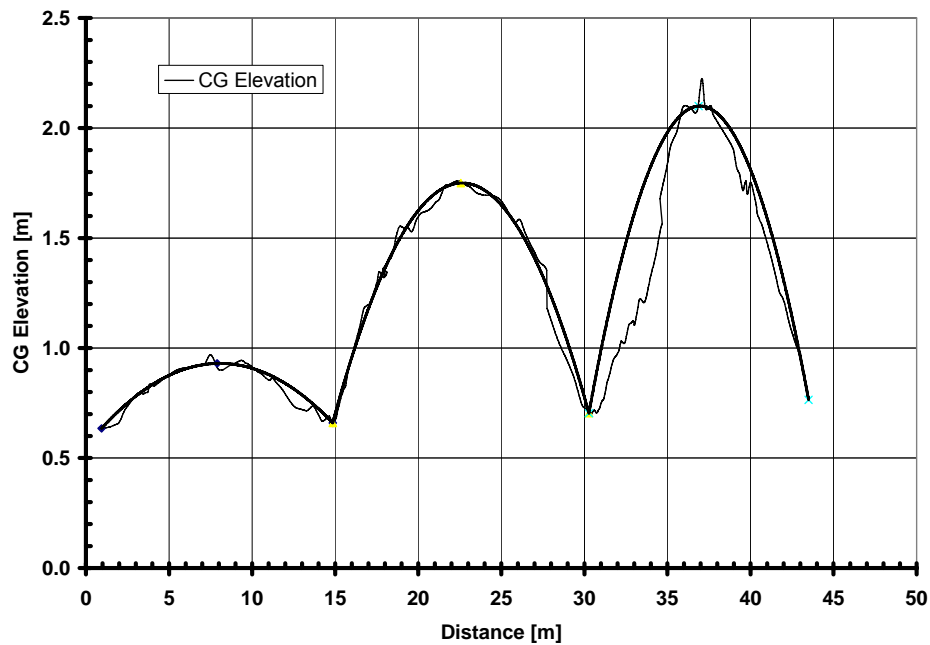


Figure 6-2: Test 1 — Center of Gravity Elevation vs. Distance For Three Successive Trajectories



**Figure 6-3: Test 1 — Center of Gravity Elevation vs. Distance for Three Successive Airborne Segments Showing Multiple Parabolic Fit**

The first segment analyzed covered a distance of 13.31 m. The film analysis shows that the center of gravity is 0.65 m. above the ground at the beginning and 0.71 m above the ground at the end as shown in Table 6-2. Using the reconstructed segment time based on constant drag factors, and the initial and final center of gravity elevations, the trajectory model was applied. The results show that the calculated descent height was approximately 0.41-0.46 m. The film analysis shows that decent height was approximately 0.31 m. In this case where a constant drag factor of 0.425-0.475 was used, the trajectory model over-estimated the measured descent height by 31-48 percent.

The second trajectory was analyzed in a similar manner. The segment covered 15.11 m. Using the end values of the first trajectory as the initial values of the second

trajectory the z-value at reconstructed Position 2 was 0.71 m and the z-value at reconstructed Position 3 was also 0.71 m. Using these values the descent height was calculated to be 0.77-0.86 m. The measured descent height was 1.06 m. In this situation the predicted height underestimated the measured descent height by 19-28 percent.

**Table 6-2: Trajectory Parameters and Results Using Drag Factor of 0.425-0.475g**

Segment	Position (x)			$\Delta x$ [m]	Elevation (z)		$t_d$ (calc)		$h_d$ (calc)		$h_d$ (meas) [m]	$h_d$ (cal/meas)	
	[m]						[m]		[m]				
	Initial		Final		Initial	Final	Low	High	Low	High		Low	High
1-2	1.83	8.50	14.87	13.04	0.65	0.66	0.29	0.31	0.41	0.46	0.31	1.33	1.49
2-3	14.87	22.62	30.38	15.51	0.66	0.70	0.40	0.42	0.79	0.88	1.06	0.74	0.83
3-4	30.38	36.94	43.50	13.12	0.70	0.76	0.42	0.45	0.88	0.99	1.46	0.61	0.68
$\mu_{low}=0.425g, \quad \mu_{high}=0.475g$													

For the third trajectory the segment spanned 12.78 m. Using the end values from the second trajectory for the initial values of the third trajectory, the z-value at reconstructed Position 3 was 0.71 m and the z-value at reconstructed Position 4 was 0.76 m. Using these values the descent height was calculated to be 0.90-1.01 m. The measured descent height was about 1.46 m. For the third trajectory the predicted height underestimated the measured descent height by 31-38 percent (see Figure 6-4).

The situation where the first segment descent height was overestimated suggests that descent time was also overestimated, due to the greater drag factor at the beginning of the roll sequence compared to the overall average. If the assumed constant drag factor were increased to improve agreement in the first trajectory, the descent height calculations for the second and third trajectories would be underestimated.

Table 6-3 shows the results of the analysis using an effective drag factor range of 0.38-0.64. This results show that for the first trajectory a larger drag factor larger than the overall average is required to produce a conservative estimate, and a drag factor lower than the overall average more accurately estimates all other trajectories. Figure 6-5 shows an overlay of the measured z-value with the range of calculated z values. Decelerations of a rolling vehicle along its roll path is clearly non-uniform.

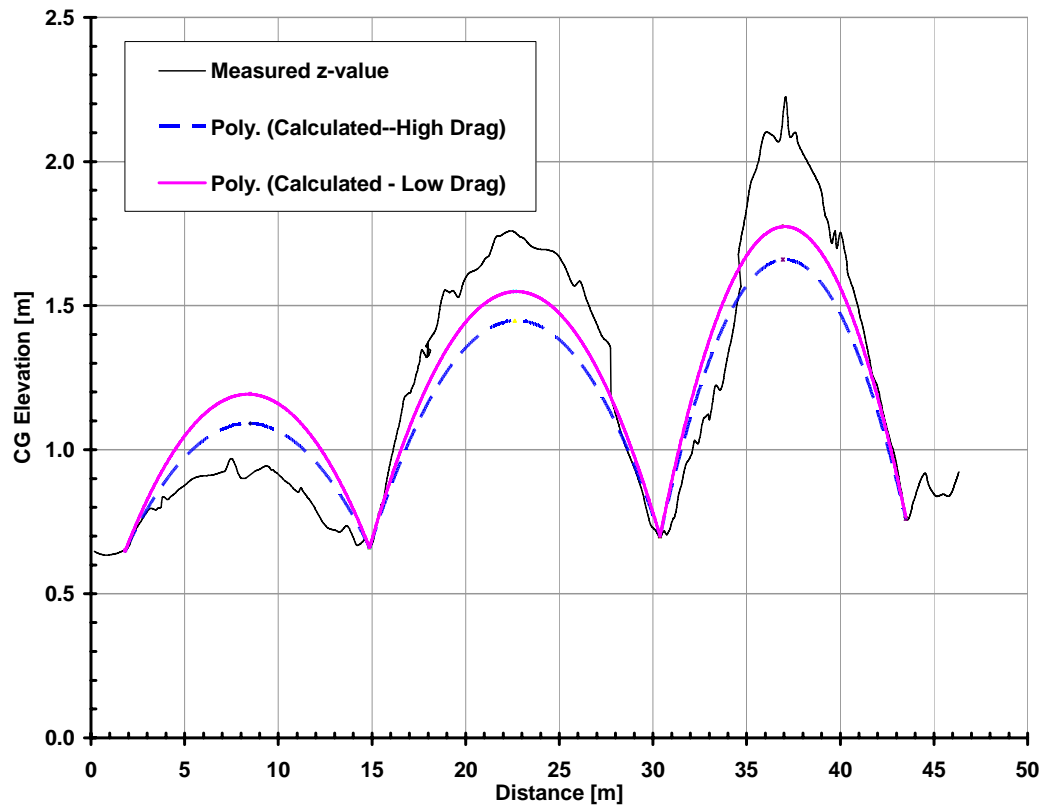


**Figure 6-4: Predicted and Measured Trajectories with  $\mu_{low}=0.425$  and  $\mu_{high}=0.475$**



Table 6-3: Trajectory Parameters and Results Using Drag of 0.38-0.64g

Segment	Position (x)			$\Delta x$ [m]	Elevation (z)		$t_d$ (calc) [m]		$h_d$ (calc) [m]		$h_d$ (meas) [m]	$h_d$ (cal/meas)	
	[m]				Initial	Final	Low	High	Low	High		Low	High
	Initial		Final										
1-2	1.83	8.50	14.87	13.04	0.65	0.66	0.25	0.32	0.30	0.52	0.31	0.98	1.67
2-3	14.87	22.62	30.38	15.51	0.66	0.70	0.34	0.45	0.58	0.99	1.06	0.55	0.93
3-4	30.38	36.94	43.50	13.12	0.70	0.76	0.36	0.48	0.65	1.11	1.46	0.44	0.76
$\mu_{low}=0.38g, \mu_{high}=0.64g$													

$\mu_{low}=0.38g$ ,  $\mu_{high}=0.64g$

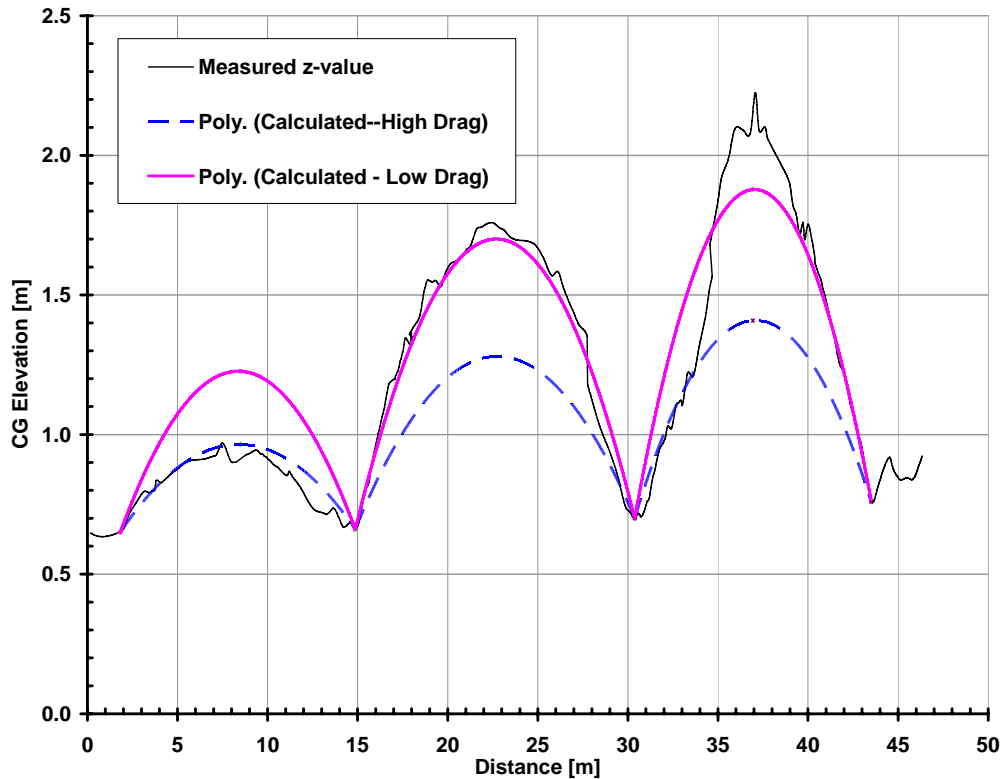


Figure 6-5: Predicted and Measured Trajectories with  $\mu_{low}=0.38$  and  $\mu_{high}=0.64$

## 6.2 Test 2 (1998 Ford Expedition)

The reconstruction diagram with three trajectory templates near the middle of the roll sequence for Test 2 is shown in Figure 6-6. Figures 6-6 through 6-10 show frame captures at the selected roll positions and intermediate positions representing maximum Center of gravity elevations within the trajectories. The reconstructed roll

positions were chosen with the intent to obtain minimum and maximum elevations based on accident evidence. Both segments are relatively short and therefore should yield relatively low trajectories.

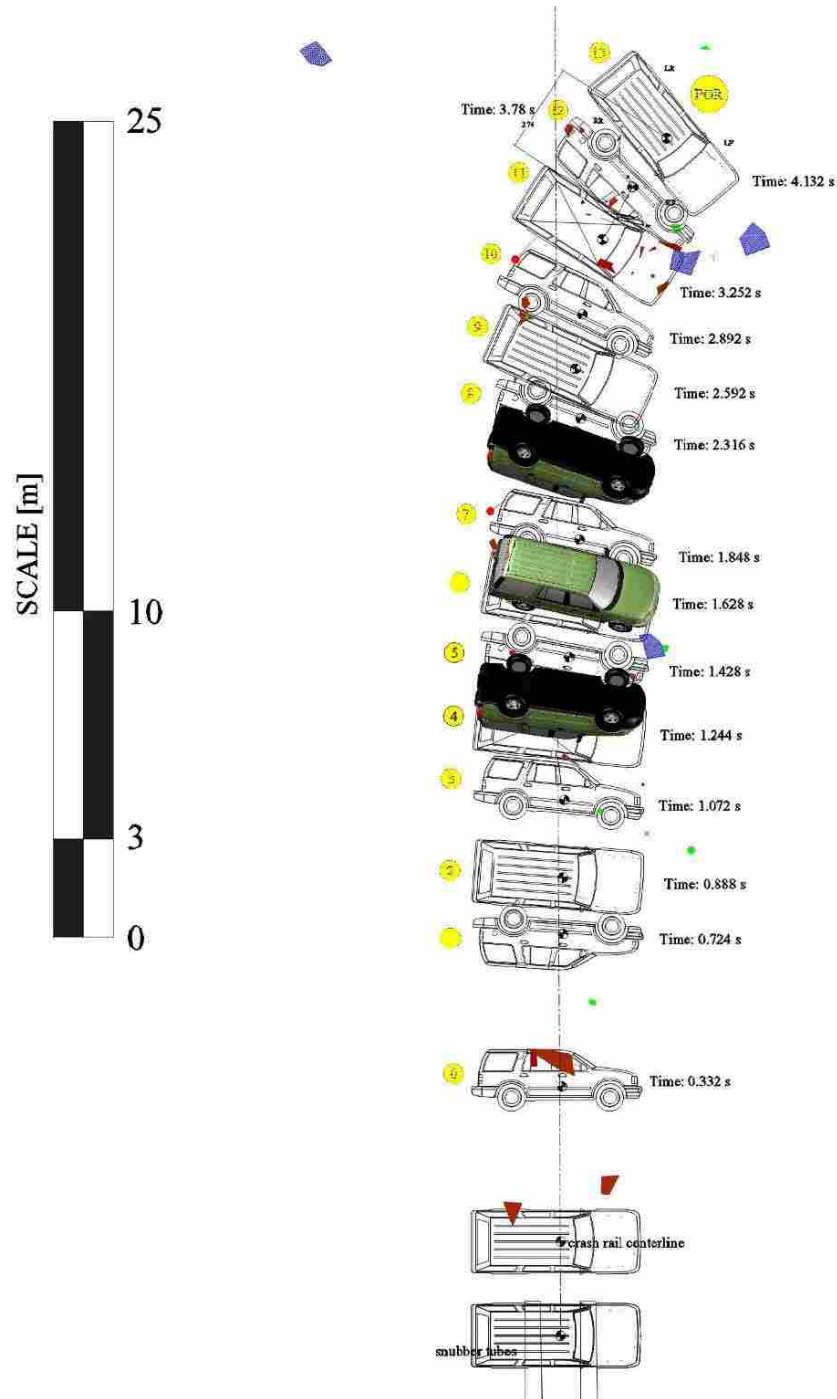


Figure 6-6: Test 2—Reconstruction Diagram with Three Trajectory Templates



**Figure 6-7: Beginning of First Trajectory**



**Figure 6-8: Maximum Elevation of First Trajectory**



**Figure 6-9: End of First Trajectory and Beginning of Second Trajectory**



**Figure 6-10: Maximum Elevation of Second Trajectory**



**Figure 6-11: End of Second Trajectory**

The roll mechanics for the reconstructed roll positions for Test 2 are summarized in Table 6-4 along with the trajectory parameters and results using the effective drag factor range of 0.425-0.475g. Both trajectories yield conservative results. The higher drag factor yields more conservative estimates as shown in Figures 6-12 and 6-13.

**Table 6-4: Test 2 — Roll Mechanics Based on Reconstructed Roll Positions**

Roll Position	Dist. [m]	Speed [kph]		Time [sec]		Roll Angle [deg]		Change in Roll Angle [deg]	Roll Rate [deg/sec]	
		Low	High	Low	High	Initial	Final		Low	High
1	16.80	61.0	64.4	1.094	1.157	90	610	520	475	450
2		43.6	46.1							
3	3.59			0.296	0.313	610	1000	390	1316	1245
4	3.81			0.360	0.380	1000	1160	160	445	421
5	10.20			2.093	2.212	1160	1440	280	134	127
		0.0	0.0							
Σ	34.40			3.843	4.063					
μ <sub>low</sub> =0.425g, μ <sub>high</sub> =0.475g										
									351	332

Table 6-6 shows the analysis using extremes in drag factor similar to that of Test 1. Utilization of the 0.64g drag factor for Test 1 reduced the descent height estimates significantly, resulting in a reasonable calculation for the first trajectory as shown in Figures 6-14 and 6-15.

**Table 6-5: Test 2 — Trajectory Parameters and Results Using Drag of 0.425-0.475**

Segment	Position (x) [m]		Δx [m]	Elevation (z) [m]			t <sub>d</sub> (calc) [sec]		h <sub>d</sub> (calc) [m]		h <sub>d</sub> (meas) [m]	h <sub>d</sub> (cal/meas)	
	Initial	Final		Initial	Maximum	Final	Low	High	Low	High		Low	High
2-3	16.80	20.39	3.59	0.71	1.05	0.76	0.13	0.14	0.08	0.10	0.29	0.29	0.33
3-4	20.39	24.20	3.81	0.76	1.21	0.94	0.13	0.14	0.08	0.10	0.27	0.30	0.37
μ <sub>low</sub> =0.425g, μ <sub>high</sub> =0.475g													

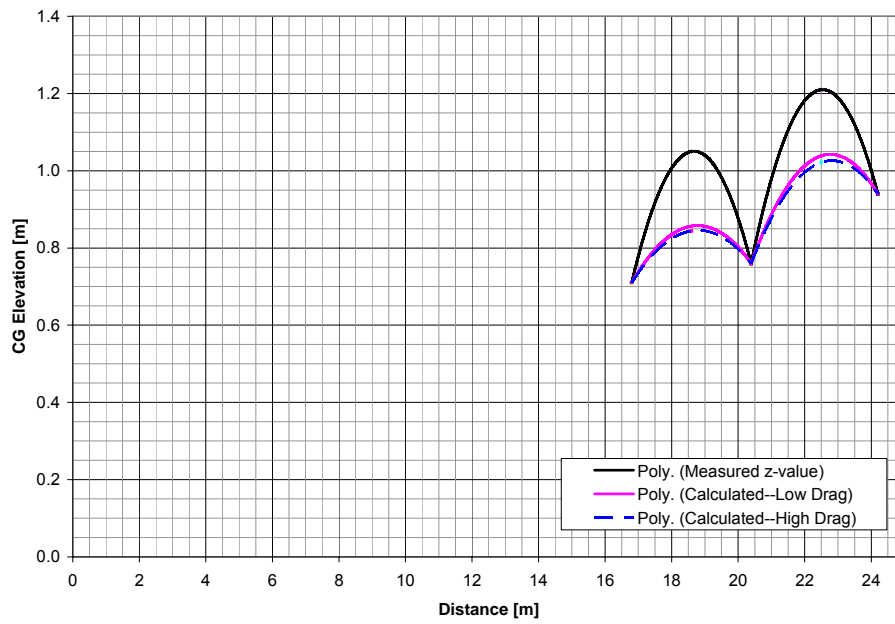


**Figure 6-12: Predicted and Measured Trajectories with  $\mu_{low}=0.425$  and  $\mu_{high}=0.475$**

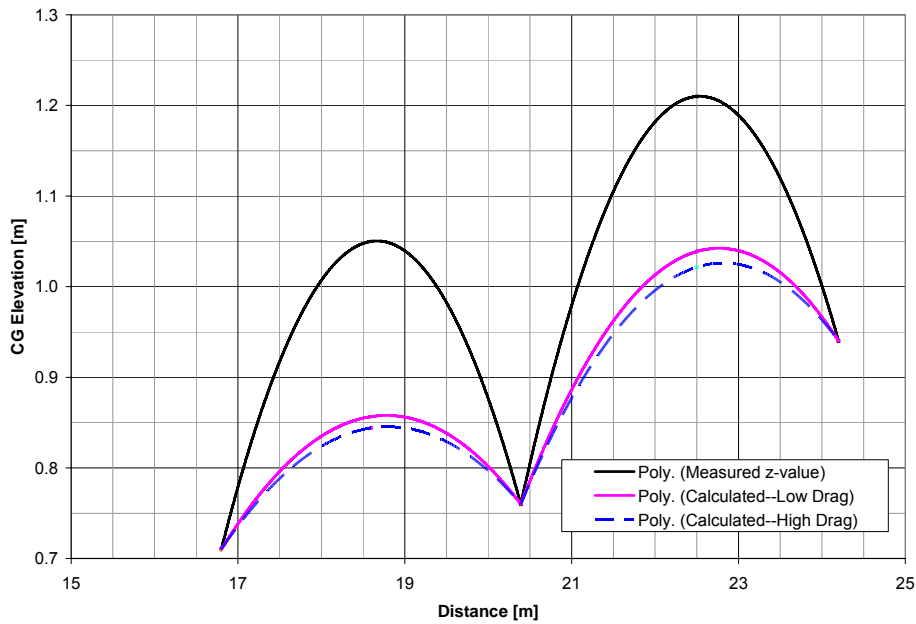


**Figure 6-13: Magnified View of Predicted and Measured Trajectories with  $\mu_{low}=0.425$  and  $\mu_{high}=0.475$**

**Table 6-6: Test 2 — Trajectory Parameters and Results Using Drag of 0.38-0.64**

Segment	Position (x)		$\Delta x$ [m]	Elevation (z)			$t_d$ (calc)		$h_d$ (calc)		$h_d$ (meas) [m]	$h_d$	
	[m]			[m]			[sec]		[m]			(cal/meas)	
	Initial	Final		Initial	Maximum	Final	Low	High	Low	High		Low	High
2-3	16.80	20.39	3.59	0.71	1.05	0.76	0.11	0.15	0.06	0.11	0.29	0.20	0.38
3-4	20.39	24.20	3.81	0.76	1.21	0.94	0.10	0.16	0.05	0.12	0.27	0.17	0.44
$U_{low}=0.38g, U_{high}=0.64g$													

$\mu_{low}=0.38g$ ,  $\mu_{high}=0.64g$

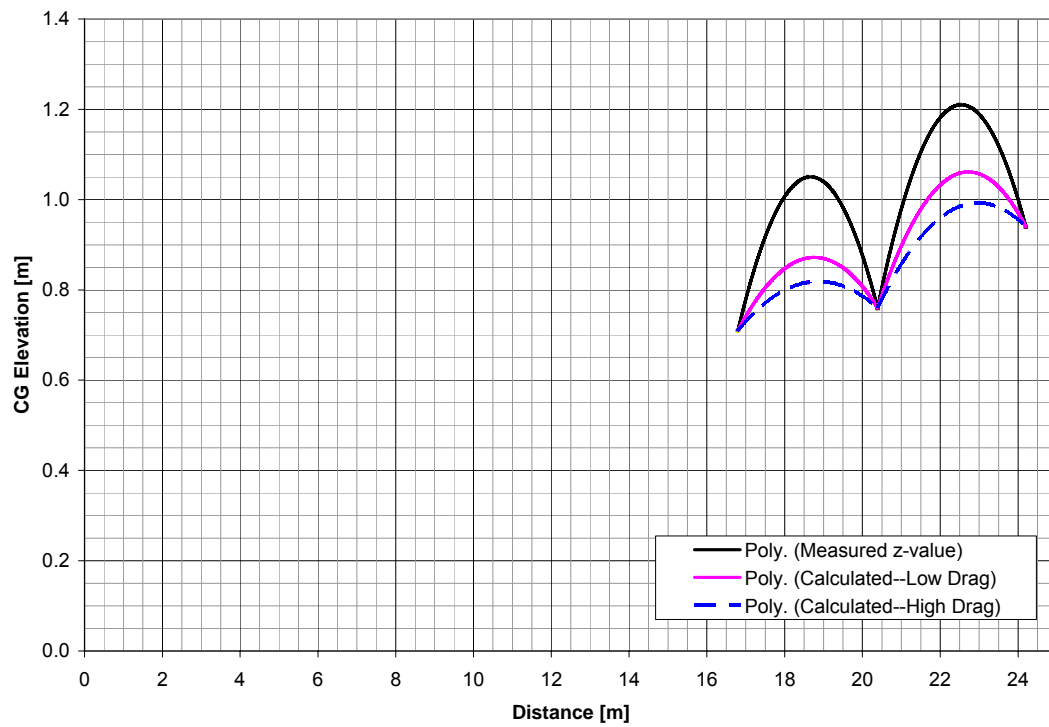


**Figure 6-14: Predicted and Measured Trajectories with  $\mu_{low}=0.38$  and  $\mu_{high}=0.64$**

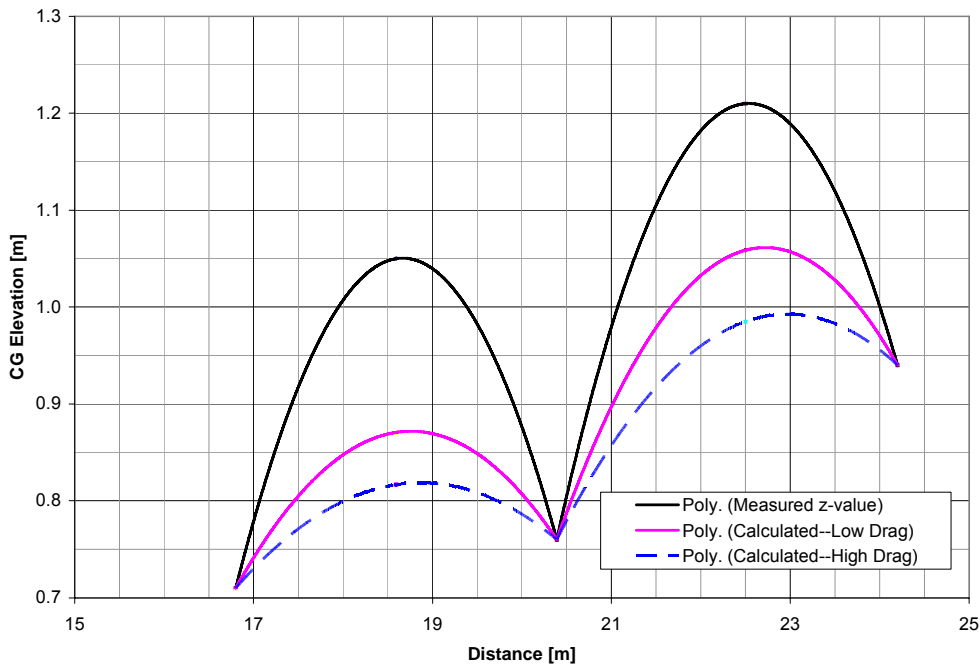


**Figure 6-15: Magnified View of Predicted and Measured Trajectories with  $\mu_{low}=0.38$  and  $\mu_{high}=0.64$**

### 6.3 Trajectory Summary

The trajectory results demonstrate the influence of drag factor on descent height calculations. Utilization of uniform drag factors tends to overestimate descent height early in a roll sequence and underestimate descent height later in the sequence. Drag factors greater than the overall average more accurately predict trajectory mechanics early in a roll sequence and use of lower drag factors predict trajectory mechanics more accurately later in a roll sequence. This results from the fact that actual drag factors are much higher early in a roll sequence and lower later in the sequence. Using a published average drag factor in the trajectory model produces conservative descent height estimates in the middle and latter parts of a roll sequence.

Care should be exercised in determining if sufficient evidence supports computational trajectory analysis. Specifically, great care should be taken not to apply the trajectory model to roll segments where there are significant intermediate vehicle ground interactions. Overlooking significant ground contacts could over-estimate segment time and therefore descent distance.

For a well-documented rollover sequence or segment, the trajectory model can be used with appropriate physical parameters to estimate descent distance.





## **7 Discussion of Results**

Detailed film analysis as described earlier can be very useful in determining vehicle position and orientation along a roll path. In crash tests and rollover accidents where video is the only form of documentation, this research can expand the analysis possibilities. Vertical location of vehicle center of gravity is a previously undocumented parameter in rollover crash tests.

The translational velocity history of a rolling vehicle on soft surfaces (e.g., desert soil) is directly influenced by the orientation and nature of each ground contact, which can either decrease or increase the roll angular velocity as the total vehicle kinetic energy is dissipated (see Appendix E).

During the rollover sequence, the energy dissipation due to vehicle deformation, sliding friction and other ground interactions results in a decrease in translational velocity throughout the sequence. The decrease may be imperceptible for certain vehicle-to-ground interactions following an airborne segment in which the center of rotation momentarily shifts from the axis of rotation through the vehicle center of gravity toward the impact location. A vehicle orientation that can produce this effect involves ground contact of the trailing side wheels/tires. When the vehicle rolls across the ground on its side body, and the outer surfaces of the trailing wheels and tires approach full ground contact, the roll center shifts toward the momentarily

stopped or nearly stopped wheels and tires. The vehicle center of gravity rotates approximately about the contact area, with only a slight decrease in the translational velocity and corresponding decrease in total energy of the vehicle.

A similar effect, involving the leading tires and wheels, can occur during short segments of a rollover sequence with the vehicle essentially in an upright position. The tread edges and sidewalls of the tires, and the lower portions of the wheel faces, momentarily approximately coincide with the roll center. The applied torque about the center of gravity of the vehicle from the tire/wheel ground contact forces increases the roll velocity, causing the center of gravity velocity to decrease less rapidly than would be computed by Equation 2.1. The influence of this mechanism on roll rate and center of gravity translational velocity is diminished due to the large effective increase in roll moment of inertia during the ground contact transients in which the roll center is remote from the vehicle roll axis.

The trajectory results demonstrate the influence of drag factor descent height calculations. Typical constant drag factors tend to overestimate descent height early in a roll sequence and underestimate descent height later in the sequence. This is a result of actual drag factors being much higher early in a roll sequence. Using a typical average drag factor in the trajectory model produces conservative descent height estimates in the middle and latter parts of a roll sequence.

Care should be exercised in assuring that sufficient evidence supports trajectory analysis. Specifically, the trajectory model is not applied to roll segments during which there are significant intermediate vehicle ground interactions. A

variable-drag model would produce accurate trajectory calculations at all locations along an entire roll sequence.

The trajectory model is a useful tool to aid in understanding rollover mechanics although a rolling vehicle may be in contact with the ground for a significant fraction of a roll segment. The model should not be used at locations in roll sequences where there are extremes in center of gravity accelerations. These extremes include the segments immediately following overturn where there are large angular accelerations and large differences between the tangential velocity of the vehicle perimeter and the translational velocity of the center of gravity. Also included are segments that include vehicle impacts with irregular terrain, trees or posts.



## **8 Conclusions, Contributions and Recommendations**

### **CONCLUSIONS**

The previous chapters have described the current state of art that is both published and unpublished relating to the rollover phase of accident reconstruction. The latter chapters describe tests that were analyzed in great detail using both film analysis and available measurements. The detail in which these tests were analyzed is unprecedented. The data that can be pulled from this analysis is a valuable contribution to the body of science. The following list summarizes the results of this analysis:

1. While the actual vehicle velocities and decelerations during specific segments of a rollover are dependent upon the orientation and nature of the vehicle ground contacts, appropriate average deceleration values can be used to reasonably estimate initial rollover velocity and approximate vehicle speeds throughout the sequence.
2. Deceleration values for the vehicles in the four rollover tests presented in this thesis have a combined average drag factor significantly higher (0.50g) than the previously published average of 0.43g.
3. Although the average drag factor for the steer-induced test was markedly lower than that from the dolly rollover tests, other roll

mechanics parameters were similar. The roll rates recorded in the featured dolly rollover tests generally do not appear to be artificially high. Roll rates of up to 600 degrees per second, and higher, are comparable to those recorded in full scale steer-induced rollover tests, as well as roll rates estimated from camera coverage of actual real world rollovers.

4. Trajectories of rolling vehicles can be mathematically modeled if sufficient information is available to determine multiple vehicle locations and orientations, and rollover path topography. Utilizing the published average drag factor yields liberal trajectory computations early in the roll sequence and conservative results during the latter portion of a roll sequence.
5. Great care should be taken in applying the trajectory model to avoid gross overestimations in descent height calculations.

## **CONTRIBUTIONS**

This thesis is the first published work to utilize detailed film analysis for the purpose of rollover accident reconstruction. This methodology allows a researcher to obtain spatial measurements of vehicles in rollover crash tests documented by video.

Accounting of roll mechanics parameters in rollover crash tests has not previously been performed with the detail documented here. The detailed accounting yields trends useful for understanding general roll mechanics.

Roll segment trajectory mechanics calculations are new to the accident reconstruction field. Trajectory mechanics estimates allow the reconstructionist to quantify vertical descent distance of vehicles from one ground impact to the next.

## **RECOMMENDATIONS FOR FUTURE WORK**

More data, time and funding would greatly compliment this work. Specifically, recommendations for future work include the following:

1. As was shown from the analysis, effective drag factors for a rolling vehicle is nonlinear. Development of a nonlinear deceleration model would be of great worth to the science of accident reconstruction and a useful contribution to this work.
2. Detailed ground impact analysis, including torques and exchange in momentum would be useful further quantifying ground impact severity.
3. Development of an optimization routine to determine ground impact parameters using pre- and post-impact conditions is recommended.
4. More data from steer-induced rollover tests should be analyzed to compare with the larger body of data from dolly rollover tests. This data would also provide the explanation for the lower drag factor for the steer-induced test compared to the dolly rollover tests. The data point could either an outlier or a description of the difference between dolly rollover tests and steer-induced rollover tests.



5. Apply film analysis techniques presented here to more rollover crash tests to provide enough data to perform confidence analysis on all roll mechanics parameters discussed here.
6. Highly-instrumented, controlled tests need to be performed to develop an accurate, comprehensive database for accident reconstruction.

## References

- [1] Baker, S. J., Fricke, L. B., Traffic Accident Reconstruction, The Traffic Institute, Northwestern University, 1990.
- [2] Viano, D. C. and Parenteau, C. S., “Rollover Crash Sensing and Safety Overview.” SAE 2004-01-0342, 2004.
- [3] McGuigan, R., and Bondy, N., “A Descriptive Study of Rollover Crashes.” 1980.
- [4] Brach, R. M. and Brach, R. M., Vehicle Accident Analysis and Reconstruction Methods, SAE International, Warrendale, PA, 2005.
- [5] “NHTSA Study of Rollover Crash Safety,” 49 CFR Part 575, Docket No. NHTSA-2000-8298.
- [6] Digges, K. H., “Summary Report of Rollover Crashes,” FHWA/NHTSA National Crash Analysis Center, 2002.
- [7] Jones, I., and Wilson, L., “Techniques for the Reconstruction of Rollover Accidents Involving Sport Utility Vehicles, Light Trucks and Minivans.” SAE 2000-08-0851, 2000.
- [8] Bready, J., May, A., and Alsop, D., “Physical Evidence Analysis and Roll Velocity Effects in Accident Reconstruction.” SAE 2001-01-1284, 2001.
- [9] Hughes, R., Lewis, L., and Hare, B., et al., “A Dynamic Test Procedure for Evaluation of Tripped Rollover Crashes.” SAE 2002-01-0693, 2002.
- [10] Hibbeler, R., Engineering Mechanics, Dynamics, 8<sup>th</sup> Ed., Prentice Hall, Upper Saddle River, NJ, 1998.
- [11] Baumeister, T., Standard Handbook for Mechanical Engineers, 7<sup>th</sup> Ed., McGraw-Hill, Inc., 1967.
- [12] Lindeburg, M., Engineer-in-Training Reference Manual, 8<sup>th</sup> Ed., Professional Publications, Inc., Belmont, CA, 1998.
- [13] Altman, S., Santistevan, D., Hitchings, C., Wallingford, J., and Greenlees, B., “A Comparison of Rollover Characteristics for Passenger Cars, Light Duty Trucks and Sport Utility Vehicles.” SAE 2002-01-0942, 2002.

- [14] Cooperrider, N., Hammoud, S., and Colwell, J., "Characteristics of Soil-Tripped Rollovers," SAE 980022, 1998.
- [15] Cooperrider, N., Thomas, T., Hammoud, S., "Testing and Analysis of Vehicle Rollover Behavior," SAE 900366, 1990.
- [16] Orlowski, K., Moffatt, E., Bundorf, R., and Holcomb, M., "Reconstruction of Rollover Collisions," SAE 890857, 1989.
- [17] Viano, D., and Parenteau, C., Occupant and Vehicle Responses in Rollovers, SAE International, Warrendale, PA, 2004.
- [18] Warner, C., Smith, G., James, M., and Germane, G., "Friction Applications in Accident Reconstruction," SAE 830612, 1983.
- [19] Heydinger, G., and Bixel, R., et al., "Measured Vehicle Inertial Parameters- NHTSA's Data Through November 1998," SAE 1999-01-1336, 1999.
- [20] Larson, R., Smith, J., Werner, S., and Fowler, G., "Vehicle rollover Testing, Methodologies in Recreating Rollover Collisions," SAE Paper No. 2000-01-1641, 2000.
- [21] Luepke, P., Carhart, M., Croteau, J., Morrison, R., Loibl, J., and Ridenour, J., "An Evaluation of Laminated Side Window Glass Performance During Rollover," SAE 2007-01-0367, 2007.
- [22] Code of Federal Regulations, Department of Transportation, National Highway Traffic Safety Administration, Part 571.208.

## Appendix A – Nomenclature


$T$	Kinetic energy
$m$	Vehicle Mass
$V$	Velocity of vehicle at CG
$I_x$	Roll moment of inertia
$I_y$	Pitch moment of inertia
$I_z$	Yaw moment of inertia
$\omega$	Roll rate
$g$	Acceleration of gravity
$z$	Elevation of CG
$t_s$	Time duration of trajectory of CG
$t_a$	Time duration of trajectory from $z_f$ to maximum elevation
$t_d$	Time duration of trajectory from maximum elevation to $z_f$
$\mu$	Drag Factor
$\Delta x$	Change in distance

### Subscripts

$i$	Initial
$f$	Final
$s$	Segment total
$a$	Ascent
$d$	Descent



## Appendix B – Detailed Crash Test documentation



### CAMERA SET-UP RECORD

PROJECT No.: PH04668FB      TEST DATE: 1/10/95

PROJECT NAME: CASTILLO V GM

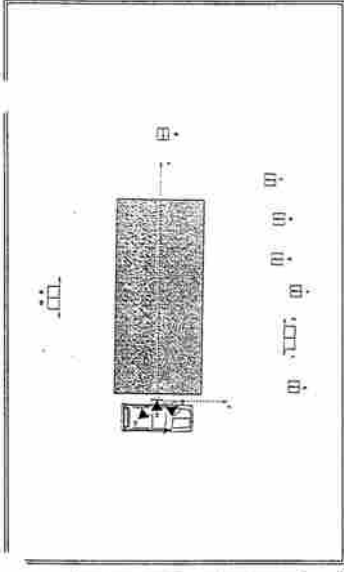
TEST TYPE: LATERAL ROLLOVER - DIRT TRIP

TARGET VEHICLE (T):

BULLET VEHICLE (B):

APPROX TEST SPEEDS - (T):      (B):

COMMENTS:



NOTE: ALL DIMENSIONS IN FEET.

LEGEND: ☒ OVERHEAD   ☒ PIT   ☒ ONBOARD   ☒ GROUND   ☒ PANNING

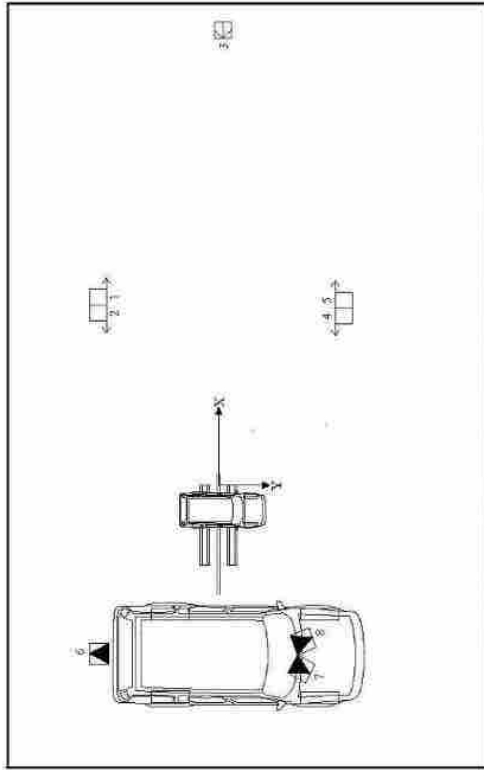
LOC. NO.	CAMERA TYPE	FIELD OF VIEW	IMPACT DISTANCE-X	CENTERLINE DISTANCE-Y	CAMERA HEIGHT-Z	SET SPEED (fps)	LENS SIZE (mm)
1	VIDEO	PANNING EVENT	31.5	100.7	5.3	RT	--
2	PS	PANNING EVENT	32.5	100.7	5.0	500	13
3	LOCAM	MED. CLOSEUP - BEGINNING OF ROLL	15.0	107.0	4.4	500	25
4	LOCAM	MED. CLOSEUP - OVERLAP OF #3	45.0	107.0	4.4	500	25
5	LOCAM	MED. CLOSEUP - OVERLAP OF #4	75.0	68.0	5.0	500	16
6	LOCAM	MED. CLOSEUP - OVERLAP OF #5	105.0	68.0	6.1	500	16
7	LOCAM	MED. CLOSEUP - OVERLAP OF #6	135.0	45.0	5.6	500	10
8	LOCAM	WIDE VIEW	225.0	16.0	11.5	500	25
9	VIDEO	PANNING EVENT	61.0	-99.0	5.0	RT	--
10	PS	PANNING EVENT	60.0	-99.0	4.8	500	35
11	PS	WIDE VIEW - DUMMY MOTION	---	---	---	500	8
12	PS	CLOSEUP - S.B. BUCKLE	---	---	---	500	13
13	PS	MED. CLOSEUP - D-RING	---	---	---	500	13
14							
15							

Rev# 1002283

Camera coverage sheet for Test 1—1989 Chevrolet S10 Blazer dolly rollover at 89 kph

## CAMERA SET-UP RECORD

PROJECT NO:	PH09825	TEST DATE:	10/19/2005
PROJECT NAME:	TEC9825		
TEST TYPE:	DOLLY ROLLOVER TEST		
TARGET VEHICLE (T):	N/A		
BULLET VEHICLE (B):	1998 FORD EXPEDITION		
TEST SPEEDS (T):	N/A	(B):	43 MPH
COMMENTS:	NONE		



NOTES: ALL DIMENSIONS IN FEET. NOT TO SCALE. Z-AXIS MEASURED UP FROM GROUND.

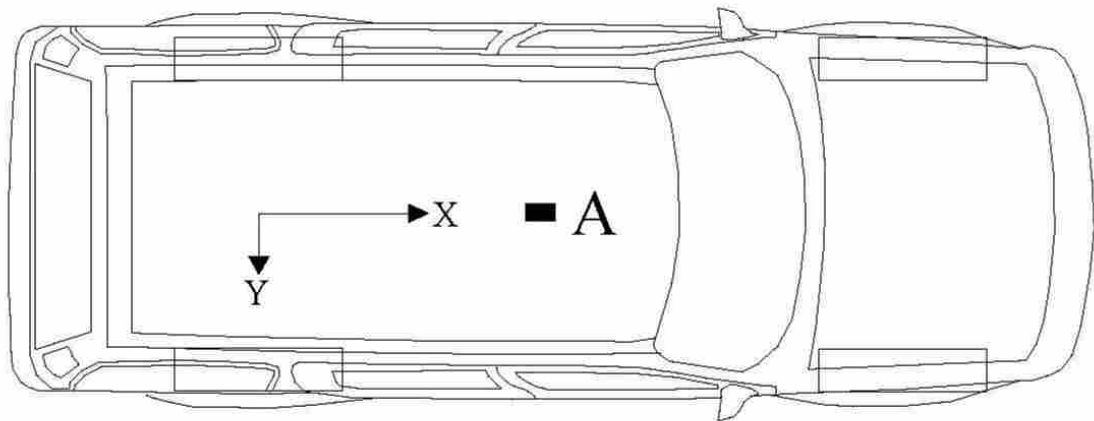
LOC NO	CAMERA TYPE	FIELD OF VIEW	IMPACT DISTANCE (ft)	CENTERLINE DISTANCE (ft)	CAMERA HEIGHT (ft)	SET SPEED (fps)	LENS SIZE (mm)
1	VIDEO	PANNING EVENT REAR	90.0	-140.0	4.9	RT	--
2	HS VIDEO	PANNING EVENT REAR	90.0	-140.0	4.8	250	25
3	LOCAM	WIDE VIEW, DOWN STREAM	230.0	0.0	5.2	250	50
4	VIDEO	PANNING EVENT FRONT	90.0	140.0	4.9	RT	--
5	HS VIDEO	PANNING EVENT FRONT	90.0	140.0	4.7	250	25
6	PS	VEHICLE INTERIOR FROM REAR	--	--	--	250	5.6
7	HS VIDEO	VEHICLE INTERIOR FROM FRONT	--	--	--	250	6.5
8	HS VIDEO	VEHICLE INTERIOR FROM FRONT	--	--	--	250	6.5
9							
10							
11							
12							
13							
14							
15							

NOTE: AN EDITED VIDEO DUB WAS PRODUCED USING THE CAMERA FOOTAGE DESCRIBED ON THIS PAGE

Camera coverage sheet for Test 2 – 1998 Ford Expedition Dolly Rollover at 69.5 kph

## VEHICLE TRANSDUCER LOCATION RECORD

PROJECT NO:	PH09825	PROJECT NAME:	TEC9825	TEST DATE:	10/19/2005
VEHICLE YEAR:	1998	VEHICLE MAKE:	FORD	VEHICLE MODEL:	EXPEDITION
VEHICLE BODY STYLE:	4-DOOR SPORT UTILITY VEHICLE			VEHICLE COLOR:	MAROON
VEHICLE IDENTIFICATION NUMBER:	1FMPU18L9WLC42537				



NOTES: NOT TO SCALE, Z-AXIS MEASURED UP FROM GROUND

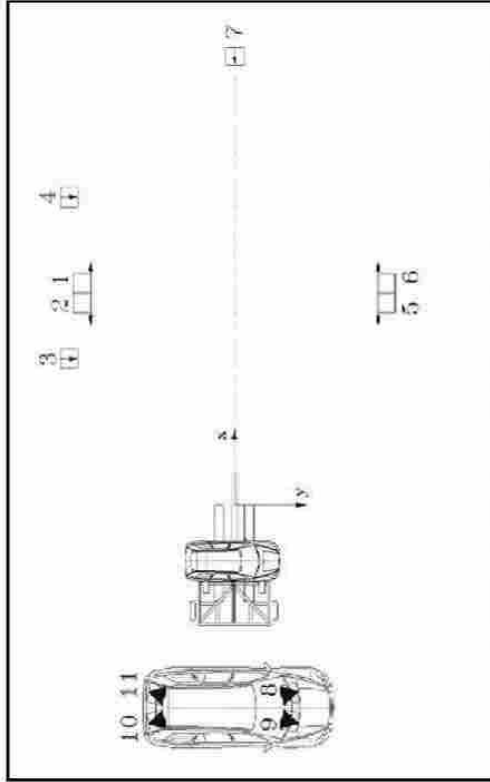
REF #	TRANSDUCER LOCATION DESCRIPTION	LONGITUDINAL (X)	LATERAL (Y)	VERTICAL (Z)
A	VEHICLE FLOOR AT CENTER CONSOLE ROLL AND YAW RATE	60.5 in.	0.0 in.	30.3 in.

Instrumentation setup for Test 2 – 1998 Ford Expedition Dolly Rollover at 69.5 kph



## CAMERA SET-UP RECORD

PROJECT NO:	PH10303	TEST DATE	7/17/2006
PROJECT NAME:	TEC10303		
TEST TYPE	DOLLY ROLLOVER TEST		
TARGET VEHICLE (T)	N/A		
BULLET VEHICLE (B)	2004 VOLVO XC90		
TEST SPEEDS (T)	N/A	(B)	42.9 MPH
COMMENTS:	NONE		



NOTES: ALL DIMENSIONS IN FEET. NOT TO SCALE. Z-AXIS MEASURED UP FROM GROUND.

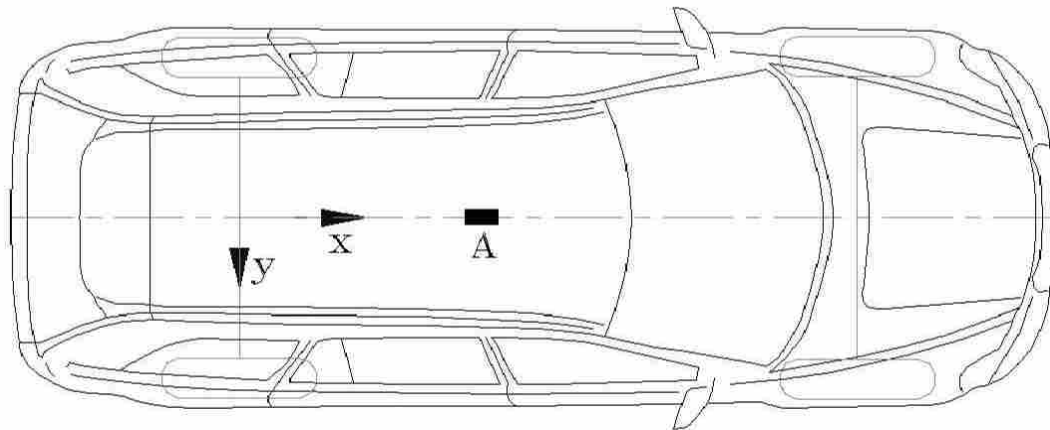
LOC NO	CAMERA TYPE	FIELD OF VIEW	IMPACT DISTANCE (X)	CENTERLINE DISTANCE (Y)	CAMERA HEIGHT (Z)	SET SPEED (fps)	LENS SIZE (mm)
1	VIDEO	PANNING EVENT REAR	90.2	-140.0	4.6	RT	--
2	HS VIDEO	PANNING EVENT REAR	89.7	-140.0	4.9	250	25
3	LOCAM	WIDE REAR VIEW, UP STREAM	84.2	-146.0	4.0	250	12.5
4	LOCAM	WIDE REAR VIEW, DOWN STREAM	153.4	-146.0	4.0	250	12.5
5	VIDEO	PANNING EVENT FRONT	89.7	140.0	4.2	RT	--
6	HS VIDEO	PANNING EVENT FRONT	90.2	140.0	4.4	250	25
7	LOCAM	WIDE VIEW, DOWN STREAM	230.0	0.0	3.6	250	50
8	HS VIDEO	VEHICLE INTERIOR FROM FRONT	--	--	--	250	6.5
9	HS VIDEO	VEHICLE INTERIOR FROM FRONT	--	--	--	250	6.5
10	PS	VEHICLE INTERIOR FROM REAR	--	--	--	250	7.5
11	PS	VEHICLE INTERIOR FROM REAR	--	--	--	250	7.5

NOTE: AN EDITED VIDEO DUB WAS PRODUCED USING THE CAMERA FOOTAGE DESCRIBED ON THIS PAGE

Camera coverage for Test 3 – 2004 Volvo XC 90 Dolly Rollover at 69 kph

## VEHICLE TRANSDUCER LOCATION RECORD

PROJECT NO:	PH10303	PROJECT NAME:	TEC10303	TEST DATE:	7/17/2006
VEHICLE YEAR:	2004	VEHICLE MAKE:	VOLVO	VEHICLE MODEL:	XC90
VEHICLE BODY STYLE:	4-DOOR SPORT UTILITY VEHICLE			VEHICLE COLOR:	GOLD
VEHICLE IDENTIFICATION NUMBER:	YV1CN59H441126781				



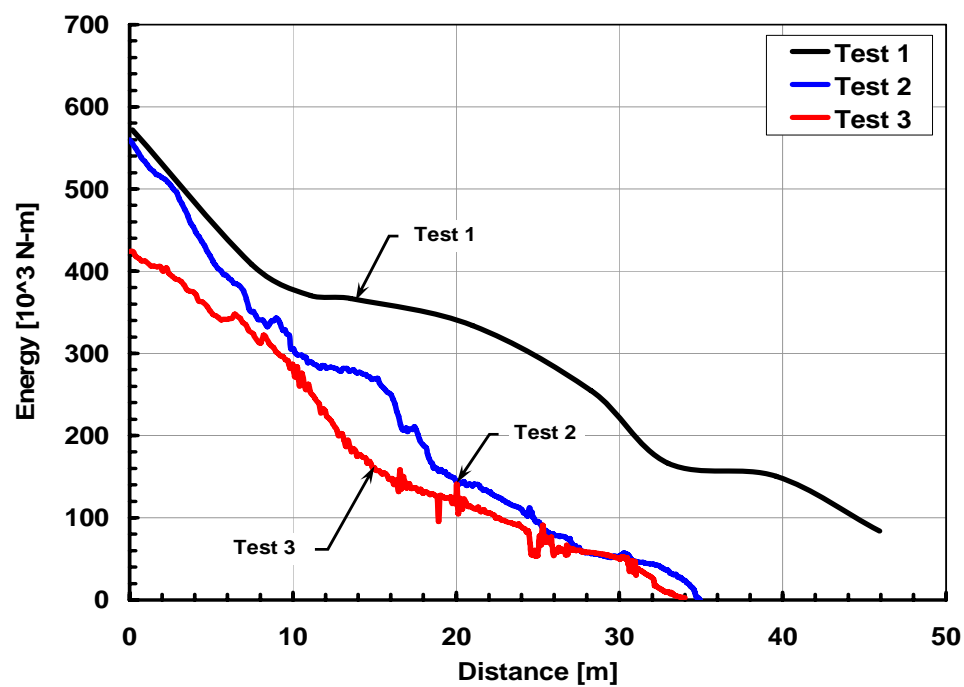
NOTES: NOT TO SCALE, Z-AXIS MEASURED UP FROM GROUND

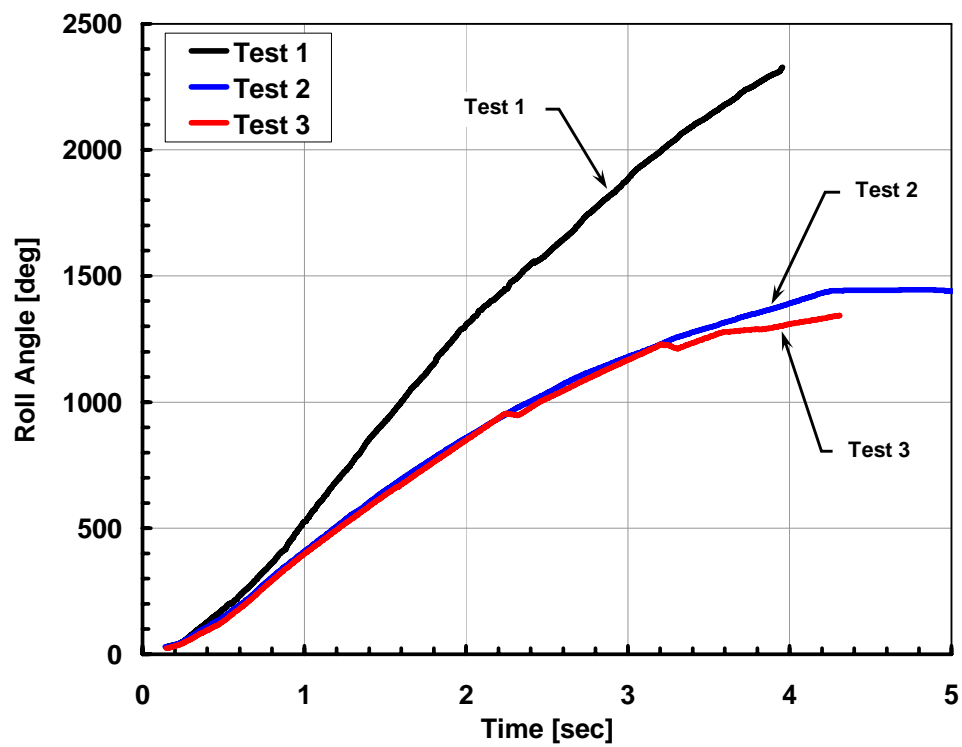
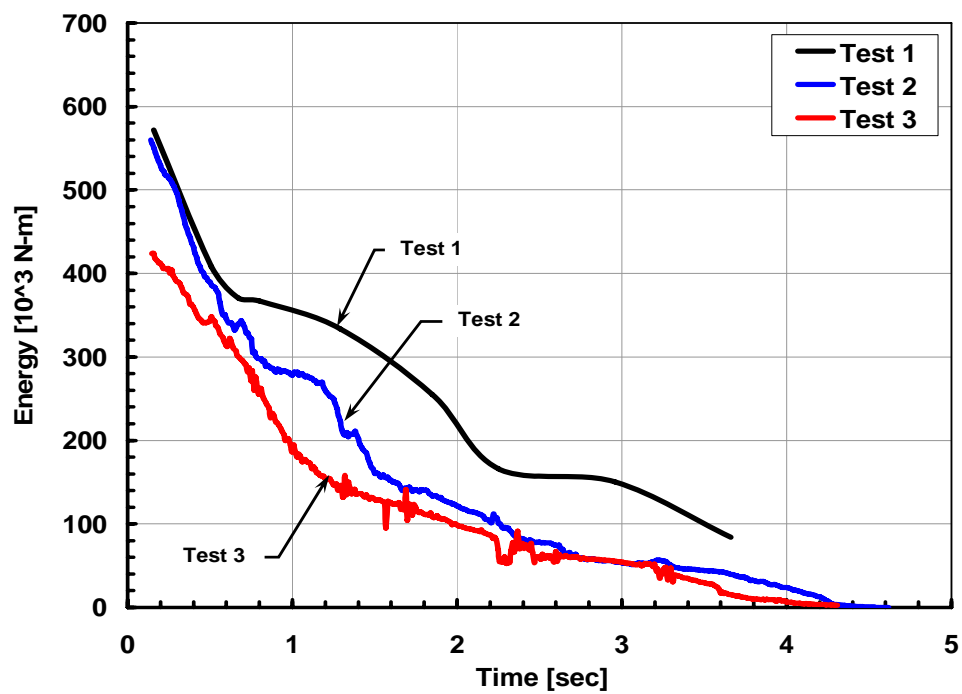
REF #	TRANSDUCER LOCATION DESCRIPTION	LONGITUDINAL (X)	LATERAL (Y)	VERTICAL (Z)
A	VEHICLE TUNNEL BEHIND CONSOLE ROLL AND YAW RATE	44.6 in.	0.0 in.	20.5 in.

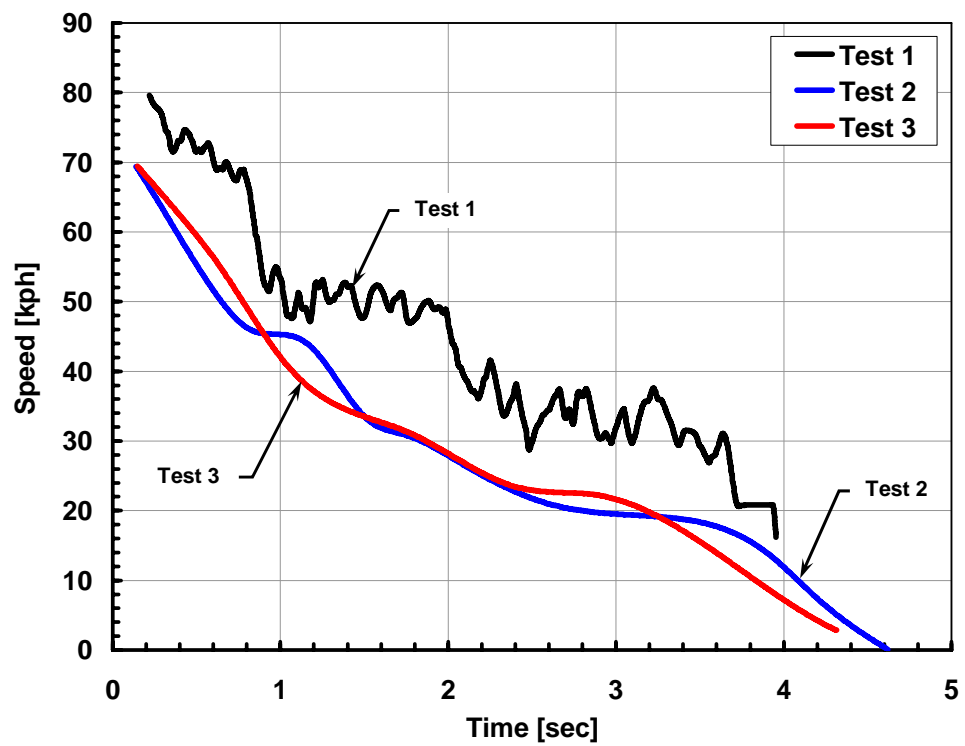
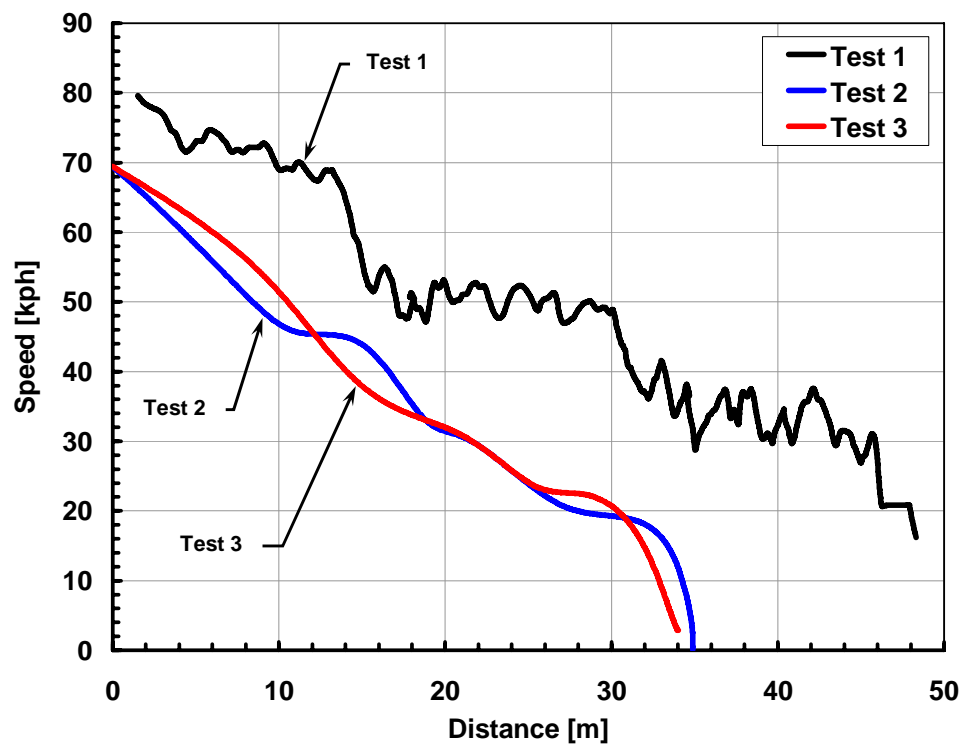
Instrumentation setup sheet for Test 3 – 2004 Volvo XC 90 Dolly Rollover at 69 kph



Appendix C – Energy Correlations

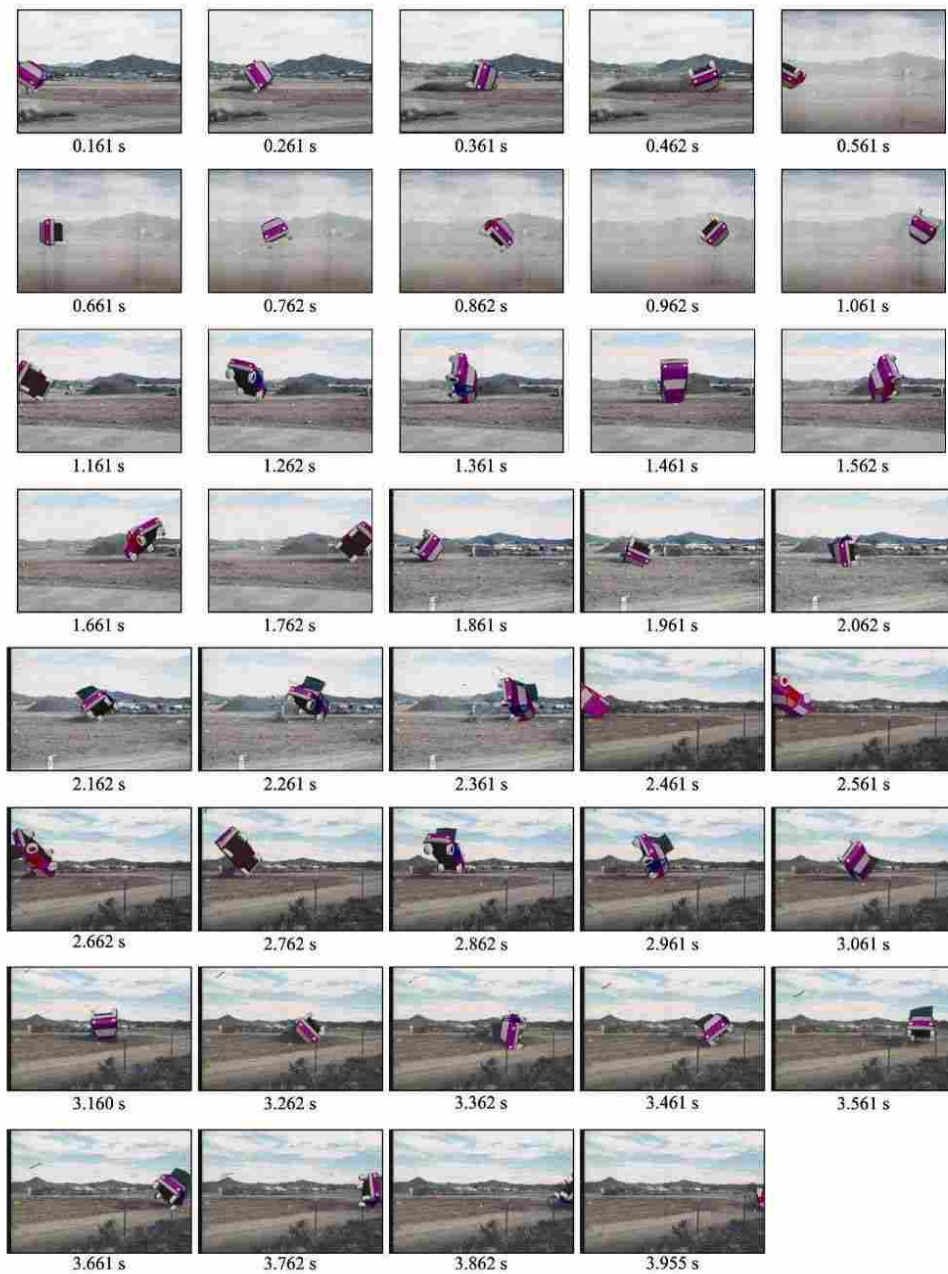








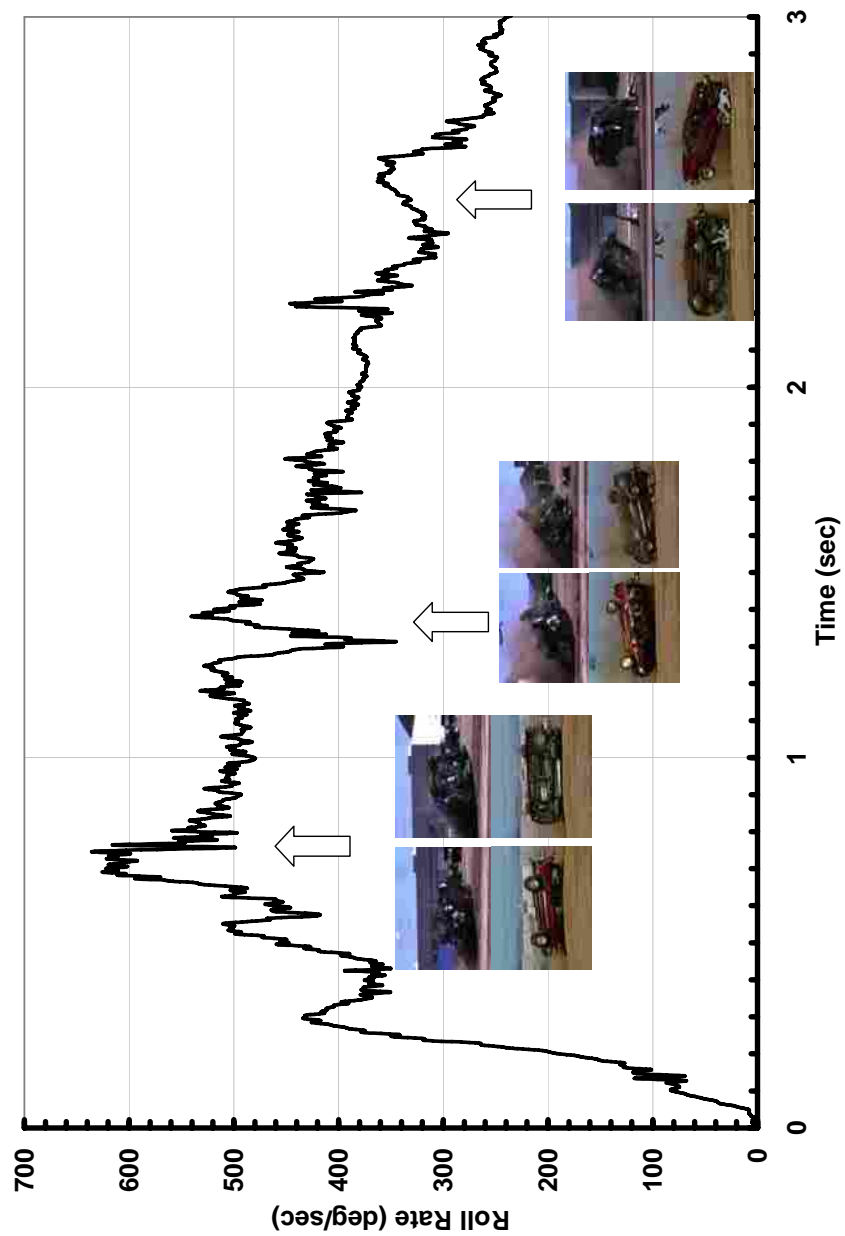
## Appendix D – Filmstrip for Test 1

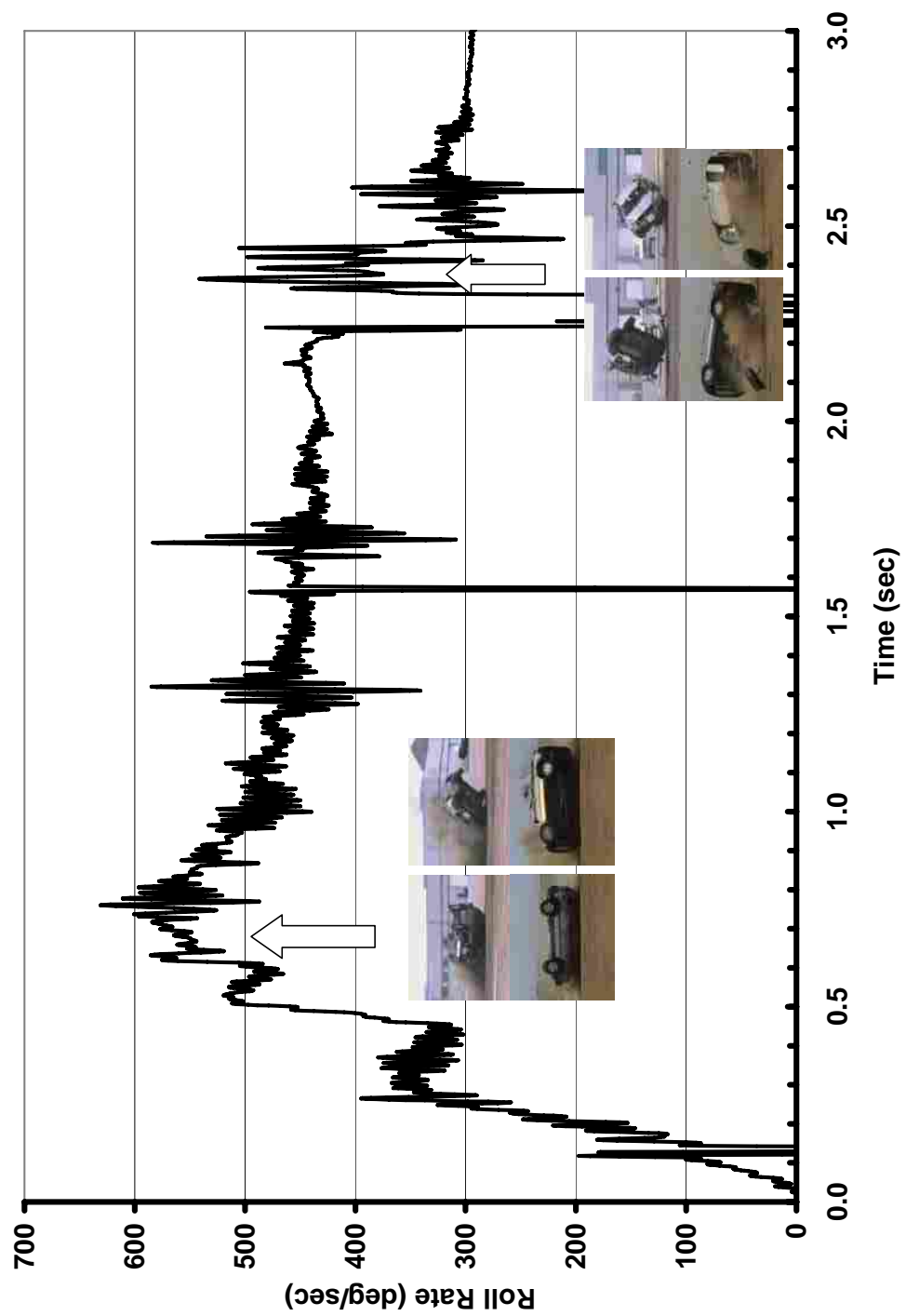






## Appendix E – Impact Effects on Roll Rate





## Appendix F – Tabular Data for Test 1

Time [sec]	Translational Distance (x) [m]	Elevation z [m]	Vehicle Angle [deg]		
			Roll	Pitch	Yaw
0.161	0.17	0.65	33.4	-0.55	-0.77
0.163	0.22	0.65	33.4	-0.55	-0.78
0.165	0.27	0.64	33.4	-0.56	-0.78
0.167	0.32	0.64	33.5	-0.56	-0.80
0.169	0.37	0.64	33.6	-0.58	-0.81
0.171	0.42	0.64	33.7	-0.59	-0.84
0.173	0.47	0.64	33.8	-0.61	-0.86
0.176	0.51	0.64	34.0	-0.63	-0.89
0.178	0.56	0.64	34.1	-0.65	-0.92
0.180	0.61	0.64	34.3	-0.67	-0.95
0.182	0.66	0.64	34.5	-0.70	-0.98
0.184	0.70	0.63	34.8	-0.73	-1.01
0.186	0.75	0.63	35.0	-0.75	-1.04
0.188	0.80	0.63	35.2	-0.78	-1.08
0.190	0.84	0.63	35.5	-0.81	-1.10
0.193	0.89	0.63	35.8	-0.85	-1.13
0.195	0.94	0.63	36.1	-0.88	-1.16
0.197	0.99	0.64	36.4	-0.91	-1.18
0.199	1.03	0.64	36.7	-0.95	-1.19
0.201	1.08	0.64	37.0	-0.98	-1.20
0.203	1.13	0.64	37.3	-1.01	-1.21
0.205	1.17	0.64	37.6	-1.05	-1.21
0.208	1.22	0.64	38.0	-1.08	-1.20
0.210	1.27	0.64	38.3	-1.11	-1.19
0.212	1.31	0.64	38.7	-1.14	-1.16
0.214	1.36	0.64	39.0	-1.17	-1.13
0.216	1.41	0.64	39.5	-1.21	-1.07
0.218	1.46	0.64	39.9	-1.24	-0.99
0.220	1.50	0.64	40.5	-1.28	-0.91
0.223	1.55	0.64	41.0	-1.31	-0.81
0.225	1.60	0.65	41.6	-1.33	-0.71
0.227	1.64	0.65	42.2	-1.35	-0.60
0.229	1.69	0.65	42.9	-1.36	-0.50
0.231	1.74	0.65	43.5	-1.36	-0.40
0.233	1.78	0.65	44.2	-1.36	-0.31
0.235	1.83	0.65	44.9	-1.36	-0.22

0.237	1.87	0.65	45.6	-1.36	-0.16
0.240	1.92	0.66	46.3	-1.36	-0.10
0.242	1.97	0.66	47.0	-1.35	-0.07
0.244	2.01	0.66	47.7	-1.34	-0.06
0.246	2.06	0.67	48.5	-1.31	-0.06
0.248	2.10	0.68	49.3	-1.28	-0.08
0.250	2.15	0.69	50.1	-1.25	-0.10
0.252	2.19	0.69	50.9	-1.22	-0.11
0.255	2.24	0.70	51.8	-1.19	-0.11
0.257	2.29	0.71	52.7	-1.17	-0.09
0.259	2.33	0.72	53.7	-1.15	-0.06
0.261	2.38	0.72	54.7	-1.15	0.00
0.263	2.42	0.73	55.7	-1.12	0.08
0.265	2.47	0.73	56.8	-1.03	0.16
0.267	2.51	0.74	57.8	-0.89	0.23
0.270	2.56	0.74	58.9	-0.71	0.26
0.272	2.61	0.75	60.1	-0.51	0.25
0.274	2.65	0.75	61.2	-0.31	0.20
0.276	2.70	0.76	62.3	-0.11	0.09
0.278	2.74	0.76	63.5	0.06	-0.07
0.280	2.79	0.76	64.6	0.19	-0.26
0.282	2.83	0.77	65.8	0.28	-0.47
0.284	2.88	0.77	66.9	0.30	-0.70
0.287	2.93	0.78	68.1	0.28	-0.90
0.289	2.97	0.78	69.3	0.21	-1.08
0.291	3.02	0.79	70.4	0.12	-1.22
0.293	3.07	0.79	71.6	0.01	-1.31
0.295	3.11	0.79	72.7	-0.09	-1.33
0.297	3.16	0.80	73.9	-0.17	-1.31
0.299	3.20	0.80	75.0	-0.23	-1.27
0.302	3.25	0.80	76.2	-0.27	-1.21
0.304	3.29	0.80	77.4	-0.30	-1.14
0.306	3.33	0.79	78.5	-0.30	-1.07
0.308	3.38	0.79	79.7	-0.30	-1.01
0.310	3.42	0.79	80.9	-0.29	-0.95
0.312	3.46	0.79	82.0	-0.27	-0.90
0.314	3.51	0.79	83.2	-0.26	-0.87
0.317	3.55	0.80	84.4	-0.25	-0.86
0.319	3.59	0.80	85.5	-0.26	-0.84
0.321	3.63	0.80	86.7	-0.26	-0.80
0.323	3.67	0.80	87.9	-0.23	-0.76
0.325	3.70	0.80	89.0	-0.15	-0.74
0.327	3.74	0.80	90.1	0.00	-0.74
0.329	3.77	0.82	91.2	0.27	-0.25
0.331	3.81	0.83	92.2	0.00	0.00
0.334	3.86	0.84	93.2	0.01	0.00
0.336	3.91	0.84	94.3	0.03	0.01
0.338	3.95	0.83	95.4	0.06	0.03
0.340	4.00	0.83	96.4	0.09	0.04
0.342	4.05	0.83	97.5	0.12	0.06
0.344	4.10	0.83	98.6	0.15	0.07

0.346	4.15	0.83	99.7	0.15	0.08
0.349	4.19	0.83	100.8	0.16	0.09
0.351	4.23	0.83	101.8	0.18	0.10
0.353	4.27	0.84	102.9	0.20	0.12
0.355	4.31	0.84	104.0	0.24	0.14
0.357	4.35	0.84	105.1	0.27	0.16
0.359	4.39	0.84	106.2	0.31	0.18
0.361	4.43	0.85	107.2	0.34	0.19
0.364	4.47	0.85	108.3	0.36	0.21
0.366	4.51	0.85	109.4	0.36	0.21
0.368	4.55	0.85	110.5	0.37	0.22
0.370	4.60	0.86	111.6	0.38	0.24
0.372	4.64	0.86	112.6	0.40	0.26
0.374	4.69	0.86	113.7	0.43	0.28
0.376	4.73	0.86	114.8	0.46	0.31
0.378	4.78	0.87	115.9	0.50	0.34
0.381	4.82	0.87	117.0	0.53	0.38
0.383	4.87	0.87	118.0	0.57	0.42
0.385	4.91	0.87	119.1	0.60	0.45
0.387	4.96	0.87	120.2	0.63	0.49
0.389	5.00	0.88	121.3	0.65	0.52
0.391	5.04	0.88	122.4	0.67	0.55
0.393	5.09	0.88	123.4	0.67	0.57
0.396	5.13	0.88	124.5	0.67	0.58
0.398	5.18	0.89	125.6	0.67	0.59
0.400	5.22	0.89	126.7	0.67	0.61
0.402	5.26	0.89	127.8	0.68	0.63
0.404	5.31	0.89	129.0	0.69	0.66
0.406	5.35	0.90	130.1	0.71	0.70
0.408	5.40	0.90	131.2	0.73	0.74
0.411	5.44	0.90	132.4	0.75	0.78
0.413	5.49	0.90	133.5	0.78	0.83
0.415	5.53	0.90	134.7	0.81	0.88
0.417	5.57	0.90	135.8	0.84	0.94
0.419	5.62	0.90	137.0	0.88	1.00
0.421	5.66	0.91	138.2	0.91	1.07
0.423	5.71	0.91	139.3	0.94	1.14
0.425	5.75	0.91	140.5	0.98	1.21
0.428	5.79	0.91	141.6	1.01	1.28
0.430	5.84	0.91	142.8	1.04	1.36
0.432	5.88	0.91	143.9	1.07	1.43
0.434	5.93	0.91	145.1	1.10	1.51
0.436	5.97	0.91	146.2	1.12	1.59
0.438	6.02	0.91	147.3	1.15	1.67
0.440	6.06	0.91	148.4	1.17	1.75
0.443	6.10	0.91	149.5	1.18	1.83
0.445	6.15	0.91	150.6	1.20	1.90
0.447	6.19	0.91	151.7	1.21	1.98
0.449	6.24	0.91	152.8	1.21	2.05
0.451	6.28	0.91	153.8	1.22	2.12
0.453	6.32	0.91	154.8	1.21	2.18

0.455	6.37	0.91	155.8	1.21	2.24
0.458	6.41	0.91	156.8	1.19	2.30
0.460	6.46	0.91	157.8	1.18	2.34
0.462	6.50	0.91	158.7	1.16	2.39
0.464	6.54	0.91	159.7	1.13	2.42
0.466	6.59	0.91	160.6	1.10	2.45
0.468	6.63	0.91	161.4	1.07	2.47
0.470	6.67	0.92	162.3	1.03	2.50
0.472	6.72	0.92	163.3	1.00	2.53
0.475	6.76	0.92	164.3	0.97	2.58
0.477	6.80	0.92	165.3	0.93	2.63
0.479	6.84	0.92	166.5	0.90	2.69
0.481	6.88	0.92	167.7	0.86	2.75
0.483	6.92	0.92	168.9	0.82	2.81
0.485	6.96	0.92	170.3	0.76	2.86
0.487	7.01	0.92	171.7	0.70	2.91
0.490	7.05	0.92	173.1	0.63	2.95
0.492	7.09	0.92	174.7	0.56	2.97
0.494	7.13	0.93	176.1	0.46	2.95
0.496	7.17	0.93	177.3	0.35	2.87
0.498	7.21	0.93	178.3	0.23	2.74
0.500	7.25	0.94	179.1	0.12	2.57
0.502	7.29	0.95	179.9	0.02	2.39
0.505	7.33	0.95	180.7	-0.07	2.20
0.507	7.37	0.96	181.5	-0.14	2.02
0.509	7.41	0.97	182.5	-0.20	1.87
0.511	7.46	0.97	183.8	-0.25	1.77
0.513	7.50	0.97	185.3	-0.30	1.72
0.515	7.54	0.97	186.9	-0.35	1.71
0.517	7.59	0.96	188.6	-0.40	1.67
0.519	7.63	0.96	190.4	-0.44	1.63
0.522	7.68	0.95	192.0	-0.48	1.57
0.524	7.73	0.94	193.6	-0.51	1.51
0.526	7.77	0.93	195.1	-0.54	1.45
0.528	7.82	0.93	196.5	-0.55	1.39
0.530	7.86	0.92	197.8	-0.57	1.33
0.532	7.90	0.91	198.8	-0.58	1.28
0.534	7.95	0.91	199.6	-0.58	1.24
0.537	7.99	0.90	200.2	-0.59	1.22
0.539	8.03	0.90	200.5	-0.59	1.21
0.541	8.07	0.90	200.8	-0.58	1.21
0.543	8.11	0.90	201.3	-0.54	1.23
0.545	8.16	0.90	202.1	-0.49	1.26
0.547	8.20	0.90	203.1	-0.43	1.28
0.549	8.24	0.90	204.1	-0.37	1.30
0.551	8.74	0.92	199.9	-1.08	3.22
0.553	8.78	0.93	201.2	-1.17	3.24
0.555	8.82	0.93	202.6	-1.25	3.24
0.557	8.86	0.93	204.0	-1.34	3.23
0.559	8.90	0.93	205.5	-1.42	3.20
0.561	8.94	0.93	206.9	-1.51	3.16

0.563	8.98	0.93	208.3	-1.61	3.12
0.565	9.02	0.93	209.5	-1.71	3.08
0.567	9.06	0.93	210.7	-1.81	3.03
0.569	9.10	0.94	211.8	-1.92	2.97
0.571	9.14	0.94	212.8	-2.03	2.92
0.573	9.18	0.94	213.8	-2.14	2.85
0.575	9.22	0.94	214.9	-2.26	2.78
0.576	9.25	0.94	215.9	-2.37	2.71
0.578	9.29	0.94	216.9	-2.48	2.63
0.580	9.33	0.94	218.1	-2.58	2.55
0.582	9.37	0.94	219.2	-2.69	2.46
0.584	9.41	0.94	220.5	-2.78	2.36
0.586	9.45	0.94	221.8	-2.88	2.27
0.588	9.49	0.94	223.3	-2.96	2.17
0.590	9.53	0.94	224.9	-3.04	2.07
0.592	9.57	0.93	226.7	-3.10	1.97
0.594	9.61	0.93	228.3	-3.15	1.87
0.596	9.65	0.93	229.7	-3.17	1.78
0.598	9.69	0.93	231.0	-3.17	1.69
0.600	9.72	0.93	232.2	-3.18	1.60
0.602	9.76	0.93	233.7	-3.21	1.52
0.604	9.80	0.92	235.1	-3.29	1.44
0.606	9.83	0.92	236.2	-3.45	1.38
0.608	9.87	0.92	237.1	-3.63	1.32
0.610	9.90	0.92	238.0	-3.82	1.25
0.612	9.94	0.92	238.9	-3.96	1.17
0.614	9.97	0.92	240.0	-4.03	1.08
0.616	10.01	0.91	241.2	-3.99	0.97
0.618	10.04	0.91	242.6	-3.85	0.84
0.620	10.08	0.91	244.0	-3.64	0.71
0.622	10.11	0.91	245.4	-3.41	0.60
0.624	10.15	0.91	246.9	-3.19	0.51
0.626	10.19	0.90	248.2	-3.03	0.47
0.628	10.23	0.90	249.5	-2.96	0.47
0.630	10.26	0.90	250.7	-2.99	0.51
0.632	10.30	0.89	251.9	-3.08	0.59
0.634	10.34	0.89	253.1	-3.22	0.69
0.636	10.38	0.89	254.2	-3.38	0.83
0.638	10.42	0.89	255.4	-3.56	0.99
0.639	10.46	0.89	256.5	-3.74	1.17
0.641	10.50	0.89	257.6	-3.90	1.35
0.643	10.54	0.88	258.8	-4.04	1.53
0.645	10.57	0.88	259.9	-4.14	1.68
0.647	10.61	0.88	261.0	-4.21	1.79
0.649	10.65	0.88	262.2	-4.23	1.85
0.651	10.69	0.87	263.3	-4.19	1.86
0.653	10.73	0.87	264.5	-4.11	1.83
0.655	10.77	0.87	265.6	-4.00	1.77
0.657	10.81	0.87	266.7	-3.88	1.69
0.659	10.85	0.86	267.8	-3.73	1.60
0.661	10.89	0.86	269.0	-3.59	1.49



0.663	10.93	0.86	270.1	-3.46	1.38
0.665	10.97	0.86	271.3	-3.34	1.26
0.667	11.01	0.85	272.5	-3.25	1.15
0.669	11.05	0.85	273.7	-3.20	1.04
0.671	11.09	0.85	275.0	-3.20	0.94
0.673	11.13	0.86	276.5	-3.43	0.71
0.675	11.17	0.87	278.2	-3.79	0.28
0.677	11.21	0.87	279.8	-3.96	-0.10
0.679	11.25	0.86	281.1	-3.93	-0.32
0.681	11.29	0.86	282.5	-3.83	-0.52
0.683	11.33	0.86	283.8	-3.69	-0.71
0.685	11.36	0.85	285.1	-3.51	-0.87
0.687	11.40	0.85	286.5	-3.30	-1.00
0.689	11.44	0.84	287.8	-3.07	-1.10
0.691	11.47	0.84	289.1	-2.82	-1.17
0.693	11.51	0.84	290.4	-2.58	-1.22
0.695	11.55	0.84	291.7	-2.33	-1.24
0.697	11.58	0.83	293.0	-2.10	-1.25
0.699	11.62	0.83	294.3	-1.88	-1.24
0.701	11.65	0.83	295.6	-1.69	-1.22
0.703	11.69	0.82	296.9	-1.52	-1.21
0.704	11.73	0.82	298.2	-1.38	-1.20
0.706	11.76	0.82	299.5	-1.28	-1.21
0.708	11.80	0.81	300.8	-1.20	-1.25
0.710	11.84	0.81	302.2	-1.13	-1.28
0.712	11.87	0.81	303.5	-1.04	-1.28
0.714	11.91	0.80	304.8	-0.92	-1.25
0.716	11.95	0.80	306.1	-0.79	-1.18
0.718	11.98	0.79	307.4	-0.65	-1.07
0.720	12.02	0.79	308.7	-0.51	-0.94
0.722	12.06	0.78	310.0	-0.38	-0.78
0.724	12.09	0.78	311.3	-0.26	-0.59
0.726	12.13	0.77	312.6	-0.15	-0.39
0.728	12.17	0.77	313.9	-0.06	-0.17
0.730	12.21	0.77	315.2	0.02	0.06
0.732	12.24	0.76	316.5	0.07	0.29
0.734	12.28	0.76	317.8	0.11	0.52
0.736	12.32	0.75	319.1	0.12	0.74
0.738	12.35	0.75	320.4	0.12	0.95
0.740	12.39	0.75	321.8	0.10	1.14
0.742	12.43	0.74	323.1	0.07	1.30
0.744	12.47	0.74	324.4	0.04	1.43
0.746	12.50	0.74	325.7	-0.01	1.54
0.748	12.54	0.73	327.0	-0.05	1.60
0.750	12.58	0.73	328.3	-0.10	1.62
0.752	12.61	0.73	329.6	-0.13	1.62
0.754	12.65	0.73	330.8	-0.17	1.64
0.756	12.69	0.73	332.0	-0.20	1.67
0.758	12.73	0.73	333.1	-0.24	1.71
0.760	12.77	0.72	334.2	-0.27	1.76
0.762	12.81	0.72	335.4	-0.30	1.82

0.764	12.85	0.72	336.5	-0.33	1.88
0.766	12.89	0.72	337.6	-0.35	1.94
0.767	12.93	0.72	338.8	-0.37	2.01
0.769	12.97	0.72	340.0	-0.39	2.07
0.771	13.00	0.72	341.3	-0.41	2.14
0.773	13.04	0.72	342.6	-0.42	2.19
0.775	13.08	0.72	344.0	-0.43	2.25
0.777	13.12	0.72	345.6	-0.43	2.29
0.779	13.16	0.72	347.2	-0.43	2.33
0.781	13.19	0.72	349.0	-0.42	2.35
0.783	13.23	0.71	350.9	-0.40	2.36
0.785	13.26	0.71	352.9	-0.36	2.50
0.787	13.30	0.71	354.8	-0.27	2.83
0.789	13.34	0.72	356.5	-0.10	3.26
0.791	13.37	0.72	357.7	0.12	3.67
0.793	13.41	0.72	358.4	0.33	3.98
0.795	13.45	0.72	358.3	0.45	4.10
0.797	13.49	0.73	358.7	0.43	4.19
0.799	13.52	0.73	360.4	0.32	4.43
0.801	13.55	0.73	362.8	0.14	4.73
0.803	13.58	0.73	365.2	-0.07	5.02
0.805	13.62	0.74	366.8	-0.25	5.24
0.807	13.66	0.74	366.9	-0.33	5.33
0.809	13.70	0.73	366.6	-0.33	5.35
0.811	13.75	0.73	367.3	-0.31	5.43
0.813	13.79	0.73	368.6	-0.29	5.52
0.815	13.84	0.72	370.5	-0.27	5.63
0.817	13.88	0.71	372.6	-0.25	5.73
0.819	13.92	0.71	374.8	-0.24	5.80
0.821	13.96	0.70	376.9	-0.23	5.83
0.823	14.00	0.70	378.6	-0.27	5.85
0.825	14.04	0.69	380.1	-0.35	5.92
0.827	14.08	0.68	381.4	-0.47	6.01
0.829	14.12	0.68	382.6	-0.61	6.10
0.830	14.16	0.67	383.9	-0.74	6.19
0.832	14.20	0.67	385.3	-0.83	6.25
0.834	14.24	0.67	387.0	-0.87	6.27
0.836	14.27	0.67	389.2	-0.87	6.28
0.838	14.30	0.67	391.5	-0.88	6.29
0.840	14.33	0.67	393.0	-0.89	6.30
0.842	14.36	0.67	394.1	-0.99	6.29
0.844	14.39	0.67	396.0	-1.23	6.26
0.846	14.41	0.68	397.9	-1.47	6.21
0.848	14.44	0.68	399.3	-1.69	6.24
0.850	14.48	0.68	400.1	-1.96	6.36
0.852	14.51	0.68	401.0	-2.23	6.47
0.854	14.54	0.68	402.4	-2.48	6.47
0.856	14.56	0.69	404.2	-2.76	6.45
0.858	14.59	0.69	405.7	-3.11	6.49
0.860	14.62	0.69	406.7	-3.42	6.55
0.862	14.66	0.69	407.1	-3.55	6.57

0.864	14.71	0.68	407.4	-3.37	6.76
0.866	14.77	0.67	408.3	-3.00	7.09
0.868	14.82	0.66	409.4	-2.80	7.26
0.870	14.85	0.66	410.4	-2.75	7.21
0.872	14.88	0.66	411.2	-2.63	7.06
0.874	14.91	0.66	411.8	-2.48	6.84
0.876	14.95	0.67	412.4	-2.32	6.56
0.878	14.98	0.67	413.1	-2.19	6.24
0.880	15.00	0.67	414.0	-2.10	5.90
0.882	15.03	0.68	415.3	-2.08	5.57
0.884	15.06	0.68	417.0	-2.14	5.26
0.886	15.09	0.69	419.3	-2.31	5.00
0.888	15.11	0.70	422.3	-2.60	4.78
0.890	15.14	0.71	425.3	-2.87	4.48
0.892	15.17	0.72	427.8	-2.98	4.05
0.893	15.19	0.73	430.0	-2.95	3.57
0.895	15.22	0.74	432.1	-2.83	3.08
0.897	15.25	0.74	434.2	-2.70	2.65
0.899	15.28	0.75	436.6	-2.61	2.31
0.901	15.30	0.76	439.4	-2.64	2.10
0.903	15.33	0.77	442.2	-2.74	1.92
0.905	15.35	0.78	444.1	-2.80	1.74
0.907	15.38	0.78	444.9	-2.82	1.65
0.909	15.40	0.79	445.7	-3.50	1.88
0.911	15.42	0.79	447.3	-4.24	2.50
0.913	15.46	0.80	450.6	-4.49	2.90
0.915	15.47	0.81	451.5	-4.50	2.68
0.917	15.48	0.81	452.2	-4.48	2.62
0.919	15.50	0.81	454.0	-4.41	2.46
0.921	15.54	0.81	456.2	-4.33	2.27
0.923	15.57	0.82	458.4	-4.27	2.09
0.925	15.60	0.82	460.0	-4.26	1.96
0.927	15.63	0.83	461.3	-4.24	1.86
0.929	15.66	0.84	463.1	-4.15	1.73
0.931	15.69	0.85	465.1	-4.03	1.60
0.933	15.71	0.87	467.1	-3.93	1.48
0.935	15.74	0.88	469.0	-3.90	1.39
0.937	15.77	0.89	470.9	-3.90	1.28
0.939	15.80	0.90	472.8	-3.85	1.15
0.941	15.83	0.91	474.6	-3.77	0.99
0.943	15.86	0.92	476.5	-3.65	0.84
0.945	15.89	0.93	478.4	-3.52	0.70
0.947	15.92	0.94	480.3	-3.39	0.58
0.949	15.96	0.95	482.1	-3.28	0.50
0.951	15.99	0.96	483.9	-3.20	0.46
0.953	16.02	0.97	485.6	-3.16	0.47
0.955	16.05	0.98	487.3	-3.14	0.50
0.956	16.08	0.98	489.0	-3.09	0.53
0.958	16.11	0.99	490.6	-3.02	0.56
0.960	16.14	1.00	492.2	-2.93	0.59
0.962	16.18	1.01	493.9	-2.83	0.62

0.964	16.21	1.02	495.5	-2.71	0.65
0.966	16.24	1.03	497.0	-2.58	0.69
0.968	16.27	1.04	498.6	-2.46	0.73
0.970	16.30	1.05	500.2	-2.33	0.78
0.972	16.33	1.06	501.8	-2.20	0.84
0.974	16.37	1.07	503.3	-2.09	0.90
0.976	16.40	1.07	504.9	-1.98	0.98
0.978	16.43	1.08	506.4	-1.88	1.08
0.980	16.46	1.09	508.0	-1.78	1.20
0.982	16.49	1.10	509.7	-1.69	1.37
0.984	16.51	1.11	511.5	-1.56	1.62
0.986	16.54	1.12	513.5	-1.39	1.92
0.988	16.57	1.13	515.5	-1.13	2.24
0.990	16.60	1.14	517.5	-0.79	2.55
0.992	16.63	1.15	519.5	-0.38	2.82
0.994	16.66	1.16	521.3	0.08	3.02
0.996	16.68	1.17	522.9	0.56	3.13
0.998	16.71	1.18	524.2	0.99	3.17
1.000	16.73	1.18	525.3	1.35	3.16
1.002	16.76	1.19	525.9	1.59	3.14
1.004	16.78	1.19	526.2	1.67	3.12
1.006	16.81	1.19	526.6	1.69	3.20
1.008	16.83	1.19	527.6	1.72	3.41
1.010	16.86	1.19	529.1	1.75	3.69
1.012	16.89	1.19	530.8	1.75	3.97
1.014	16.92	1.19	532.6	1.70	4.21
1.016	16.94	1.19	534.2	1.61	4.33
1.018	16.97	1.20	536.2	1.50	4.50
1.019	17.00	1.20	538.6	1.39	4.78
1.021	17.03	1.20	540.0	1.33	4.93
1.023	17.06	1.20	542.0	1.15	5.07
1.025	17.08	1.20	542.4	1.21	5.24
1.027	17.09	1.21	543.5	1.34	5.61
1.029	17.11	1.21	545.2	1.49	5.98
1.031	17.13	1.21	547.3	1.62	6.13
1.033	17.16	1.22	549.7	1.70	6.04
1.035	17.20	1.22	552.1	1.82	6.10
1.037	17.23	1.23	554.4	1.94	6.16
1.039	17.26	1.23	556.5	2.08	6.31
1.041	17.30	1.24	558.2	2.21	6.46
1.043	17.33	1.25	559.4	2.30	6.56
1.045	17.35	1.26	559.8	2.32	6.58
1.047	17.37	1.26	562.0	2.17	6.65
1.049	17.39	1.27	564.2	2.18	7.25
1.051	17.42	1.27	567.8	2.33	7.19
1.053	17.45	1.28	569.2	2.44	7.87
1.055	17.47	1.29	570.9	2.55	8.19
1.057	17.50	1.30	571.1	2.40	8.32
1.059	17.54	1.31	571.8	2.01	8.63
1.061	17.57	1.32	572.8	1.43	9.00
1.063	17.60	1.34	574.0	0.75	9.34

1.065	17.64	1.35	575.5	0.08	9.57
1.067	17.67	1.35	577.1	-0.42	9.64
1.069	17.69	1.34	578.8	-0.78	9.70
1.071	17.72	1.34	580.8	-1.11	9.87
1.073	17.74	1.34	583.0	-1.43	10.12
1.075	17.77	1.34	585.2	-1.73	10.41
1.077	17.79	1.33	587.5	-2.02	10.70
1.079	17.81	1.33	589.6	-2.29	10.94
1.081	17.84	1.33	591.7	-2.53	11.10
1.082	17.86	1.32	593.5	-2.74	11.13
1.084	17.89	1.32	595.1	-2.93	11.11
1.086	17.92	1.32	596.7	-3.13	11.14
1.088	17.95	1.32	598.2	-3.33	11.22
1.090	17.98	1.37	599.8	-3.53	11.33
1.092	18.01	1.33	601.2	-3.74	11.46
1.094	18.04	1.33	602.7	-3.96	11.62
1.096	18.07	1.33	604.2	-4.18	11.78
1.098	18.10	1.34	605.6	-4.40	11.95
1.100	18.13	1.34	607.0	-4.62	12.10
1.102	17.86	1.36	606.2	11.29	-10.57
1.104	17.89	1.36	607.8	11.54	-10.72
1.106	17.92	1.37	609.5	11.78	-10.86
1.108	17.96	1.37	611.2	12.03	-10.98
1.110	17.99	1.37	612.9	12.27	-11.10
1.112	18.02	1.38	614.6	12.50	-11.20
1.114	18.05	1.38	616.3	12.73	-11.28
1.116	18.08	1.38	618.1	12.94	-11.34
1.118	18.11	1.39	619.8	13.13	-11.38
1.120	18.14	1.39	621.5	13.30	-11.40
1.123	18.17	1.39	623.2	13.44	-11.39
1.125	18.19	1.39	625.0	13.55	-11.36
1.127	18.22	1.40	626.7	13.63	-11.30
1.129	18.24	1.40	628.4	13.71	-11.24
1.131	18.27	1.40	630.2	13.84	-11.21
1.133	18.29	1.40	632.0	14.00	-11.20
1.135	18.31	1.40	633.8	14.20	-11.20
1.137	18.33	1.41	635.6	14.41	-11.21
1.139	18.35	1.41	637.5	14.63	-11.22
1.141	18.37	1.41	639.3	14.85	-11.22
1.143	18.38	1.41	641.2	15.07	-11.22
1.145	18.40	1.42	643.0	15.27	-11.20
1.147	18.42	1.42	644.8	15.45	-11.16
1.149	18.44	1.42	646.6	15.59	-11.09
1.151	18.47	1.43	648.3	15.69	-11.00
1.153	18.49	1.44	650.0	15.77	-10.89
1.155	18.52	1.45	651.7	15.86	-10.79
1.157	18.55	1.46	653.3	15.96	-10.70
1.159	18.58	1.47	654.9	16.06	-10.61
1.161	18.61	1.49	656.5	16.16	-10.51
1.163	18.64	1.50	658.1	16.26	-10.42
1.165	18.67	1.51	659.7	16.35	-10.31

1.167	18.70	1.52	661.4	16.42	-10.20
1.169	18.73	1.52	663.0	16.50	-10.08
1.171	18.76	1.53	664.7	16.61	-9.94
1.173	18.79	1.54	666.5	16.73	-9.81
1.175	18.81	1.54	668.2	16.85	-9.67
1.177	18.84	1.55	669.9	16.98	-9.54
1.179	18.87	1.55	671.6	17.08	-9.43
1.181	18.90	1.55	673.1	17.17	-9.34
1.183	18.92	1.55	674.6	17.23	-9.29
1.185	18.95	1.55	675.9	17.25	-9.26
1.187	18.98	1.55	677.4	17.46	-9.27
1.189	19.01	1.55	679.3	17.95	-9.29
1.191	19.03	1.55	681.3	18.54	-9.29
1.193	19.06	1.55	683.2	19.03	-9.28
1.195	19.09	1.55	684.7	19.24	-9.28
1.197	19.12	1.55	686.0	19.35	-9.30
1.199	19.16	1.55	687.4	19.65	-9.37
1.201	19.19	1.55	688.9	20.06	-9.45
1.203	19.22	1.55	690.4	20.54	-9.55
1.206	19.25	1.55	692.0	21.02	-9.64
1.208	19.28	1.55	693.4	21.44	-9.72
1.210	19.31	1.55	694.8	21.74	-9.77
1.212	19.35	1.55	696.1	21.85	-9.79
1.214	19.38	1.55	697.3	21.96	-9.81
1.216	19.41	1.55	698.8	22.25	-9.85
1.218	19.44	1.54	700.3	22.68	-9.90
1.220	19.47	1.54	701.9	23.19	-9.94
1.222	19.50	1.54	703.6	23.73	-9.96
1.224	19.53	1.53	705.3	24.26	-9.94
1.226	19.56	1.53	706.9	24.73	-9.86
1.228	19.59	1.53	708.5	25.07	-9.73
1.230	19.62	1.53	710.1	25.25	-9.52
1.232	19.65	1.53	711.5	25.32	-9.26
1.234	19.67	1.54	713.0	25.39	-8.96
1.236	19.70	1.54	714.4	25.45	-8.64
1.238	19.73	1.55	715.9	25.51	-8.30
1.240	19.76	1.55	717.3	25.57	-7.96
1.242	19.78	1.56	718.7	25.62	-7.62
1.244	19.81	1.57	720.1	25.67	-7.29
1.246	19.84	1.57	721.6	25.71	-6.98
1.248	19.87	1.58	723.0	25.75	-6.70
1.250	19.90	1.58	724.4	25.80	-6.46
1.252	19.93	1.59	725.8	25.84	-6.26
1.254	19.96	1.59	727.2	25.90	-6.09
1.256	19.99	1.60	728.5	25.96	-5.94
1.258	20.02	1.60	729.9	26.03	-5.81
1.260	20.05	1.60	731.3	26.10	-5.69
1.262	20.08	1.61	732.6	26.17	-5.58
1.264	20.11	1.61	734.0	26.23	-5.48
1.266	20.14	1.61	735.4	26.29	-5.37
1.268	20.17	1.61	736.9	26.35	-5.26

1.270	20.20	1.61	738.4	26.39	-5.14
1.272	20.22	1.62	739.9	26.42	-5.01
1.274	20.25	1.62	741.5	26.44	-4.86
1.276	20.28	1.62	743.1	26.46	-4.70
1.278	20.31	1.62	744.8	26.49	-4.53
1.280	20.33	1.62	746.5	26.52	-4.36
1.282	20.36	1.62	748.2	26.55	-4.18
1.284	20.39	1.62	749.9	26.58	-3.99
1.286	20.41	1.62	751.7	26.61	-3.80
1.289	20.44	1.62	753.4	26.64	-3.61
1.291	20.47	1.62	755.2	26.68	-3.41
1.293	20.49	1.62	757.0	26.71	-3.22
1.295	20.52	1.62	758.8	26.74	-3.02
1.297	20.55	1.62	760.6	26.77	-2.83
1.299	20.58	1.63	762.5	26.80	-2.64
1.301	20.60	1.63	764.3	26.83	-2.45
1.303	20.63	1.63	766.1	26.85	-2.27
1.305	20.66	1.63	767.9	26.88	-2.09
1.307	20.69	1.63	769.7	26.90	-1.92
1.309	20.71	1.63	771.5	26.92	-1.76
1.311	20.74	1.63	773.3	26.94	-1.61
1.313	20.77	1.64	775.1	26.96	-1.47
1.315	20.80	1.64	776.8	26.98	-1.34
1.317	20.83	1.64	778.5	26.99	-1.23
1.319	20.86	1.64	780.2	27.01	-1.13
1.321	20.88	1.65	781.9	27.02	-1.04
1.323	20.91	1.65	783.5	27.03	-0.97
1.325	20.94	1.65	785.1	27.03	-0.92
1.327	20.97	1.66	786.7	27.04	-0.89
1.329	21.00	1.66	788.2	27.04	-0.88
1.331	21.03	1.66	789.6	27.02	-0.87
1.333	21.06	1.66	791.0	26.96	-0.82
1.335	21.10	1.67	792.4	26.88	-0.76
1.337	21.13	1.67	793.8	26.79	-0.69
1.339	21.16	1.67	795.1	26.69	-0.61
1.341	21.19	1.67	796.6	26.59	-0.54
1.343	21.22	1.67	798.1	26.51	-0.48
1.345	21.25	1.67	799.7	26.45	-0.44
1.347	21.28	1.68	801.4	26.43	-0.43
1.349	21.31	1.68	803.3	26.47	-0.44
1.351	21.34	1.69	805.2	26.58	-0.49
1.353	21.37	1.69	807.3	26.74	-0.56
1.355	21.39	1.70	809.4	26.92	-0.65
1.357	21.42	1.70	811.6	27.13	-0.74
1.359	21.45	1.71	813.8	27.34	-0.84
1.361	21.47	1.71	816.0	27.53	-0.93
1.363	21.50	1.72	818.1	27.68	-1.01
1.365	21.53	1.73	820.3	27.79	-1.06
1.367	21.56	1.73	822.3	27.82	-1.08
1.369	21.59	1.73	824.3	27.84	-1.05
1.372	21.62	1.74	826.4	27.86	-0.96

1.374	21.65	1.74	828.4	27.90	-0.84
1.376	21.68	1.74	830.5	27.95	-0.69
1.378	21.71	1.74	832.5	28.00	-0.53
1.380	21.74	1.74	834.5	28.05	-0.37
1.382	21.77	1.74	836.5	28.10	-0.22
1.384	21.80	1.74	838.4	28.14	-0.09
1.386	21.83	1.74	840.2	28.16	-0.01
1.388	21.86	1.74	841.9	28.17	0.02
1.390	21.89	1.74	843.6	28.16	0.03
1.392	21.92	1.75	845.3	28.14	0.03
1.394	21.95	1.75	846.9	28.11	0.04
1.396	21.98	1.75	848.6	28.06	0.05
1.398	22.01	1.75	850.3	28.01	0.06
1.400	22.04	1.75	851.9	27.95	0.08
1.402	22.07	1.75	853.5	27.88	0.09
1.404	22.10	1.75	855.2	27.81	0.11
1.406	22.13	1.75	856.8	27.74	0.13
1.408	22.16	1.75	858.4	27.66	0.15
1.410	22.19	1.76	860.0	27.58	0.17
1.412	22.22	1.76	861.5	27.51	0.18
1.414	22.25	1.76	863.1	27.44	0.20
1.416	22.28	1.76	864.6	27.37	0.22
1.418	22.31	1.76	866.1	27.31	0.23
1.420	22.34	1.76	867.6	27.25	0.24
1.422	22.37	1.76	869.0	27.21	0.25
1.424	22.40	1.76	870.4	27.18	0.26
1.426	22.42	1.76	871.8	27.15	0.27
1.428	22.45	1.76	873.2	27.15	0.27
1.430	22.48	1.76	874.6	27.14	0.29
1.432	22.51	1.76	876.0	27.13	0.34
1.434	22.53	1.76	877.4	27.11	0.43
1.436	22.56	1.76	878.9	27.08	0.54
1.438	22.59	1.76	880.4	27.04	0.68
1.440	22.61	1.75	881.9	27.00	0.84
1.442	22.64	1.75	883.4	26.96	1.01
1.444	22.67	1.75	884.9	26.91	1.20
1.446	22.69	1.75	886.5	26.85	1.39
1.448	22.72	1.75	888.0	26.80	1.59
1.450	22.75	1.75	889.6	26.74	1.78
1.452	22.77	1.75	891.1	26.69	1.97
1.455	22.80	1.74	892.6	26.63	2.15
1.457	22.82	1.74	894.1	26.58	2.32
1.459	22.85	1.74	895.6	26.53	2.47
1.461	22.88	1.74	897.0	26.49	2.60
1.463	22.90	1.74	898.4	26.45	2.71
1.465	22.93	1.74	899.8	26.43	2.79
1.467	22.95	1.74	901.2	26.41	2.84
1.469	22.98	1.74	902.4	26.40	2.86
1.471	23.01	1.74	903.7	26.40	2.87
1.473	23.03	1.74	905.0	26.38	2.87
1.475	23.06	1.74	906.4	26.35	2.88



1.477	23.09	1.73	907.8	26.32	2.90
1.479	23.11	1.73	909.2	26.28	2.92
1.481	23.14	1.73	910.6	26.23	2.94
1.483	23.17	1.73	912.1	26.18	2.96
1.485	23.20	1.73	913.5	26.13	2.98
1.487	23.22	1.73	915.0	26.08	3.00
1.489	23.25	1.72	916.5	26.04	3.02
1.491	23.28	1.72	917.9	26.00	3.03
1.493	23.31	1.72	919.4	25.96	3.05
1.495	23.33	1.72	920.8	25.93	3.06
1.497	23.36	1.71	922.2	25.92	3.07
1.499	23.39	1.71	923.6	25.91	3.07
1.501	23.42	1.71	925.0	25.89	3.06
1.503	23.44	1.71	926.4	25.84	3.04
1.505	23.47	1.71	927.7	25.76	3.01
1.507	23.50	1.71	929.0	25.66	2.97
1.509	23.53	1.70	930.3	25.54	2.93
1.511	23.55	1.70	931.7	25.41	2.88
1.513	23.58	1.70	933.0	25.27	2.82
1.515	23.61	1.70	934.3	25.13	2.77
1.517	23.64	1.70	935.7	24.99	2.72
1.519	23.66	1.70	937.1	24.86	2.67
1.521	23.69	1.70	938.5	24.74	2.63
1.523	23.72	1.70	939.9	24.64	2.59
1.525	23.75	1.70	941.4	24.56	2.57
1.527	23.78	1.70	942.9	24.51	2.55
1.529	23.81	1.70	944.4	24.49	2.54
1.531	23.84	1.70	946.0	24.49	2.53
1.533	23.87	1.70	947.6	24.49	2.51
1.535	23.90	1.70	949.2	24.50	2.47
1.538	23.93	1.70	950.8	24.50	2.42
1.540	23.96	1.70	952.4	24.51	2.36
1.542	23.99	1.70	954.0	24.51	2.29
1.544	24.02	1.70	955.6	24.52	2.22
1.546	24.05	1.70	957.2	24.52	2.14
1.548	24.08	1.69	958.8	24.53	2.06
1.550	24.11	1.69	960.5	24.54	1.97
1.552	24.14	1.69	962.1	24.54	1.88
1.554	24.17	1.69	963.7	24.55	1.80
1.556	24.21	1.69	965.4	24.55	1.72
1.558	24.24	1.69	967.0	24.56	1.65
1.560	24.27	1.69	968.6	24.56	1.58
1.562	24.30	1.69	970.2	24.56	1.52
1.564	24.33	1.69	971.8	24.57	1.47
1.566	24.35	1.69	973.4	24.57	1.43
1.568	24.38	1.69	975.0	24.57	1.41
1.570	24.41	1.69	976.6	24.57	1.40
1.572	24.44	1.69	978.2	24.58	1.43
1.574	24.47	1.69	979.8	24.60	1.53
1.576	24.50	1.69	981.4	24.64	1.67
1.578	24.53	1.69	983.0	24.69	1.86

1.580	24.56	1.69	984.7	24.75	2.07
1.582	24.58	1.69	986.3	24.81	2.31
1.584	24.61	1.69	987.9	24.87	2.56
1.586	24.64	1.69	989.5	24.93	2.81
1.588	24.67	1.69	991.2	24.98	3.06
1.590	24.70	1.69	992.8	25.03	3.28
1.592	24.72	1.69	994.3	25.07	3.47
1.594	24.75	1.68	995.9	25.10	3.62
1.596	24.78	1.68	997.4	25.12	3.72
1.598	24.81	1.68	998.9	25.12	3.76
1.600	24.84	1.68	1000.4	25.12	3.76
1.602	24.87	1.68	1002.0	25.10	3.78
1.604	24.90	1.68	1003.6	25.08	3.80
1.606	24.92	1.67	1005.3	25.05	3.84
1.608	24.95	1.67	1007.0	25.02	3.87
1.610	24.98	1.67	1008.8	24.98	3.92
1.612	25.01	1.67	1010.6	24.93	3.97
1.614	25.04	1.66	1012.4	24.89	4.01
1.616	25.07	1.66	1014.2	24.84	4.06
1.618	25.10	1.66	1016.0	24.80	4.11
1.621	25.13	1.65	1017.8	24.76	4.16
1.623	25.16	1.65	1019.6	24.72	4.20
1.625	25.19	1.65	1021.3	24.68	4.24
1.627	25.21	1.64	1023.0	24.65	4.27
1.629	25.24	1.64	1024.7	24.63	4.29
1.631	25.27	1.64	1026.3	24.61	4.31
1.633	25.30	1.63	1027.9	24.61	4.31
1.635	25.32	1.63	1029.4	24.60	4.33
1.637	25.35	1.63	1031.1	24.59	4.36
1.639	25.38	1.62	1032.8	24.57	4.42
1.641	25.40	1.62	1034.5	24.55	4.50
1.643	25.43	1.61	1036.2	24.52	4.60
1.645	25.46	1.61	1038.0	24.49	4.71
1.647	25.48	1.61	1039.8	24.45	4.84
1.649	25.51	1.60	1041.7	24.40	4.98
1.651	25.53	1.60	1043.5	24.36	5.13
1.653	25.56	1.59	1045.3	24.31	5.29
1.655	25.58	1.59	1047.1	24.26	5.45
1.657	25.61	1.59	1048.9	24.21	5.62
1.659	25.63	1.58	1050.7	24.16	5.80
1.661	25.66	1.58	1052.4	24.11	5.97
1.663	25.69	1.58	1054.1	24.06	6.14
1.665	25.71	1.57	1055.7	24.01	6.31
1.667	25.74	1.57	1057.3	23.97	6.48
1.669	25.77	1.57	1058.8	23.93	6.64
1.671	25.80	1.57	1060.2	23.87	6.80
1.673	25.83	1.57	1061.5	23.75	6.96
1.675	25.86	1.57	1062.7	23.59	7.12
1.677	25.89	1.57	1063.8	23.41	7.28
1.679	25.92	1.58	1064.8	23.20	7.44
1.681	25.96	1.58	1065.9	22.99	7.60

1.683	25.99	1.58	1066.9	22.78	7.75
1.685	26.02	1.58	1068.0	22.59	7.90
1.687	26.05	1.58	1069.1	22.42	8.06
1.689	26.09	1.58	1070.2	22.29	8.22
1.691	26.12	1.58	1071.5	22.21	8.38
1.693	26.15	1.58	1072.9	22.14	8.53
1.695	26.18	1.58	1074.3	22.06	8.67
1.697	26.21	1.57	1075.7	21.95	8.79
1.699	26.23	1.57	1077.2	21.84	8.91
1.702	26.26	1.56	1078.7	21.72	9.01
1.704	26.29	1.55	1080.3	21.60	9.11
1.706	26.32	1.55	1081.8	21.49	9.21
1.708	26.35	1.54	1083.3	21.39	9.32
1.710	26.38	1.54	1084.8	21.30	9.43
1.712	26.40	1.53	1086.3	21.24	9.56
1.714	26.43	1.52	1087.7	21.17	9.69
1.716	26.46	1.52	1089.1	21.09	9.80
1.718	26.48	1.52	1090.5	20.99	9.91
1.720	26.51	1.51	1091.9	20.88	10.01
1.722	26.54	1.51	1093.2	20.76	10.10
1.724	26.56	1.50	1094.6	20.62	10.18
1.726	26.59	1.50	1096.0	20.48	10.26
1.728	26.62	1.49	1097.3	20.32	10.33
1.730	26.65	1.49	1098.7	20.17	10.40
1.732	26.67	1.48	1100.0	20.01	10.47
1.734	26.70	1.48	1101.4	19.85	10.53
1.736	26.73	1.48	1102.8	19.70	10.60
1.738	26.75	1.47	1104.2	19.54	10.67
1.740	26.78	1.47	1105.6	19.39	10.74
1.742	26.80	1.46	1107.0	19.25	10.82
1.744	26.83	1.46	1108.4	19.12	10.90
1.746	26.86	1.46	1109.9	19.00	10.99
1.748	26.88	1.45	1111.3	18.89	11.09
1.750	26.91	1.45	1112.8	18.79	11.20
1.752	26.94	1.45	1114.328	18.7	11.3
1.754	26.96	1.44	1115.877	18.6	11.4
1.756	26.99	1.44	1117.48	18.5	11.5
1.758	27.01	1.43	1119.13	18.3	11.6
1.760	27.04	1.43	1120.82	18.2	11.7
1.762	27.07	1.43	1122.542	18.0	11.7
1.764	27.09	1.42	1124.288	17.7	11.8
1.766	27.12	1.42	1126.051	17.5	11.8
1.768	27.14	1.41	1127.821	17.3	11.9
1.770	27.17	1.41	1129.592	17.1	11.9
1.772	27.19	1.40	1131.352	16.9	11.9
1.774	27.22	1.40	1133.094	16.6	12.0
1.776	27.25	1.40	1134.808	16.4	12.1
1.778	27.27	1.39	1136.485	16.3	12.2
1.780	27.30	1.39	1138.115	16.1	12.3
1.782	27.33	1.39	1139.7	16.0	12.4
1.785	27.35	1.39	1141.2	15.8	12.5

1.787	27.38	1.39	1142.7	15.6	12.6
1.789	27.41	1.38	1144.1	15.3	12.7
1.791	27.43	1.38	1145.5	15.0	12.7
1.793	27.46	1.38	1146.8	14.7	12.6
1.795	27.49	1.38	1148.2	14.3	12.6
1.797	27.52	1.38	1149.5	13.9	12.6
1.799	27.54	1.38	1150.8	13.5	12.5
1.801	27.57	1.37	1152.2	13.2	12.5
1.803	27.60	1.37	1153.5	12.8	12.4
1.805	27.63	1.37	1154.9	12.5	12.4
1.807	27.65	1.37	1156.4	12.2	12.4
1.809	27.68	1.36	1157.8	12.0	12.4
1.811	27.71	1.36	1159.4	11.9	12.5
1.813	27.74	1.35	1161.0	11.8	12.6
1.815	27.76	1.18	1172.8	-11.44	-11.38
1.817	27.78	1.17	1174.2	-11.18	-11.41
1.819	27.81	1.17	1175.6	-10.91	-11.42
1.821	27.84	1.16	1177.1	-10.63	-11.42
1.823	27.86	1.16	1178.5	-10.35	-11.41
1.825	27.89	1.15	1179.9	-10.07	-11.40
1.827	27.92	1.14	1181.4	-9.78	-11.37
1.829	27.95	1.14	1182.8	-9.49	-11.34
1.831	27.97	1.13	1184.3	-9.20	-11.30
1.833	28.00	1.13	1185.7	-8.91	-11.26
1.835	28.03	1.12	1187.1	-8.63	-11.20
1.837	28.06	1.11	1188.6	-8.35	-11.15
1.839	28.08	1.11	1190.0	-8.08	-11.09
1.841	28.11	1.10	1191.4	-7.81	-11.03
1.843	28.14	1.09	1192.9	-7.55	-10.97
1.845	28.17	1.09	1194.3	-7.30	-10.91
1.847	28.19	1.08	1195.8	-7.06	-10.85
1.849	28.22	1.07	1197.2	-6.83	-10.79
1.851	28.25	1.07	1198.6	-6.61	-10.74
1.853	28.28	1.06	1200.0	-6.40	-10.70
1.855	28.31	1.06	1201.5	-6.21	-10.66
1.857	28.34	1.05	1202.9	-6.02	-10.64
1.859	28.36	1.04	1204.3	-5.85	-10.62
1.861	28.39	1.04	1205.7	-5.69	-10.62
1.863	28.42	1.03	1207.2	-5.55	-10.63
1.865	28.45	1.03	1208.6	-5.42	-10.65
1.867	28.48	1.02	1210.0	-5.31	-10.70
1.869	28.51	1.02	1211.4	-5.19	-10.72
1.871	28.54	1.01	1212.8	-5.06	-10.69
1.873	28.56	1.01	1214.2	-4.93	-10.62
1.875	28.59	1.00	1215.7	-4.78	-10.51
1.877	28.62	1.00	1217.1	-4.64	-10.37
1.879	28.65	0.99	1218.5	-4.49	-10.20
1.881	28.68	0.99	1219.9	-4.35	-10.03
1.883	28.71	0.98	1221.3	-4.21	-9.84
1.885	28.73	0.98	1222.7	-4.08	-9.66
1.887	28.76	0.98	1224.2	-3.95	-9.49

1.889	28.79	0.97	1225.6	-3.84	-9.33
1.891	28.82	0.97	1227.0	-3.73	-9.20
1.893	28.84	0.96	1228.5	-3.65	-9.10
1.895	28.87	0.96	1229.9	-3.57	-9.04
1.897	28.90	0.95	1231.4	-3.52	-9.03
1.899	28.93	0.95	1232.8	-3.46	-9.04
1.901	28.95	0.95	1234.3	-3.40	-9.02
1.903	28.98	0.94	1235.9	-3.32	-8.97
1.905	29.01	0.94	1237.4	-3.24	-8.91
1.907	29.03	0.93	1238.9	-3.15	-8.83
1.909	29.06	0.93	1240.5	-3.06	-8.74
1.911	29.08	0.92	1242.1	-2.97	-8.65
1.913	29.11	0.92	1243.6	-2.89	-8.55
1.915	29.13	0.91	1245.1	-2.81	-8.45
1.917	29.16	0.91	1246.7	-2.74	-8.35
1.919	29.19	0.90	1248.2	-2.67	-8.27
1.921	29.21	0.90	1249.7	-2.62	-8.19
1.923	29.24	0.89	1251.1	-2.58	-8.13
1.925	29.26	0.89	1252.6	-2.55	-8.10
1.927	29.29	0.88	1254.0	-2.54	-8.08
1.929	29.32	0.88	1255.4	-2.54	-8.08
1.931	29.35	0.87	1257.0	-2.54	-8.07
1.933	29.38	0.87	1258.6	-2.53	-8.05
1.935	29.40	0.86	1260.4	-2.53	-8.03
1.937	29.43	0.85	1262.2	-2.52	-8.00
1.939	29.46	0.84	1264.0	-2.51	-7.97
1.941	29.49	0.84	1265.9	-2.49	-7.93
1.943	29.52	0.83	1267.9	-2.48	-7.89
1.945	29.55	0.82	1269.8	-2.46	-7.84
1.947	29.58	0.81	1271.7	-2.45	-7.79
1.949	29.61	0.81	1273.7	-2.43	-7.74
1.951	29.64	0.80	1275.5	-2.41	-7.69
1.953	29.67	0.79	1277.4	-2.39	-7.64
1.955	29.69	0.78	1279.2	-2.37	-7.58
1.957	29.72	0.77	1280.9	-2.36	-7.52
1.959	29.75	0.77	1282.5	-2.34	-7.47
1.961	29.78	0.76	1284.0	-2.32	-7.41
1.963	29.80	0.75	1285.4	-2.30	-7.36
1.966	29.83	0.75	1286.6	-2.28	-7.30
1.968	29.86	0.74	1287.7	-2.26	-7.25
1.970	29.88	0.74	1288.6	-2.25	-7.20
1.972	29.91	0.73	1289.4	-2.23	-7.15
1.974	29.93	0.73	1289.9	-2.22	-7.10
1.976	29.96	0.73	1290.3	-2.20	-7.06
1.978	29.98	0.73	1290.4	-2.19	-7.03
1.980	30.01	0.73	1290.7	-2.16	-7.00
1.982	30.03	0.73	1291.6	-2.12	-6.99
1.984	30.06	0.73	1292.6	-2.06	-6.99
1.986	30.08	0.72	1293.4	-2.02	-6.99
1.988	30.11	0.72	1293.8	-2.00	-6.99
1.990	30.13	0.72	1294.7	-1.87	-7.04

1.992	30.16	0.72	1297.1	-1.55	-7.15
1.994	30.19	0.71	1299.9	-1.15	-7.25
1.996	30.22	0.71	1302.5	-0.81	-7.31
1.998	30.25	0.71	1304.7	-0.51	-7.35
2.000	30.27	0.70	1307.0	-0.18	-7.40
2.002	30.30	0.70	1309.1	0.15	-7.44
2.004	30.33	0.70	1310.9	0.43	-7.46
2.006	30.35	0.70	1312.1	0.63	-7.48
2.008	30.38	0.70	1312.5	0.70	-7.49
2.010	30.40	0.70	1313.4	0.65	-7.44
2.012	30.42	0.70	1314.3	0.54	-7.38
2.014	30.44	0.70	1314.6	0.30	-7.31
2.016	30.47	0.71	1315.3	-0.22	-7.11
2.018	30.49	0.71	1316.0	-0.72	-6.88
2.020	30.51	0.71	1316.4	-0.93	-6.76
2.022	30.54	0.71	1318.0	-0.67	-6.68
2.024	30.56	0.72	1319.3	-0.44	-6.53
2.026	30.58	0.72	1320.7	-0.21	-6.37
2.028	30.61	0.72	1321.6	-0.08	-6.29
2.030	30.63	0.71	1323.8	-0.66	-6.50
2.032	30.66	0.71	1325.7	-1.14	-6.55
2.034	30.68	0.71	1327.0	-1.70	-6.50
2.036	30.70	0.71	1328.3	-1.79	-6.43
2.038	30.72	0.71	1329.6	-1.83	-6.28
2.040	30.75	0.71	1330.8	-1.83	-6.09
2.042	30.77	0.71	1332.1	-1.81	-5.85
2.044	30.79	0.71	1333.4	-1.77	-5.60
2.046	30.82	0.71	1334.6	-1.73	-5.35
2.048	30.84	0.72	1335.9	-1.70	-5.12
2.050	30.86	0.72	1337.1	-1.70	-4.93
2.052	30.88	0.72	1338.3	-1.72	-4.78
2.054	30.91	0.73	1339.4	-1.78	-4.71
2.056	30.93	0.73	1340.3	-1.88	-4.62
2.058	30.95	0.73	1341.0	-2.00	-4.47
2.060	30.97	0.74	1341.7	-2.13	-4.28
2.062	31.00	0.75	1342.5	-2.26	-4.10
2.064	31.02	0.75	1343.6	-2.41	-3.96
2.066	31.04	0.76	1345.0	-2.61	-3.80
2.068	31.06	0.76	1346.7	-2.81	-3.57
2.070	31.08	0.76	1348.9	-2.96	-3.36
2.072	31.11	0.76	1351.9	-3.01	-3.27
2.074	31.13	0.76	1355.0	-3.06	-3.27
2.076	31.15	0.77	1357.5	-3.17	-3.27
2.078	31.17	0.77	1359.4	-3.36	-3.27
2.080	31.19	0.78	1360.8	-3.61	-3.27
2.082	31.22	0.78	1361.9	-3.91	-3.24
2.084	31.24	0.79	1362.6	-4.25	-3.20
2.086	31.26	0.80	1363.1	-4.62	-3.14
2.088	31.28	0.81	1363.6	-5.00	-3.06
2.090	31.30	0.82	1364.0	-5.40	-2.96
2.092	31.33	0.83	1364.5	-5.79	-2.86

2.094	31.35	0.84	1365.2	-6.16	-2.77
2.096	31.37	0.84	1366.2	-6.50	-2.70
2.098	31.39	0.85	1367.6	-6.81	-2.68
2.100	31.41	0.85	1369.4	-7.06	-2.72
2.102	31.43	0.86	1371.4	-7.29	-2.81
2.104	31.45	0.86	1373.1	-7.52	-2.89
2.106	31.47	0.87	1374.7	-7.76	-2.97
2.108	31.49	0.87	1376.0	-8.00	-3.05
2.110	31.51	0.88	1377.3	-8.24	-3.12
2.112	31.53	0.89	1378.3	-8.49	-3.20
2.114	31.56	0.89	1379.3	-8.74	-3.27
2.116	31.58	0.90	1380.2	-8.99	-3.34
2.118	31.60	0.91	1381.0	-9.24	-3.41
2.120	31.62	0.91	1381.8	-9.50	-3.48
2.122	31.64	0.92	1382.6	-9.76	-3.55
2.124	31.66	0.92	1383.4	-10.02	-3.62
2.126	31.68	0.93	1384.2	-10.28	-3.70
2.128	31.70	0.94	1385.0	-10.55	-3.78
2.130	31.73	0.94	1386.0	-10.82	-3.87
2.132	31.75	0.95	1387.0	-11.09	-3.96
2.134	31.77	0.95	1388.1	-11.38	-4.06
2.136	31.79	0.95	1389.3	-11.70	-4.18
2.138	31.81	0.95	1390.6	-12.05	-4.31
2.140	31.83	0.96	1391.9	-12.42	-4.45
2.142	31.85	0.96	1393.3	-12.80	-4.60
2.144	31.86	0.96	1394.6	-13.18	-4.75
2.146	31.88	0.96	1395.9	-13.57	-4.91
2.148	31.90	0.96	1397.2	-13.94	-5.06
2.150	31.92	0.97	1398.4	-14.30	-5.20
2.152	31.94	0.97	1399.5	-14.63	-5.34
2.154	31.96	0.97	1400.6	-14.93	-5.46
2.156	31.98	0.97	1401.4	-15.19	-5.57
2.158	32.01	0.98	1402.1	-15.41	-5.66
2.160	32.03	0.98	1402.7	-15.57	-5.73
2.162	32.05	0.98	1403.0	-15.67	-5.78
2.164	32.07	0.99	1403.1	-15.71	-5.79
2.166	32.10	0.99	1403.4	-15.77	-5.89
2.168	32.12	1.00	1404.1	-15.92	-6.17
2.170	32.14	1.01	1405.2	-16.12	-6.58
2.172	32.16	1.02	1406.5	-16.33	-7.08
2.174	32.17	1.02	1407.9	-16.52	-7.62
2.176	32.19	1.03	1409.3	-16.64	-8.16
2.178	32.21	1.03	1410.6	-16.68	-8.63
2.181	32.23	1.03	1411.6	-16.60	-8.97
2.183	32.25	1.03	1412.5	-16.60	-9.30
2.185	32.27	1.03	1413.6	-16.83	-9.74
2.187	32.29	1.03	1414.8	-17.21	-10.26
2.189	32.31	1.03	1416.0	-17.65	-10.82
2.191	32.33	1.02	1417.3	-18.09	-11.38
2.193	32.35	1.02	1418.5	-18.46	-11.91
2.195	32.37	1.02	1419.8	-18.67	-12.34

2.197	32.39	1.02	1421.0	-18.66	-12.64
2.199	32.41	1.02	1422.1	-18.54	-12.85
2.201	32.43	1.02	1423.4	-18.44	-13.07
2.203	32.46	1.03	1424.6	-18.37	-13.29
2.205	32.48	1.04	1425.8	-18.31	-13.51
2.207	32.50	1.04	1427.0	-18.26	-13.74
2.209	32.53	1.05	1428.2	-18.23	-13.97
2.211	32.55	1.06	1429.4	-18.19	-14.20
2.213	32.57	1.07	1430.6	-18.16	-14.44
2.215	32.60	1.08	1431.8	-18.11	-14.68
2.217	32.62	1.09	1432.9	-18.05	-14.93
2.219	32.64	1.10	1434.0	-17.97	-15.17
2.221	32.67	1.10	1435.0	-17.87	-15.42
2.223	32.69	1.11	1436.0	-17.74	-15.67
2.225	32.72	1.11	1436.9	-17.58	-15.92
2.227	32.74	1.11	1437.8	-17.37	-16.17
2.229	32.76	1.11	1438.8	-17.16	-16.52
2.231	32.79	1.11	1440.2	-16.95	-17.07
2.233	32.81	1.11	1441.8	-16.75	-17.74
2.235	32.83	1.12	1443.5	-16.54	-18.47
2.237	32.86	1.12	1445.2	-16.33	-19.22
2.239	32.88	1.12	1446.8	-16.13	-19.91
2.241	32.90	1.12	1448.1	-15.95	-20.48
2.243	32.93	1.12	1449.0	-15.83	-20.86
2.245	32.95	1.12	1449.3	-15.78	-21.01
2.247	32.97	1.12	1449.3	-15.92	-21.14
2.249	32.98	1.11	1449.2	-16.22	-21.44
2.251	32.99	1.11	1449.2	-16.52	-21.74
2.253	33.01	1.10	1449.2	-16.65	-21.87
2.255	33.03	1.11	1449.8	-16.47	-22.07
2.257	33.05	1.11	1451.5	-15.97	-22.60
2.259	33.08	1.12	1454.0	-15.21	-23.32
2.261	33.10	1.13	1456.9	-14.26	-24.14
2.263	33.12	1.14	1459.9	-13.20	-24.92
2.265	33.14	1.15	1462.6	-12.15	-25.57
2.267	33.16	1.16	1464.8	-11.25	-26.02
2.269	33.18	1.17	1466.7	-10.50	-26.36
2.271	33.21	1.18	1468.5	-9.79	-26.76
2.273	33.23	1.19	1470.4	-9.11	-27.18
2.275	33.25	1.20	1472.2	-8.47	-27.60
2.277	33.27	1.20	1473.9	-7.85	-27.99
2.279	33.28	1.21	1475.6	-7.25	-28.33
2.281	33.30	1.22	1477.0	-6.67	-28.59
2.283	33.32	1.22	1478.2	-6.12	-28.76
2.285	33.34	1.22	1479.3	-5.61	-28.88
2.287	33.36	1.22	1480.3	-5.15	-29.03
2.289	33.38	1.22	1481.1	-4.72	-29.20
2.291	33.40	1.22	1482.0	-4.32	-29.40
2.293	33.42	1.22	1482.7	-3.94	-29.62
2.295	33.44	1.22	1483.5	-3.57	-29.84
2.297	33.46	1.22	1484.2	-3.21	-30.08



2.299	33.48	1.21	1484.9	-2.84	-30.32
2.301	33.50	1.21	1485.6	-2.47	-30.55
2.303	33.52	1.21	1486.3	-2.07	-30.78
2.305	33.54	1.21	1487.1	-1.65	-30.98
2.307	33.56	1.21	1488.0	-1.20	-31.17
2.309	33.57	1.21	1488.9	-0.72	-31.32
2.311	33.59	1.21	1489.8	-0.19	-31.43
2.313	33.61	1.21	1490.9	0.38	-31.50
2.315	33.63	1.21	1492.1	1.01	-31.51
2.317	33.65	1.21	1493.4	1.68	-31.48
2.319	33.67	1.22	1494.7	2.38	-31.42
2.321	33.69	1.22	1496.2	3.11	-31.33
2.323	33.70	1.22	1497.6	3.86	-31.21
2.325	33.72	1.23	1499.1	4.63	-31.07
2.327	33.74	1.24	1500.6	5.41	-30.90
2.329	33.76	1.24	1502.2	6.19	-30.70
2.331	33.77	1.25	1503.8	6.98	-30.48
2.333	33.79	1.25	1505.4	7.77	-30.24
2.335	33.81	1.26	1506.9	8.54	-29.98
2.337	33.83	1.27	1508.5	9.31	-29.70
2.339	33.85	1.27	1510.1	10.06	-29.41
2.341	33.86	1.28	1511.6	10.80	-29.11
2.343	33.88	1.29	1513.1	11.51	-28.80
2.345	33.90	1.30	1514.6	12.21	-28.48
2.347	33.92	1.30	1516.1	12.88	-28.17
2.349	33.94	1.31	1517.5	13.53	-27.86
2.351	33.96	1.32	1518.8	14.15	-27.56
2.353	33.98	1.32	1520.1	14.74	-27.26
2.355	34.00	1.33	1521.3	15.30	-26.93
2.357	34.02	1.34	1522.6	15.83	-26.58
2.359	34.04	1.34	1523.8	16.33	-26.22
2.361	34.06	1.35	1524.9	16.80	-25.85
2.363	34.09	1.35	1526.1	17.25	-25.46
2.365	34.11	1.36	1527.2	17.68	-25.06
2.367	34.13	1.37	1528.3	18.10	-24.66
2.369	34.15	1.37	1529.4	18.49	-24.25
2.371	34.17	1.38	1530.5	18.88	-23.84
2.373	34.20	1.39	1531.5	19.26	-23.43
2.375	34.22	1.39	1532.6	19.63	-23.02
2.377	34.24	1.40	1533.7	19.99	-22.60
2.379	34.26	1.41	1534.7	20.36	-22.19
2.381	34.28	1.41	1535.8	20.73	-21.78
2.383	34.30	1.42	1536.9	21.11	-21.38
2.385	34.33	1.43	1538.0	21.49	-20.97
2.387	34.35	1.44	1539.1	21.88	-20.56
2.389	34.37	1.45	1540.3	22.24	-20.13
2.391	34.39	1.46	1541.5	22.59	-19.69
2.393	34.41	1.46	1542.7	22.92	-19.24
2.396	34.43	1.47	1544.0	23.24	-18.78
2.398	34.45	1.48	1545.2	23.54	-18.31
2.400	34.47	1.49	1546.4	23.84	-17.85

2.402	34.49	1.50	1547.6	24.14	-17.38
2.404	34.51	1.51	1548.8	24.43	-16.92
2.406	34.53	1.52	1549.8	24.72	-16.46
2.408	34.55	1.53	1550.9	24.99	-16.00
2.410	34.57	1.53	1552.0	25.23	-15.55
2.412	34.60	1.54	1553.2	25.45	-15.09
2.414	34.62	1.55	1554.4	25.65	-14.62
2.416	34.64	1.56	1555.6	25.86	-14.14
2.418	34.67	1.56	1556.8	26.07	-13.64
2.420	34.69	1.57	1557.9	26.31	-13.12
2.421	34.55	1.68	1550.8	18.77	-14.92
2.423	34.57	1.68	1551.8	19.18	-14.71
2.425	34.59	1.69	1552.8	19.60	-14.50
2.427	34.60	1.70	1553.8	20.01	-14.29
2.429	34.62	1.70	1554.7	20.43	-14.07
2.431	34.64	1.71	1555.6	20.85	-13.85
2.434	34.66	1.72	1556.5	21.27	-13.62
2.436	34.67	1.72	1557.4	21.68	-13.39
2.438	34.69	1.73	1558.3	22.09	-13.14
2.440	34.71	1.73	1559.1	22.50	-12.88
2.442	34.72	1.74	1559.9	22.91	-12.61
2.444	34.74	1.75	1560.7	23.30	-12.33
2.446	34.76	1.75	1561.5	23.69	-12.03
2.448	34.78	1.76	1562.3	24.07	-11.72
2.451	34.79	1.76	1563.2	24.44	-11.39
2.453	34.81	1.77	1564.0	24.80	-11.04
2.455	34.83	1.78	1564.8	25.15	-10.67
2.457	34.84	1.78	1565.6	25.47	-10.29
2.459	34.86	1.79	1566.5	25.79	-9.88
2.461	34.88	1.79	1567.4	26.08	-9.46
2.463	34.90	1.80	1568.3	26.35	-9.01
2.465	34.91	1.80	1569.2	26.60	-8.54
2.467	34.93	1.81	1570.2	26.83	-8.05
2.470	34.95	1.82	1571.2	27.03	-7.53
2.472	34.96	1.82	1572.2	27.20	-6.99
2.474	34.98	1.83	1573.3	27.34	-6.44
2.476	35.00	1.84	1574.4	27.48	-5.84
2.478	35.01	1.84	1575.6	27.66	-5.21
2.480	35.03	1.85	1576.7	27.86	-4.53
2.482	35.04	1.85	1577.9	28.07	-3.82
2.484	35.05	1.86	1579.1	28.29	-3.07
2.487	35.07	1.87	1580.3	28.50	-2.28
2.489	35.08	1.87	1581.5	28.71	-1.48
2.491	35.09	1.88	1582.7	28.89	-0.65
2.493	35.11	1.89	1583.9	29.06	0.20
2.495	35.12	1.89	1585.2	29.19	1.05
2.497	35.14	1.90	1586.4	29.28	1.91
2.499	35.15	1.90	1587.7	29.33	2.75
2.501	35.17	1.91	1589.0	29.34	3.58
2.504	35.19	1.92	1590.3	29.30	4.38
2.506	35.21	1.92	1591.6	29.20	5.15

2.508	35.23	1.93	1593.0	29.09	5.90
2.510	35.26	1.93	1594.3	29.00	6.64
2.512	35.28	1.94	1595.6	28.91	7.39
2.514	35.31	1.94	1596.9	28.83	8.14
2.516	35.34	1.95	1598.2	28.74	8.88
2.518	35.37	1.95	1599.5	28.65	9.62
2.520	35.41	1.96	1600.8	28.55	10.35
2.523	35.44	1.96	1602.0	28.43	11.06
2.525	35.47	1.97	1603.2	28.30	11.77
2.527	35.50	1.97	1604.4	28.13	12.45
2.529	35.52	1.98	1605.6	27.94	13.11
2.531	35.55	1.98	1606.8	27.71	13.73
2.533	35.57	1.99	1607.9	27.45	14.33
2.535	35.60	1.99	1609.1	27.16	14.90
2.537	35.62	2.00	1610.3	26.88	15.46
2.540	35.64	2.00	1611.6	26.60	16.02
2.542	35.66	2.01	1612.8	26.32	16.57
2.544	35.68	2.02	1614.1	26.04	17.11
2.546	35.70	2.02	1615.4	25.75	17.65
2.548	35.72	2.03	1616.7	25.46	18.18
2.550	35.73	2.04	1618.1	25.16	18.69
2.552	35.75	2.04	1619.4	24.85	19.20
2.554	35.77	2.05	1620.7	24.54	19.71
2.556	35.79	2.06	1622.1	24.22	20.20
2.559	35.81	2.06	1623.4	23.90	20.68
2.561	35.82	2.07	1624.7	23.56	21.15
2.563	35.84	2.07	1625.9	23.21	21.61
2.565	35.86	2.08	1627.2	22.85	22.05
2.567	35.88	2.08	1628.4	22.47	22.48
2.569	35.90	2.09	1629.5	22.09	22.90
2.571	35.92	2.09	1630.7	21.69	23.30
2.573	35.94	2.09	1631.7	21.27	23.68
2.576	35.96	2.10	1632.8	20.85	24.05
2.578	35.98	2.10	1633.9	20.43	24.40
2.580	36.00	2.10	1634.9	20.00	24.74
2.582	36.02	2.10	1636.0	19.58	25.06
2.584	36.04	2.10	1637.1	19.15	25.38
2.586	36.06	2.10	1638.2	18.72	25.68
2.588	36.08	2.10	1639.3	18.29	25.97
2.590	36.11	2.10	1640.4	17.85	26.25
2.593	36.13	2.10	1641.5	17.41	26.52
2.595	36.15	2.10	1642.6	16.97	26.79
2.597	36.17	2.10	1643.7	16.53	27.04
2.599	36.19	2.10	1644.8	16.07	27.29
2.601	36.22	2.10	1645.9	15.62	27.54
2.603	36.24	2.10	1647.0	15.15	27.77
2.605	36.26	2.10	1648.1	14.68	28.00
2.607	36.28	2.09	1649.2	14.21	28.23
2.609	36.30	2.09	1650.3	13.72	28.45
2.612	36.33	2.09	1651.3	13.22	28.67
2.614	36.35	2.09	1652.4	12.71	28.88

2.616	36.37	2.09	1653.5	12.19	29.08
2.618	36.39	2.09	1654.6	11.67	29.29
2.620	36.41	2.09	1655.7	11.15	29.51
2.622	36.43	2.09	1656.8	10.63	29.73
2.624	36.45	2.09	1658.0	10.11	29.95
2.626	36.47	2.08	1659.1	9.59	30.18
2.629	36.50	2.08	1660.3	9.06	30.41
2.631	36.52	2.08	1661.5	8.53	30.64
2.633	36.54	2.08	1662.7	7.99	30.86
2.635	36.56	2.08	1663.9	7.44	31.08
2.637	36.58	2.07	1665.1	6.88	31.30
2.639	36.60	2.07	1666.4	6.30	31.50
2.641	36.62	2.07	1667.6	5.72	31.70
2.643	36.64	2.07	1668.9	5.13	31.88
2.645	36.66	2.07	1670.1	4.52	32.05
2.648	36.69	2.07	1671.4	3.90	32.20
2.650	36.71	2.07	1672.7	3.26	32.33
2.652	36.73	2.07	1674.0	2.62	32.43
2.654	36.75	2.07	1675.2	1.96	32.52
2.656	36.77	2.07	1676.5	1.29	32.57
2.658	36.79	2.08	1677.8	0.61	32.60
2.660	36.82	2.08	1679.1	-0.10	32.63
2.662	36.84	2.09	1680.5	-0.84	32.71
2.665	36.86	2.11	1681.9	-1.61	32.80
2.667	36.89	2.12	1683.4	-2.40	32.91
2.669	36.91	2.14	1685.0	-3.23	33.02
2.671	36.94	2.16	1686.5	-4.07	33.12
2.673	36.96	2.17	1688.1	-4.92	33.21
2.675	36.99	2.19	1689.7	-5.78	33.26
2.677	37.01	2.20	1691.2	-6.63	33.27
2.679	37.03	2.21	1692.7	-7.46	33.24
2.682	37.05	2.22	1694.2	-8.26	33.16
2.684	37.07	2.22	1695.6	-9.03	33.01
2.686	37.09	2.22	1697.0	-9.74	32.80
2.688	37.11	2.22	1698.4	-10.42	32.53
2.690	37.12	2.21	1699.9	-11.05	32.23
2.692	37.14	2.20	1701.4	-11.65	31.88
2.694	37.15	2.19	1703.0	-12.23	31.52
2.696	37.16	2.18	1704.6	-12.78	31.13
2.698	37.18	2.17	1706.2	-13.31	30.74
2.701	37.19	2.15	1707.8	-13.84	30.35
2.703	37.20	2.14	1709.5	-14.37	29.96
2.705	37.22	2.13	1711.1	-14.91	29.58
2.707	37.23	2.11	1712.8	-15.46	29.22
2.709	37.25	2.10	1714.4	-16.04	28.89
2.711	37.27	2.09	1716.1	-16.66	28.58
2.713	37.29	2.09	1717.7	-17.33	28.30
2.715	37.31	2.09	1719.3	-18.03	28.03
2.718	37.33	2.08	1721.0	-18.74	27.73
2.720	37.35	2.08	1722.7	-19.45	27.41
2.722	37.37	2.08	1724.4	-20.16	27.06

2.724	37.40	2.09	1726.1	-20.88	26.68
2.726	37.42	2.09	1727.8	-21.58	26.28
2.728	37.45	2.09	1729.5	-22.27	25.85
2.730	37.47	2.09	1731.2	-22.94	25.40
2.732	37.50	2.10	1732.8	-23.59	24.93
2.734	37.52	2.10	1734.4	-24.22	24.44
2.737	37.55	2.10	1735.9	-24.82	23.93
2.739	37.57	2.10	1737.4	-25.38	23.41
2.741	37.59	2.10	1738.8	-25.92	22.88
2.743	37.62	2.10	1740.1	-26.41	22.34
2.745	37.64	2.10	1741.3	-26.86	21.79
2.747	37.65	2.09	1742.4	-27.21	21.21
2.749	37.67	2.09	1743.4	-27.39	20.58
2.751	37.68	2.09	1744.4	-27.47	19.92
2.754	37.69	2.08	1745.4	-27.46	19.24
2.756	37.70	2.08	1746.3	-27.42	18.57
2.758	37.72	2.07	1747.2	-27.38	17.91
2.760	37.73	2.07	1748.2	-27.39	17.28
2.762	37.74	2.06	1749.2	-27.49	16.68
2.764	37.76	2.06	1750.2	-27.71	16.12
2.766	37.78	2.06	1751.3	-28.00	15.58
2.768	37.81	2.05	1752.4	-28.27	15.03
2.771	37.83	2.05	1753.5	-28.53	14.47
2.773	37.85	2.05	1754.6	-28.78	13.90
2.775	37.87	2.04	1755.8	-29.02	13.32
2.777	37.90	2.04	1757.0	-29.24	12.73
2.779	37.92	2.04	1758.1	-29.44	12.14
2.781	37.94	2.04	1759.3	-29.64	11.55
2.783	37.96	2.03	1760.5	-29.82	10.94
2.785	37.99	2.03	1761.7	-29.98	10.34
2.787	38.01	2.03	1763.0	-30.13	9.73
2.790	38.03	2.02	1764.2	-30.27	9.11
2.792	38.06	2.02	1765.4	-30.39	8.49
2.794	38.08	2.02	1766.7	-30.51	7.88
2.796	38.11	2.02	1767.9	-30.60	7.26
2.798	38.13	2.01	1769.2	-30.69	6.64
2.800	38.15	2.01	1770.4	-30.76	6.02
2.802	38.18	2.01	1771.7	-30.82	5.39
2.804	38.20	2.00	1772.9	-30.87	4.77
2.807	38.22	2.00	1774.2	-30.91	4.16
2.809	38.24	2.00	1775.4	-30.93	3.54
2.811	38.27	2.00	1776.7	-30.95	2.93
2.813	38.29	1.99	1777.9	-30.95	2.31
2.815	38.31	1.99	1779.1	-30.95	1.71
2.817	38.33	1.99	1780.3	-30.93	1.10
2.819	38.36	1.99	1781.5	-30.90	0.50
2.821	38.38	1.98	1782.7	-30.87	-0.09
2.823	38.40	1.98	1783.9	-30.82	-0.69
2.826	38.42	1.98	1785.1	-30.77	-1.27
2.828	38.44	1.97	1786.2	-30.71	-1.85
2.830	38.46	1.97	1787.4	-30.64	-2.43

2.832	38.48	1.97	1788.6	-30.55	-3.00
2.834	38.50	1.97	1789.7	-30.46	-3.56
2.836	38.52	1.96	1790.9	-30.36	-4.12
2.838	38.54	1.96	1792.0	-30.24	-4.67
2.840	38.56	1.96	1793.2	-30.12	-5.22
2.843	38.58	1.96	1794.4	-29.99	-5.76
2.845	38.60	1.96	1795.6	-29.85	-6.29
2.847	38.61	1.95	1796.8	-29.70	-6.82
2.849	38.63	1.95	1797.9	-29.54	-7.35
2.851	38.65	1.95	1799.1	-29.37	-7.87
2.853	38.67	1.95	1800.3	-29.20	-8.38
2.855	38.69	1.94	1801.5	-29.02	-8.89
2.857	38.71	1.94	1802.6	-28.83	-9.40
2.860	38.73	1.94	1803.8	-28.63	-9.90
2.862	38.74	1.94	1805.0	-28.43	-10.40
2.864	38.76	1.93	1806.1	-28.22	-10.89
2.866	38.78	1.93	1807.3	-28.00	-11.38
2.868	38.80	1.93	1808.4	-27.77	-11.87
2.870	38.82	1.93	1809.5	-27.54	-12.35
2.872	38.83	1.92	1810.6	-27.31	-12.84
2.874	38.85	1.92	1811.8	-27.06	-13.31
2.876	38.87	1.92	1812.9	-26.81	-13.79
2.879	38.89	1.92	1813.9	-26.56	-14.27
2.881	38.91	1.91	1815.0	-26.30	-14.74
2.883	38.92	1.91	1816.1	-26.03	-15.21
2.885	38.94	1.91	1817.1	-25.75	-15.68
2.887	38.96	1.90	1818.2	-25.47	-16.15
2.889	38.98	1.90	1819.2	-25.21	-16.63
2.891	39.00	1.89	1820.2	-24.97	-17.14
2.893	39.01	1.89	1821.3	-24.76	-17.67
2.896	39.03	1.88	1822.3	-24.56	-18.22
2.898	39.05	1.87	1823.4	-24.37	-18.78
2.900	39.06	1.87	1824.4	-24.17	-19.35
2.902	39.08	1.86	1825.5	-23.96	-19.91
2.904	39.10	1.85	1826.5	-23.73	-20.47
2.906	39.11	1.84	1827.6	-23.47	-21.00
2.908	39.13	1.83	1828.6	-23.18	-21.51
2.910	39.15	1.83	1829.7	-22.85	-21.98
2.912	39.17	1.82	1830.7	-22.47	-22.41
2.915	39.18	1.82	1831.8	-22.03	-22.77
2.917	39.20	1.81	1833.0	-21.51	-23.04
2.919	39.22	1.81	1834.3	-20.94	-23.24
2.921	39.24	1.81	1835.6	-20.32	-23.37
2.923	39.26	1.80	1837.0	-19.67	-23.45
2.925	39.28	1.80	1838.3	-19.00	-23.50
2.927	39.30	1.80	1839.6	-18.33	-23.51
2.929	39.31	1.80	1841.0	-17.66	-23.52
2.932	39.33	1.79	1842.2	-17.01	-23.52
2.934	39.35	1.79	1843.4	-16.38	-23.55
2.936	39.37	1.78	1844.5	-15.76	-23.56
2.938	39.39	1.77	1845.8	-15.11	-23.51

2.940	39.41	1.76	1847.0	-14.45	-23.42
2.942	39.43	1.75	1848.3	-13.80	-23.31
2.944	39.45	1.74	1849.7	-13.16	-23.19
2.946	39.47	1.74	1851.0	-12.53	-23.07
2.949	39.49	1.73	1852.3	-11.92	-22.97
2.951	39.51	1.72	1853.6	-11.35	-22.90
2.953	39.53	1.72	1854.9	-10.80	-22.89
2.955	39.55	1.72	1856.2	-10.29	-22.94
2.957	39.57	1.72	1857.4	-9.81	-23.08
2.959	39.58	1.72	1858.7	-9.35	-23.33
2.961	39.60	1.73	1860.4	-8.88	-23.66
2.963	39.61	1.73	1862.2	-8.39	-24.04
2.965	39.63	1.74	1864.0	-7.87	-24.41
2.968	39.64	1.74	1865.7	-7.34	-24.72
2.970	39.66	1.75	1867.1	-6.80	-24.93
2.972	39.68	1.75	1868.3	-6.30	-25.08
2.974	39.69	1.75	1869.2	-5.84	-25.26
2.976	39.71	1.76	1870.2	-5.38	-25.42
2.978	39.72	1.76	1871.3	-4.87	-25.55
2.980	39.74	1.76	1872.4	-4.32	-25.55
2.982	39.75	1.75	1873.3	-3.75	-25.38
2.985	39.76	1.73	1874.0	-3.16	-25.14
2.987	39.78	1.71	1874.8	-2.57	-24.88
2.989	39.79	1.70	1875.8	-1.96	-24.69
2.991	39.81	1.70	1877.2	-1.31	-24.63
2.993	39.84	1.70	1878.9	-0.60	-24.57
2.995	39.86	1.71	1880.6	0.16	-24.34
2.997	39.89	1.72	1882.5	0.93	-24.00
2.999	39.92	1.73	1884.3	1.70	-23.61
3.002	39.95	1.74	1886.1	2.44	-23.23
3.004	39.97	1.75	1887.9	3.14	-22.91
3.006	40.00	1.75	1889.7	3.82	-22.72
3.008	40.02	1.75	1891.3	4.47	-22.57
3.010	40.05	1.75	1893.0	5.09	-22.36
3.012	40.07	1.74	1894.5	5.68	-22.09
3.014	40.09	1.74	1896.0	6.24	-21.79
3.016	40.12	1.73	1897.5	6.78	-21.46
3.018	40.14	1.72	1899.0	7.31	-21.14
3.021	40.16	1.71	1900.4	7.82	-20.82
3.023	40.19	1.71	1901.9	8.34	-20.54
3.025	40.21	1.70	1903.5	8.87	-20.28
3.027	40.23	1.69	1905.1	9.37	-19.94
3.029	40.25	1.68	1906.8	9.79	-19.42
3.031	40.28	1.68	1908.5	10.14	-18.80
3.033	40.30	1.67	1910.1	10.42	-18.15
3.035	40.32	1.66	1911.7	10.66	-17.55
3.038	40.34	1.65	1913.0	10.88	-17.08
3.040	40.35	1.64	1914.0	11.12	-16.79
3.042	40.36	1.64	1915.0	11.21	-16.51
3.044	40.37	1.63	1916.1	11.02	-16.06
3.046	40.37	1.63	1917.4	10.65	-15.48

3.048	40.37	1.63	1918.7	10.20	-14.84
3.050	40.38	1.62	1920.1	9.77	-14.19
3.052	40.38	1.62	1921.5	9.44	-13.59
3.054	40.39	1.61	1922.8	9.29	-13.10
3.057	40.41	1.61	1924.1	9.42	-12.79
3.059	40.43	1.60	1925.2	9.83	-12.57
3.061	40.46	1.60	1926.1	10.44	-12.31
3.063	40.50	1.59	1927.0	11.17	-12.01
3.065	40.54	1.58	1927.9	11.93	-11.65
3.067	40.58	1.58	1928.9	12.66	-11.24
3.069	40.61	1.57	1930.0	13.27	-10.82
3.071	40.64	1.57	1931.5	13.68	-10.41
3.074	40.67	1.56	1933.0	13.91	-10.01
3.076	40.69	1.56	1934.3	14.05	-9.59
3.078	40.71	1.55	1935.5	14.09	-9.16
3.080	40.73	1.55	1936.5	14.08	-8.72
3.082	40.75	1.55	1937.5	14.01	-8.29
3.084	40.77	1.54	1938.4	13.90	-7.87
3.086	40.78	1.54	1939.2	13.79	-7.47
3.088	40.80	1.53	1940.1	13.67	-7.09
3.091	40.82	1.53	1940.9	13.58	-6.73
3.093	40.84	1.52	1941.9	13.52	-6.40
3.095	40.85	1.52	1942.8	13.52	-6.09
3.097	40.87	1.51	1943.9	13.59	-5.80
3.099	40.89	1.51	1945.0	13.67	-5.52
3.101	40.91	1.50	1946.1	13.69	-5.23
3.103	40.93	1.50	1947.1	13.65	-4.92
3.105	40.95	1.49	1948.0	13.57	-4.61
3.107	40.97	1.49	1949.0	13.46	-4.30
3.110	40.99	1.48	1949.9	13.33	-3.99
3.112	41.01	1.48	1950.9	13.18	-3.69
3.114	41.03	1.47	1951.8	13.04	-3.39
3.116	41.05	1.47	1952.8	12.90	-3.09
3.118	41.07	1.46	1953.8	12.79	-2.80
3.120	41.09	1.45	1954.9	12.71	-2.52
3.122	41.11	1.45	1956.0	12.67	-2.24
3.124	41.13	1.44	1957.3	12.68	-1.96
3.127	41.15	1.44	1958.5	12.70	-1.67
3.129	41.17	1.43	1959.6	12.66	-1.38
3.131	41.19	1.43	1960.7	12.58	-1.08
3.133	41.21	1.42	1961.8	12.46	-0.79
3.135	41.23	1.42	1962.8	12.31	-0.50
3.137	41.25	1.41	1963.8	12.13	-0.21
3.139	41.27	1.40	1964.8	11.93	0.08
3.141	41.29	1.40	1965.8	11.72	0.36
3.143	41.32	1.39	1966.7	11.50	0.63
3.146	41.34	1.38	1967.6	11.29	0.90
3.148	41.36	1.38	1968.5	11.08	1.16
3.150	41.38	1.37	1969.5	10.88	1.42
3.152	41.40	1.37	1970.4	10.70	1.69
3.154	41.42	1.36	1971.3	10.54	1.95



3.156	41.44	1.35	1972.3	10.42	2.23
3.158	41.46	1.35	1973.3	10.33	2.51
3.160	41.48	1.34	1974.3	10.20	2.79
3.163	41.50	1.33	1975.3	9.96	3.04
3.165	41.52	1.33	1976.3	9.63	3.25
3.167	41.55	1.32	1977.3	9.24	3.42
3.169	41.57	1.31	1978.3	8.80	3.57
3.171	41.59	1.30	1979.3	8.33	3.69
3.173	41.61	1.29	1980.3	7.84	3.78
3.175	41.63	1.29	1981.3	7.37	3.86
3.177	41.66	1.28	1982.3	6.92	3.94
3.180	41.68	1.27	1983.3	6.50	4.02
3.182	41.70	1.27	1984.4	6.14	4.13
3.184	41.72	1.26	1985.4	5.85	4.27
3.186	41.74	1.26	1986.5	5.62	4.47
3.188	41.76	1.25	1987.5	5.40	4.69
3.190	41.78	1.25	1988.6	5.12	4.88
3.192	41.80	1.24	1989.7	4.81	5.03
3.194	41.82	1.24	1990.8	4.46	5.15
3.196	41.84	1.24	1991.9	4.10	5.24
3.199	41.87	1.24	1993.1	3.72	5.30
3.201	41.89	1.23	1994.2	3.33	5.34
3.203	41.91	1.23	1995.3	2.96	5.37
3.205	41.93	1.23	1996.5	2.59	5.40
3.207	41.95	1.23	1997.6	2.23	5.43
3.209	41.97	1.22	1998.8	1.88	5.48
3.211	41.99	1.22	1999.9	1.54	5.55
3.213	42.02	1.21	2001.0	1.20	5.67
3.216	42.04	1.21	2002.2	0.84	5.83
3.218	42.06	1.20	2003.3	0.45	6.03
3.220	42.09	1.19	2004.5	0.03	6.23
3.222	42.11	1.19	2005.6	-0.44	6.44
3.224	42.13	1.18	2006.8	-0.94	6.63
3.226	42.16	1.17	2008.0	-1.47	6.79
3.228	42.18	1.16	2009.2	-2.03	6.91
3.230	42.21	1.15	2010.3	-2.60	6.98
3.232	42.23	1.15	2011.5	-3.16	6.98
3.235	42.25	1.14	2012.6	-3.71	6.93
3.237	42.28	1.13	2013.8	-4.22	6.81
3.239	42.30	1.12	2014.9	-4.67	6.62
3.241	42.32	1.12	2016.0	-5.04	6.39
3.243	42.34	1.11	2017.1	-5.36	6.14
3.245	42.36	1.11	2018.1	-5.67	5.92
3.247	42.38	1.10	2019.2	-5.96	5.72
3.249	42.40	1.10	2020.2	-6.25	5.53
3.252	42.42	1.09	2021.2	-6.53	5.35
3.254	42.44	1.09	2022.2	-6.81	5.18
3.256	42.46	1.08	2023.3	-7.07	5.01
3.258	42.47	1.08	2024.3	-7.34	4.84
3.260	42.49	1.07	2025.3	-7.59	4.65
3.262	42.51	1.07	2026.3	-7.83	4.46

3.264	42.53	1.06	2027.3	-8.06	4.24
3.266	42.55	1.06	2028.4	-8.28	4.00
3.269	42.57	1.06	2029.4	-8.47	3.73
3.271	42.59	1.05	2030.5	-8.64	3.43
3.273	42.61	1.05	2031.5	-8.79	3.10
3.275	42.63	1.04	2032.6	-8.90	2.73
3.277	42.65	1.04	2033.6	-9.00	2.35
3.279	42.67	1.03	2034.6	-9.07	1.96
3.281	42.69	1.03	2035.5	-9.13	1.55
3.283	42.71	1.02	2036.4	-9.16	1.14
3.285	42.73	1.02	2037.3	-9.17	0.72
3.288	42.75	1.01	2038.2	-9.16	0.30
3.290	42.77	1.01	2039.1	-9.12	-0.12
3.292	42.80	1.00	2040.0	-9.07	-0.53
3.294	42.82	1.00	2041.0	-9.00	-0.94
3.296	42.84	0.99	2042.0	-8.91	-1.34
3.298	42.86	0.99	2043.0	-8.80	-1.73
3.300	42.88	0.98	2044.1	-8.68	-2.10
3.302	42.90	0.98	2045.3	-8.55	-2.46
3.305	42.92	0.97	2046.6	-8.41	-2.81
3.307	42.94	0.97	2047.9	-8.26	-3.14
3.309	42.97	0.96	2049.4	-8.11	-3.46
3.311	42.99	0.96	2050.9	-7.96	-3.75
3.313	43.01	0.95	2052.6	-7.81	-4.03
3.315	43.03	0.94	2054.4	-7.66	-4.29
3.317	43.04	0.93	2056.3	-7.57	-4.57
3.319	43.06	0.93	2057.9	-7.57	-4.88
3.321	43.08	0.92	2059.4	-7.63	-5.22
3.324	43.10	0.91	2060.7	-7.76	-5.61
3.326	43.11	0.91	2061.9	-7.92	-6.02
3.328	43.13	0.90	2063.0	-8.12	-6.47
3.330	43.15	0.90	2064.0	-8.33	-6.93
3.332	43.16	0.89	2065.0	-8.54	-7.40
3.334	43.18	0.88	2065.8	-8.75	-7.87
3.336	43.19	0.88	2066.7	-8.94	-8.34
3.338	43.21	0.87	2067.5	-9.10	-8.79
3.341	43.22	0.87	2068.3	-9.23	-9.21
3.343	43.24	0.86	2069.1	-9.30	-9.59
3.345	43.26	0.86	2069.9	-9.31	-9.92
3.347	43.27	0.85	2070.7	-9.26	-10.18
3.349	43.29	0.85	2071.6	-9.13	-10.37
3.351	43.31	0.84	2072.6	-8.96	-10.51
3.353	43.32	0.83	2073.5	-8.78	-10.64
3.355	43.34	0.83	2074.4	-8.60	-10.75
3.358	43.36	0.82	2075.4	-8.41	-10.84
3.360	43.38	0.81	2076.3	-8.23	-10.92
3.362	43.39	0.80	2077.2	-8.06	-10.98
3.364	43.41	0.80	2078.2	-7.89	-11.04
3.366	43.43	0.79	2079.1	-7.73	-11.08
3.368	43.44	0.78	2080.0	-7.58	-11.12
3.370	43.46	0.78	2081.0	-7.44	-11.15

3.372	43.48	0.77	2081.9	-7.32	-11.18
3.374	43.50	0.76	2082.8	-7.21	-11.20
3.377	43.52	0.76	2083.8	-7.12	-11.22
3.379	43.53	0.76	2084.7	-7.06	-11.24
3.381	43.55	0.76	2085.7	-7.01	-11.26
3.383	43.57	0.76	2086.7	-6.99	-11.29
3.385	43.59	0.76	2087.7	-7.02	-11.34
3.387	43.61	0.76	2088.6	-7.07	-11.41
3.389	43.63	0.76	2089.6	-7.15	-11.49
3.391	43.65	0.76	2090.6	-7.26	-11.59
3.394	43.67	0.76	2091.6	-7.39	-11.69
3.396	43.69	0.77	2092.6	-7.53	-11.80
3.398	43.71	0.77	2093.6	-7.69	-11.92
3.400	43.73	0.78	2094.6	-7.86	-12.03
3.402	43.75	0.78	2095.6	-8.04	-12.15
3.404	43.77	0.78	2096.6	-8.21	-12.26
3.406	43.79	0.79	2097.5	-8.39	-12.36
3.408	43.81	0.79	2098.5	-8.55	-12.46
3.410	43.82	0.80	2099.5	-8.71	-12.54
3.413	43.84	0.80	2100.5	-8.84	-12.61
3.415	43.86	0.81	2101.4	-8.96	-12.67
3.417	43.88	0.81	2102.4	-9.05	-12.72
3.419	43.90	0.82	2103.3	-9.10	-12.75
3.421	43.92	0.82	2104.2	-9.12	-12.76
3.423	43.94	0.83	2105.1	-9.12	-12.77
3.425	43.96	0.83	2106.0	-9.13	-12.81
3.427	43.97	0.83	2106.9	-9.15	-12.87
3.430	43.99	0.84	2107.7	-9.16	-12.94
3.432	44.01	0.84	2108.4	-9.18	-13.03
3.434	44.03	0.84	2109.2	-9.20	-13.14
3.436	44.04	0.85	2109.9	-9.22	-13.25
3.438	44.06	0.85	2110.7	-9.24	-13.37
3.440	44.08	0.86	2111.4	-9.27	-13.48
3.442	44.10	0.86	2112.1	-9.29	-13.60
3.444	44.11	0.86	2112.8	-9.31	-13.71
3.447	44.13	0.87	2113.5	-9.32	-13.82
3.449	44.15	0.87	2114.2	-9.34	-13.91
3.451	44.16	0.87	2114.9	-9.35	-13.99
3.453	44.18	0.88	2115.6	-9.36	-14.05
3.455	44.20	0.88	2116.3	-9.37	-14.09
3.457	44.22	0.88	2117.1	-9.37	-14.10
3.459	44.24	0.89	2117.8	-9.37	-14.11
3.461	44.26	0.89	2118.6	-9.38	-14.11
3.463	44.27	0.89	2119.4	-9.38	-14.13
3.466	44.29	0.89	2120.2	-9.39	-14.15
3.468	44.31	0.90	2121.0	-9.41	-14.17
3.470	44.33	0.90	2121.8	-9.42	-14.19
3.472	44.35	0.90	2122.7	-9.43	-14.22
3.474	44.37	0.91	2123.5	-9.45	-14.24
3.476	44.39	0.91	2124.4	-9.46	-14.27
3.478	44.41	0.91	2125.2	-9.48	-14.30

3.480	44.43	0.91	2126.1	-9.49	-14.32
3.483	44.45	0.91	2127.0	-9.51	-14.35
3.485	44.46	0.92	2127.9	-9.52	-14.37
3.487	44.48	0.92	2128.8	-9.53	-14.38
3.489	44.50	0.92	2129.8	-9.54	-14.40
3.491	44.52	0.92	2130.7	-9.54	-14.41
3.493	44.54	0.92	2131.6	-9.54	-14.41
3.495	44.55	0.92	2132.6	-9.56	-14.43
3.497	44.57	0.92	2133.6	-9.62	-14.50
3.499	44.58	0.91	2134.7	-9.71	-14.61
3.502	44.60	0.91	2135.8	-9.82	-14.74
3.504	44.61	0.91	2136.9	-9.94	-14.89
3.506	44.63	0.90	2137.9	-10.07	-15.05
3.508	44.64	0.90	2139.0	-10.21	-15.21
3.510	44.66	0.89	2140.1	-10.33	-15.35
3.512	44.67	0.89	2141.1	-10.44	-15.48
3.514	44.68	0.88	2142.1	-10.53	-15.59
3.516	44.70	0.88	2143.1	-10.59	-15.66
3.519	44.72	0.88	2144.0	-10.61	-15.68
3.521	44.73	0.88	2144.8	-10.62	-15.71
3.523	44.75	0.87	2145.7	-10.62	-15.78
3.525	44.76	0.87	2146.6	-10.63	-15.88
3.527	44.78	0.87	2147.5	-10.64	-16.02
3.529	44.80	0.87	2148.4	-10.65	-16.18
3.531	44.81	0.86	2149.3	-10.67	-16.35
3.533	44.83	0.86	2150.2	-10.68	-16.53
3.536	44.84	0.86	2151.1	-10.69	-16.71
3.538	44.86	0.86	2151.9	-10.69	-16.89
3.540	44.88	0.86	2152.7	-10.70	-17.05
3.542	44.89	0.86	2153.5	-10.70	-17.19
3.544	44.91	0.85	2154.3	-10.71	-17.30
3.546	44.93	0.85	2154.9	-10.71	-17.37
3.548	44.94	0.85	2155.6	-10.71	-17.39
3.550	44.96	0.85	2156.2	-10.71	-17.42
3.552	44.98	0.85	2157.1	-10.70	-17.50
3.555	45.00	0.85	2158.0	-10.69	-17.64
3.557	45.01	0.84	2159.0	-10.67	-17.81
3.559	45.03	0.84	2160.1	-10.64	-18.01
3.561	45.04	0.84	2161.2	-10.60	-18.24
3.563	45.06	0.84	2162.4	-10.54	-18.49
3.565	45.08	0.84	2163.6	-10.47	-18.75
3.567	45.09	0.84	2164.7	-10.38	-19.01
3.569	45.11	0.84	2165.9	-10.27	-19.27
3.572	45.12	0.84	2167.0	-10.14	-19.51
3.574	45.14	0.84	2168.0	-9.99	-19.74
3.576	45.16	0.84	2169.0	-9.82	-19.94
3.578	45.17	0.84	2169.8	-9.63	-20.10
3.580	45.19	0.84	2170.5	-9.43	-20.22
3.582	45.21	0.84	2171.2	-9.24	-20.41
3.584	45.23	0.84	2172.0	-9.08	-20.77
3.586	45.24	0.84	2173.0	-8.93	-21.23

3.588	45.26	0.84	2174.0	-8.77	-21.77
3.591	45.27	0.84	2175.1	-8.60	-22.34
3.593	45.29	0.84	2176.2	-8.40	-22.88
3.595	45.30	0.84	2177.2	-8.17	-23.36
3.597	45.32	0.84	2178.2	-7.90	-23.72
3.599	45.34	0.84	2179.1	-7.59	-23.91
3.601	45.36	0.84	2179.9	-7.31	-24.11
3.603	45.37	0.84	2180.7	-7.11	-24.47
3.605	45.39	0.84	2181.5	-6.94	-24.89
3.608	45.41	0.84	2182.2	-6.78	-25.31
3.610	45.42	0.84	2182.9	-6.59	-25.65
3.612	45.44	0.84	2183.6	-6.35	-25.82
3.614	45.46	0.85	2184.2	-6.09	-25.89
3.616	45.48	0.85	2184.9	-5.84	-25.97
3.618	45.50	0.85	2185.6	-5.60	-26.06
3.620	45.52	0.85	2186.4	-5.37	-26.16
3.622	45.54	0.84	2187.2	-5.14	-26.26
3.625	45.56	0.84	2188.0	-4.92	-26.38
3.627	45.58	0.84	2188.8	-4.70	-26.49
3.629	45.60	0.84	2189.7	-4.49	-26.62
3.631	45.62	0.84	2190.5	-4.26	-26.74
3.633	45.64	0.84	2191.4	-4.04	-26.87
3.635	45.66	0.84	2192.3	-3.81	-26.99
3.637	45.68	0.84	2193.2	-3.57	-27.12
3.639	45.70	0.84	2194.2	-3.32	-27.24
3.641	45.72	0.84	2195.1	-3.06	-27.35
3.644	45.74	0.84	2196.0	-2.78	-27.46
3.646	45.76	0.84	2196.9	-2.49	-27.56
3.648	45.78	0.84	2197.9	-2.19	-27.65
3.650	45.80	0.84	2198.8	-1.86	-27.72
3.652	45.81	0.84	2199.7	-1.52	-27.78
3.654	45.83	0.84	2200.5	-1.15	-27.82
3.656	45.85	0.84	2201.4	-0.77	-27.84
3.658	45.87	0.84	2202.3	-0.35	-27.83
3.661	45.88	0.84	2203.3	0.11	-27.76
3.663	45.90	0.85	2204.4	0.60	-27.66
3.665	45.91	0.85	2205.6	1.11	-27.52
3.667	45.92	0.85	2206.8	1.64	-27.35
3.669	45.94	0.85	2208.0	2.18	-27.15
3.671	45.95	0.85	2209.3	2.73	-26.93
3.673	45.96	0.85	2210.7	3.27	-26.70
3.675	45.98	0.86	2212.0	3.82	-26.45
3.677	45.99	0.86	2213.3	4.35	-26.21
3.680	46.00	0.86	2214.6	4.88	-25.97
3.682	46.01	0.86	2215.9	5.40	-25.75
3.684	46.02	0.86	2217.2	5.91	-25.54
3.686	46.03	0.87	2218.4	6.41	-25.36
3.688	46.05	0.87	2219.5	6.89	-25.22
3.690	46.06	0.87	2220.7	7.37	-25.08
3.692	46.07	0.87	2221.8	7.85	-24.90
3.694	46.08	0.88	2222.9	8.32	-24.69

3.697	46.10	0.88	2224.0	8.79	-24.46
3.699	46.11	0.88	2225.1	9.24	-24.20
3.701	46.12	0.88	2226.2	9.68	-23.91
3.703	46.13	0.89	2227.2	10.10	-23.62
3.705	46.14	0.89	2228.2	10.51	-23.30
3.707	46.16	0.89	2229.3	10.90	-22.98
3.709	46.17	0.89	2230.3	11.28	-22.66
3.711	46.18	0.89	2231.2	11.65	-22.33
3.714	46.19	0.90	2232.2	11.99	-22.01
3.716	46.20	0.90	2233.1	12.33	-21.69
3.718	46.22	0.90	2234.0	12.65	-21.39
3.720	46.23	0.90	2234.9	12.95	-21.10
3.722	46.24	0.90	2235.8	13.25	-20.82
3.724	46.25	0.91	2236.6	13.53	-20.57
3.726	46.27	0.91	2237.5	13.81	-20.34
3.728	46.28	0.91	2238.3	14.08	-20.14
3.730	46.29	0.91	2239.0	14.29	-19.93
3.733	46.30	0.92	2239.7	14.40	-19.66
3.735	46.31	0.92	2240.4	14.42	-19.36
3.737	46.33	0.92	2241.0	14.37	-19.03
3.739	46.34	0.93	2241.6	14.27	-18.68
3.741	46.35	0.93	2242.2	14.13	-18.32
3.743	46.37	0.93	2242.8	13.97	-17.97
3.745	46.38	0.94	2243.4	13.81	-17.63
3.747	46.39	0.94	2244.0	13.67	-17.31
3.750	46.40	0.94	2244.7	13.55	-17.02
3.752	46.42	0.95	2245.3	13.49	-16.78
3.754	46.43	0.95	2246.0	13.49	-16.58
3.756	46.44	0.95	2246.7	13.57	-16.44
3.758	46.45	0.95	2247.4	13.65	-16.31
3.760	46.47	0.96	2248.2	13.64	-16.11
3.762	46.48	0.96	2248.9	13.56	-15.86
3.764	46.49	0.96	2249.6	13.44	-15.58
3.766	46.51	0.96	2250.2	13.29	-15.26
3.769	46.52	0.96	2250.9	13.13	-14.92
3.771	46.53	0.96	2251.7	12.99	-14.57
3.773	46.55	0.96	2252.4	12.88	-14.22
3.775	46.56	0.96	2253.1	12.81	-13.88
3.777	46.57	0.96	2253.9	12.82	-13.55
3.779	46.59	0.96	2254.7	12.91	-13.24
3.781	46.60	0.96	2255.6	13.11	-12.96
3.783	46.61	0.96	2256.5	13.35	-12.67
3.786	46.63	0.96	2257.3	13.55	-12.31
3.788	46.64	0.97	2258.2	13.71	-11.91
3.790	46.66	0.97	2259.0	13.84	-11.47
3.792	46.67	0.97	2259.9	13.92	-10.99
3.794	46.69	0.97	2260.8	13.97	-10.48
3.796	46.70	0.97	2261.6	13.98	-9.95
3.798	46.72	0.98	2262.5	13.97	-9.41
3.800	46.73	0.98	2263.4	13.93	-8.86
3.803	46.75	0.98	2264.2	13.86	-8.30

3.805	46.76	0.98	2265.1	13.78	-7.75
3.807	46.78	0.98	2266.0	13.68	-7.20
3.809	46.79	0.98	2266.8	13.58	-6.67
3.811	46.81	0.99	2267.7	13.47	-6.15
3.813	46.83	0.99	2268.6	13.37	-5.64
3.815	46.84	0.99	2269.4	13.27	-5.16
3.817	46.86	0.99	2270.3	13.20	-4.70
3.819	46.87	0.99	2271.1	13.14	-4.25
3.822	46.89	1.00	2272.0	13.12	-3.83
3.824	46.91	1.00	2272.9	13.13	-3.43
3.826	46.93	1.00	2273.7	13.19	-3.04
3.828	46.94	1.00	2274.5	13.26	-2.65
3.830	46.96	1.00	2275.3	13.30	-2.24
3.832	46.98	1.00	2276.1	13.30	-1.81
3.834	47.01	1.00	2276.9	13.27	-1.38
3.836	47.03	1.00	2277.7	13.21	-0.93
3.839	47.05	1.01	2278.5	13.13	-0.49
3.841	47.07	1.01	2279.2	13.03	-0.05
3.843	47.09	1.01	2280.0	12.92	0.38
3.845	47.12	1.01	2280.7	12.80	0.80
3.847	47.14	1.01	2281.5	12.68	1.20
3.849	47.16	1.01	2282.3	12.55	1.60
3.851	47.18	1.01	2283.1	12.44	1.98
3.853	47.20	1.01	2283.8	12.33	2.35
3.855	47.21	1.01	2284.6	12.25	2.70
3.858	47.23	1.01	2285.5	12.15	3.06
3.860	47.24	1.01	2286.5	12.01	3.42
3.862	47.25	1.01	2287.5	11.84	3.79
3.864	47.26	1.01	2288.6	11.65	4.13
3.866	47.27	1.02	2289.6	11.45	4.44
3.868	47.28	1.02	2290.5	11.25	4.72
3.870	47.29	1.02	2291.4	11.08	4.94
3.872	47.31	1.02	2292.1	10.94	5.11
3.875	47.32	1.02	2292.7	10.84	5.22
3.877	47.33	1.02	2293.0	10.81	5.26
3.879	47.35	1.02	2293.3	10.76	5.22
3.881	47.37	1.02	2293.8	10.62	5.12
3.883	47.40	1.02	2294.4	10.41	4.97
3.885	47.42	1.02	2295.2	10.17	4.79
3.887	47.45	1.02	2296.0	9.90	4.60
3.889	47.48	1.02	2296.9	9.62	4.41
3.892	47.50	1.02	2297.7	9.37	4.24
3.894	47.53	1.02	2298.5	9.16	4.10
3.896	47.55	1.02	2299.2	9.02	4.00
3.898	47.58	1.02	2299.8	8.97	3.97
3.900	47.59	1.02	2300.3	8.99	4.00
3.902	47.61	1.01	2300.8	9.05	4.07
3.904	47.63	1.01	2301.2	9.15	4.20
3.906	47.64	1.01	2301.7	9.28	4.36
3.908	47.66	1.01	2302.1	9.44	4.55
3.911	47.67	1.00	2302.6	9.61	4.77

3.913	47.68	1.00	2303.0	9.79	5.02
3.915	47.70	1.00	2303.5	9.99	5.27
3.917	47.71	1.00	2304.0	10.18	5.53
3.919	47.73	0.99	2304.6	10.38	5.79
3.921	47.74	0.99	2305.1	10.57	6.04
3.923	47.76	0.99	2305.7	10.75	6.27
3.925	47.77	0.99	2306.4	10.93	6.46
3.928	47.79	0.98	2307.1	11.10	6.62
3.930	47.81	0.98	2307.9	11.25	6.72
3.932	47.83	0.98	2308.8	11.39	6.76
3.934	47.86	0.98	2309.7	11.52	6.73
3.936	47.89	0.98	2310.7	11.62	6.62
3.938	47.92	0.98	2311.9	11.75	6.36
3.940	47.96	0.98	2313.5	11.95	5.93
3.942	48.00	0.98	2315.4	12.18	5.34
3.944	48.05	0.98	2317.4	12.42	4.64
3.947	48.11	0.98	2319.6	12.63	3.86
3.949	48.16	0.98	2321.9	12.81	3.04
3.951	48.22	0.98	2324.2	12.94	2.20
3.953	48.27	0.98	2326.4	13.03	1.40
3.955	48.32	0.97	2328.4	13.08	0.68

---





## Appendix G – Tabular Data for Test 2

Time	Distance		
[sec]	[m]		
0.14	0.00	0.42	4.93
0.15	0.18	0.43	5.09
0.16	0.36	0.44	5.26
0.17	0.54	0.45	5.42
0.18	0.72	0.46	5.59
0.19	0.90	0.47	5.75
0.20	1.08	0.48	5.91
0.21	1.26	0.49	6.07
0.22	1.44	0.50	6.23
0.23	1.62	0.51	6.38
0.24	1.80	0.52	6.54
0.25	1.98	0.53	6.69
0.26	2.16	0.54	6.84
0.27	2.34	0.55	6.99
0.28	2.51	0.56	7.14
0.29	2.69	0.57	7.29
0.30	2.87	0.58	7.44
0.31	3.04	0.59	7.59
0.32	3.22	0.60	7.73
0.33	3.39	0.61	7.87
0.34	3.57	0.62	8.01
0.35	3.74	0.63	8.15
0.36	3.91	0.64	8.29
0.37	4.08	0.65	8.43
0.38	4.25	0.66	8.57
0.39	4.42	0.67	8.71
0.40	4.59	0.68	8.84
0.41	4.76	0.69	8.98
		0.70	9.11
		0.71	9.25
		0.72	9.38

0.73	9.51	1.15	14.82
0.74	9.64	1.16	14.95
0.75	9.77	1.17	15.07
0.76	9.90	1.18	15.19
0.77	10.03	1.19	15.31
0.78	10.16	1.20	15.43
0.79	10.29	1.21	15.55
0.80	10.42	1.22	15.67
0.81	10.54	1.23	15.79
0.82	10.67	1.24	15.91
0.83	10.80	1.25	16.02
0.84	10.93	1.26	16.14
0.85	11.05	1.27	16.25
0.86	11.18	1.28	16.37
0.87	11.31	1.29	16.48
0.88	11.43	1.30	16.59
0.89	11.56	1.31	16.70
0.90	11.69	1.32	16.81
0.91	11.81	1.33	16.92
0.92	11.94	1.34	17.03
0.93	12.06	1.35	17.14
0.94	12.19	1.36	17.24
0.95	12.32	1.37	17.35
0.96	12.44	1.38	17.45
0.97	12.57	1.39	17.55
0.98	12.69	1.40	17.65
0.99	12.82	1.41	17.76
1.00	12.95	1.42	17.86
1.01	13.07	1.43	17.95
1.02	13.20	1.44	18.05
1.03	13.32	1.45	18.15
1.04	13.45	1.46	18.24
1.05	13.57	1.47	18.34
1.06	13.70	1.48	18.43
1.07	13.83	1.49	18.53
1.08	13.95	1.50	18.62
1.09	14.08	1.51	18.71
1.10	14.20	1.52	18.80
1.11	14.33	1.53	18.89
1.12	14.45	1.54	18.99
1.13	14.57	1.55	19.08
1.14	14.70	1.56	19.16

1.57	19.25	1.99	22.83
1.58	19.34	2.00	22.91
1.59	19.43	2.01	22.99
1.60	19.52	2.02	23.07
1.61	19.61	2.03	23.15
1.62	19.69	2.04	23.23
1.63	19.78	2.05	23.31
1.64	19.87	2.06	23.39
1.65	19.96	2.07	23.46
1.66	20.04	2.08	23.54
1.67	20.13	2.09	23.62
1.68	20.22	2.10	23.70
1.69	20.30	2.11	23.78
1.70	20.39	2.12	23.85
1.71	20.48	2.13	23.93
1.72	20.56	2.14	24.01
1.73	20.65	2.15	24.08
1.74	20.73	2.16	24.16
1.75	20.82	2.17	24.23
1.76	20.91	2.18	24.31
1.77	20.99	2.19	24.38
1.78	21.08	2.20	24.45
1.79	21.16	2.21	24.53
1.80	21.25	2.22	24.60
1.81	21.33	2.23	24.67
1.82	21.42	2.24	24.75
1.83	21.50	2.25	24.82
1.84	21.59	2.26	24.89
1.85	21.67	2.27	24.96
1.86	21.75	2.28	25.03
1.87	21.84	2.29	25.10
1.88	21.92	2.30	25.17
1.89	22.00	2.31	25.24
1.90	22.09	2.32	25.31
1.91	22.17	2.33	25.38
1.92	22.25	2.34	25.44
1.93	22.34	2.35	25.51
1.94	22.42	2.36	25.58
1.95	22.50	2.37	25.64
1.96	22.58	2.38	25.71
1.97	22.66	2.39	25.77
1.98	22.75	2.40	25.84

2.41	25.90	2.83	28.35
2.42	25.97	2.84	28.41
2.43	26.03	2.85	28.46
2.44	26.10	2.86	28.52
2.45	26.16	2.87	28.57
2.46	26.22	2.88	28.63
2.47	26.28	2.89	28.68
2.48	26.34	2.90	28.74
2.49	26.41	2.91	28.79
2.50	26.47	2.92	28.85
2.51	26.53	2.93	28.90
2.52	26.59	2.94	28.96
2.53	26.65	2.95	29.01
2.54	26.71	2.96	29.07
2.55	26.77	2.97	29.12
2.56	26.83	2.98	29.17
2.57	26.89	2.99	29.23
2.58	26.95	3.00	29.28
2.59	27.00	3.01	29.34
2.60	27.06	3.02	29.39
2.61	27.12	3.03	29.45
2.62	27.18	3.04	29.50
2.63	27.24	3.05	29.56
2.64	27.29	3.06	29.61
2.65	27.35	3.07	29.67
2.66	27.41	3.08	29.72
2.67	27.47	3.09	29.77
2.68	27.52	3.10	29.83
2.69	27.58	3.11	29.88
2.70	27.63	3.12	29.94
2.71	27.69	3.13	29.99
2.72	27.75	3.14	30.04
2.73	27.80	3.15	30.10
2.74	27.86	3.16	30.15
2.75	27.91	3.17	30.21
2.76	27.97	3.18	30.26
2.77	28.02	3.19	30.31
2.78	28.08	3.20	30.37
2.79	28.13	3.21	30.42
2.80	28.19	3.22	30.47
2.81	28.24	3.23	30.53
2.82	28.30	3.24	30.58

3.25	30.63	3.67	32.75
3.26	30.69	3.68	32.80
3.27	30.74	3.69	32.85
3.28	30.79	3.70	32.89
3.29	30.85	3.71	32.94
3.30	30.90	3.72	32.98
3.31	30.95	3.73	33.03
3.32	31.00	3.74	33.08
3.33	31.06	3.75	33.12
3.34	31.11	3.76	33.17
3.35	31.16	3.77	33.21
3.36	31.21	3.78	33.25
3.37	31.26	3.79	33.30
3.38	31.32	3.80	33.34
3.39	31.37	3.81	33.38
3.40	31.42	3.82	33.43
3.41	31.47	3.83	33.47
3.42	31.52	3.84	33.51
3.43	31.57	3.85	33.55
3.44	31.62	3.86	33.59
3.45	31.67	3.87	33.64
3.46	31.73	3.88	33.68
3.47	31.78	3.89	33.72
3.48	31.83	3.90	33.75
3.49	31.88	3.91	33.79
3.50	31.93	3.92	33.83
3.51	31.98	3.93	33.87
3.52	32.03	3.94	33.91
3.53	32.08	3.95	33.94
3.54	32.13	3.96	33.98
3.55	32.18	3.97	34.02
3.56	32.22	3.98	34.05
3.57	32.27	3.99	34.09
3.58	32.32	4.00	34.12
3.59	32.37	4.01	34.16
3.60	32.42	4.02	34.19
3.61	32.47	4.03	34.22
3.62	32.52	4.04	34.25
3.63	32.56	4.05	34.28
3.64	32.61	4.06	34.31
3.65	32.66	4.07	34.34
3.66	32.71	4.08	34.37

4.09	34.40	4.51	35.01
4.10	34.43	4.52	35.01
4.11	34.46	4.53	35.02
4.12	34.48	4.54	35.02
4.13	34.51	4.55	35.02
4.14	34.54	4.56	35.02
4.15	34.56	4.57	35.02
4.16	34.58	4.58	35.02
4.17	34.61	4.59	35.02
4.18	34.63	4.60	35.02
4.19	34.65	4.61	35.01
4.20	34.67	4.62	35.01
4.21	34.69	4.63	35.01
4.22	34.71	4.64	35.01
4.23	34.73	4.65	35.00
4.24	34.75	4.66	35.00
4.25	34.77	4.67	34.99
4.26	34.78	4.68	34.99
4.27	34.80	4.69	34.98
4.28	34.82	4.70	34.98
4.29	34.83	4.71	34.97
4.30	34.85	4.72	34.97
4.31	34.86	4.73	34.96
4.32	34.87	4.74	34.96
4.33	34.88	4.75	34.95
4.34	34.90	4.76	34.94
4.35	34.91	4.77	34.93
4.36	34.92	4.78	34.93
4.37	34.93	4.79	34.92
4.38	34.94	4.80	34.91
4.39	34.95	4.81	34.90
4.40	34.96	4.82	34.89
4.41	34.96	4.83	34.88
4.42	34.97	4.84	34.88
4.43	34.98	4.85	34.87
4.44	34.98	4.86	34.86
4.45	34.99	4.87	34.85
4.46	34.99	4.88	34.84
4.47	35.00	4.89	34.83
4.48	35.00	4.90	34.82
4.49	35.01	4.91	34.80
4.50	35.01	4.92	34.79

4.93	34.78
4.94	34.77
4.95	34.76
4.96	34.75
4.97	34.74
4.98	34.73
4.99	34.71
5.00	34.70
5.01	34.69
5.02	34.68
5.03	34.67
5.04	34.65
5.05	34.64
5.06	34.63
5.07	34.62
5.08	34.60
5.09	34.59
5.10	34.58
5.11	34.56
5.12	34.55
5.13	34.54
5.14	34.53

---



